STRUCTURAL SUPRAMOLECULAR ASSEMBLIES OF SPHERES AND TUBES

A Dissertation

presented to

the Faculty of the Graduate School

University of Missouri-Columbia

In Partial Fulfillment

of the Requirements for the Degree

Doctor of Philosophy

By

MICHAEL WILLIAM HEAVEN

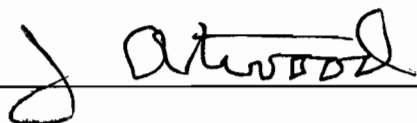Prof. Jerry L. Atwood, Dissertation Supervisor

May 2006

The undersigned, appointed by the Dean of the Graduate School,
have examined the dissertation entitled,

STRUCTURAL SUPRAMOLECULAR ASSEMBLIES
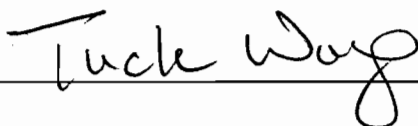## OF SPHERES AND TUBES
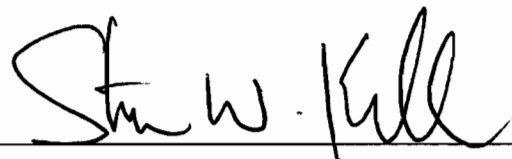
Presented by Michael William Heaven

A candidate for the degree of Doctor of Philosophy

And hereby certify that in their opinion it is worthy of acceptance.

Acknowledgments

List of Tables

List of Figures

List of Schemes

Chapter 1: Structural supramolecular chemistry

Since chemistry was discovered, when atoms were recognized and ratios of molecular weights were rationalized which led to the understanding of molecules, chemists have sought to create new and interesting structures. Through a series of covalent modifications, molecules that were discovered naturally could be synthesized in the lab with the idea that they could be made more simply than they could *via* extraction. The molecules we sought were analogues of structures that were seen to be useful in nature and could cure or prevent diseases, strengthen structures or produce useful devices.[1]

Supramolecular chemistry takes this one step further by now taking these molecules and asking what they can do when we put them together. Not covalently but through non-covalent means, as we see all around us in the cells of plants and animals. Our groups interest in supramolecular compounds relates to our ongoing program involving the construction of large host systems for molecular encapsulation and manipulation.[2-7]

Structurally, nature constructs permeable walls such as lipid bilayers.[8] The cytoskeleton of cells is a complex and vibrant supramolecular construct able to act as a barrier, scaffold or transport medium.[9] Recently long tunnels between cells called cytonemes draw out and self assemble columns of actin and relay amino acids.[10] The projects presented within humbly wish to emulate and discover some of the pieces that can help bridge between chemistry and biology.

1

The first project takes a popular but difficult to work with molecule, the cucurbituril.[11] It has been used for various supramolecular structures, particularly pseudorotaxanes, and so may one day act as artificial signaling devices for changing external stimuli as is found in nerve cells. This project dealt with the discovery of new tectons for supramolecular chemistry that may allow cucurbituril analogues to find greater efficiency and utility. As part of the discovery process, serendipitously a route was found to improve the reaction process of a biologically important compound through green principles.[12] A very important scientific lesson was dealt here too.

The second project took one of the most enigmatic molecules discovered in the past twenty years, the fullerenes, and through solid state engineering attempted to determine how structurally these compounds could be changed.[13,14] The project showed how it was possible to turn a complex two dimensional sheet of fullerenes into a helical array. This project allows one to envision that one day precise crystal engineering may be required to form regular rows of carbons so as to create nanotubes in some nanoscale engineering device.

Carbon nanotubes were the focus of the third project. Creation of regular arrays of nanotubes will improve their properties. This can be performed as per the second project by placing precursors of the nanotubes like laying down piping in a ditch. However, the other way in which arrays can be developed is through supramolecular chemistry with the coming together *via* mutually cohesive but differing molecules. This project attempted to

answer the question in that how does a disordered array of nanotubes become a more ordered gel through self assembly of nickel containing macrocycles.

Finally, the last project takes a look at the large scale formation of biology structures and determines how it can be mimicked from the much smaller supermolecules currently available.[15] A cell wall, besides the complex mix of receptor and channel proteins is a mess of chaotic but organized lipid bilayers that while relatively small in themselves organize into a much larger aggregate.[16] We have found a system that promotes the same behavior and produces spherical structure way out of proportion to their individual size. Surprisingly these large aggregates likewise perform what has been recently discovered in cells themselves; the cellular nanotubes between cells. This project seeks to discover the generality and proposes the how and why this may occur.

Each of these projects takes a different aspect of supramolecular chemistry. From the humble beginnings with the formation of small tectons to the large scale structures approaching the dimensions of cells, each of these various aspects look at how supramolecular chemistry may mimic and even improve the structures upon which we gaze enviously at nature. I hope you find that reading about the journey that has been this PhD is as interesting as I found in undertaking it.

(1)   Feiters, M. C. In *Supramolecular Technology*; Reinhoudt, D. N., Ed.; Elsevier Science Ltd.: Oxford, 1996; Vol. 10, pp 267-360.
(2)   Hardie, M. J.; Raston, C. L. *J. Chem. Soc., Dalton Trans.* **2000**, 2483-2492.
(3)   Cave, G. W. V.; Hardie, M. J.; Roberts, B. A.; Raston, C. L. *Eur. J. Org. Chem.* **2001**, *2001*, 3227-3231.
(4)   Orr, G. W.; Barbour, L. J.; Atwood, J. L. *Science* **1999**, *285*, 1049-1052.
(5)   MacGillivray, L. R.; Atwood, J. L. *Nature* **1997**, *389*, 469-472.

(6)   Atwood, J. L.; Barbour, L. J.; Jerga, A. *Chem. Commun.* **2001**, 2376-2377.

(7)   Rose, K. N.; Barbour, L. J.; Orr, G. W.; Atwood, J. L. *Chem. Commun.* **1998**, *3*, 407-408.

(8)   Fyles, T. M. In *Inclusion Aspects of Membrane Chemistry*; Osa, T., Atwood, J. L., Eds.; Kluwer Academic Publishers: Dordrecht, 1991; Vol. 2, pp 59-110.

(9)   Giner, D.; Neco, P.; Frances, M. d. M.; Lopez, I.; Viniegra, S.; Gutierrez, L. M. *J Cell Sci.* **2005**, *118*, 2871-2880.

(10)   Ramirez-Weber, F.-A.; Kornberg, T. B. *Cell* **1999**, *97*, 599-607.

(11)   Lagona, J.; Mukhopadhyay, P.; Chakrabarti, S.; Isaacs, L. *Angew. Chem. Int. Ed.* **2005**, *44*, 4844-4870.

(12)   Atwood, J. L.; Barbour, L. J.; Heaven, M. W.; Raston, C. L. *J. Chem. Crystallogr.* **2003**, *33*, 175-179.

(13)   Atwood, J. L.; Barbour, L. J.; Heaven, M. W.; Raston, C. L. *Angew. Chem. Int. Ed.* **2003**, *42*, 3254-3257.

(14)   Atwood, J. L.; Barbour, L. J.; Heaven, M. W.; Raston, C. L. *Chem. Commun.* **2003**, 2270-2271.

(15)   Antesberger, J.; Cave, G. W. V.; Ferrarelli, M. C.; Heaven, M. W.; Raston, C. L.; Atwood, J. L. *Chem. Commun.* **2005**, 892-894.

(16)   Gokel, G. W. *Chem. Commun.* **2000**, *1*, 1-9.

Chapter 2: Cucurbit[n]uril; building of structural tectons

Abstract

This project was envisioned as examining the supramolecular structural suitability of the toroidal macrocycle cucurbituril. Initially hypothesized at Monash University, Melbourne, Australia in 2000 as a way to protect carotenoids in solution from their propensity for facile isomerizations and subsequent degradation, the project evolved into the structural supramolecular chemistry project submitted after it was determined that the host-guest system was incompatible due to mutually exclusive solubilities between host and guest. This project examined a range of modifications to the cucurbituril host and after extensive exploration into modifying its chemical properties a new type of cucurbituril was discovered, along with some novel substrates and a greener method for forming commercially interesting compounds, the hydantoins. During the investigation of improving the solubilities of cucurbituril, an unusual new structure was found when using potassium nitrate with cucurbit[6]uril. It was found that the simple removal of a large encapsulated molecule will change the potassium cucurbituril solid state structure into one more resembling a cesium product.

2.1   *Cucurbit[n]uril*

2.1.1   Introduction

Since the elucidation of the structure of cucurbit[6]uril **(1)** by Mock and coworkers in 1981 (Figure 2.1),[1] this macrocycle has become a popular building block for a range of supramolecular constructs. Amongst the various uses has been the formation of pseudorotaxanes,[2] containers for small molecules,[3] molecular ball bearings,[4] reactive dye remover from aqueous solutions[5] and microreactors[6] or drug delivery carriers.[7] Most of this research has required the use of a cationic metal or nitrogen, amine or aromatic functionalized guest to solubilize cucurbit[n]uril since the macrocycle's low solubility presents a major drawback.[8,9]
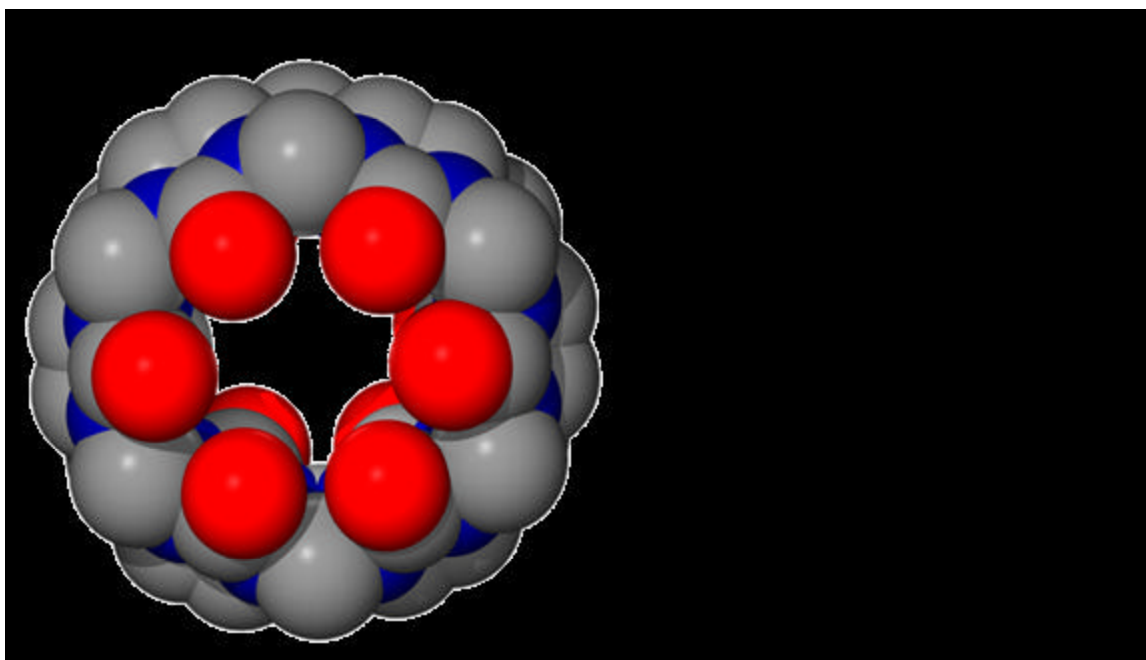
Figure 2.1. Left: Space filling view of cucurbit[6]uril, **1**, revealing the toroidal cavity encircled by carbonyl oxygen atoms. (grey = carbon, red = oxygen, blue = nitrogen, hydrogen atoms not shown for clarity). Right: Side view of cucurbit[6]uril.

2.2   *Cucurbit[n]uril synthesis*

2.2.1   Characterization of cucurbit[6]uril.

The parent compound cucurbit[n]uril (from the Latin Cucurbitaceae (*pumpkin*)) was first synthesized in 1905 by Behrend.[10] The compound required a simple synthesis, a product of an acid hydrolysis from a combination of glycoluril (**2**) and formaldehyde (**3**) (Scheme 2.1). However due to limited analytical techniques the white, amorphous solid was difficult to fully characterize. While it could be determined that the empirical formula was $(C_6H_6N_4O_2)_n$ and that complexes were formed between **1** and salts or dyes, its full characterization was to take a further seventy-six years and was mischaracterized as a polymer. At the time, in honor of its discoverer, it became known as Behrend's polymer, a now obvious misnomer.
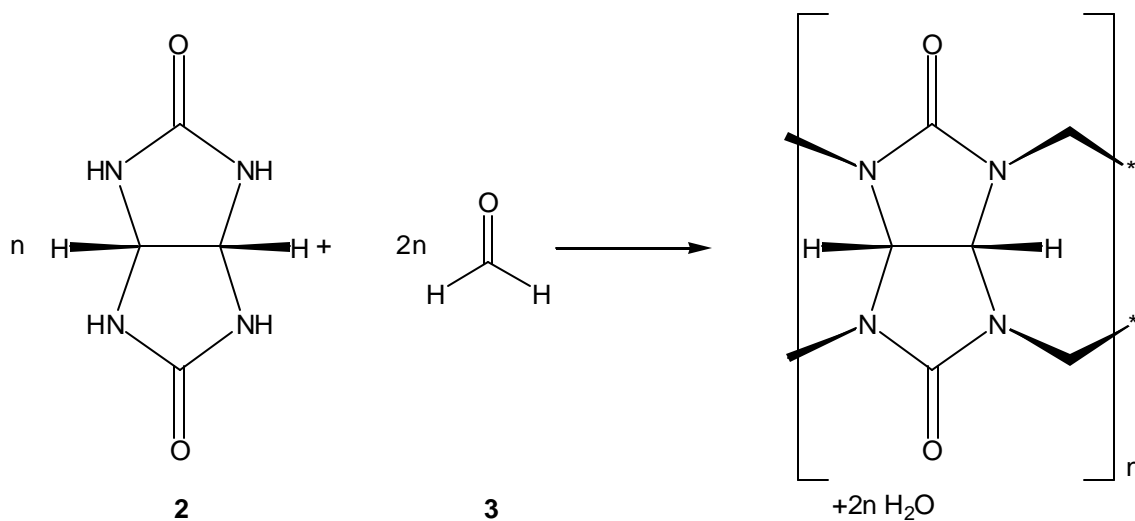
Scheme 2.1. General Synthetic procedure for cucurbit[n]uril (n = 5, 6, 7, 8, 10)

In 1981, after reading about Behrend's work, Mock and coworkers repeated the synthesis and analyzed the product with the modern techniques not available to Behrend.[1] With access to proton NMR, they were able to determine that the material was highly

symmetrical, having only three resonances (two for single protons with geminal coupling and a single peak of the two glycoluril protons). The resonances were all upfield from the aromatic region so discounting a symmetrical heterocycle. The infrared spectrum also revealed that the precursor molecule of glycoluril was retained with a C=O stretch at 1720 cm^{-1}. As with Behrend, complete characterization was still somewhat difficult as it was found that the product was not volatile enough for the mass spectrometry techniques available. Finally, resorting to single crystal X-ray crystallography, they were finally able to determine the structure from its calcium sulphate salt.

The molecule **1** was found to be a rigid macrocycle, the glycoluril and formaldehyde coming together *via* aminal bonds (Figure 2.1). The angled shape of the substrate glycoluril precursor is retained meaning that the molecule has a pinched-in portal of six carbonyl groups above and below the wider main body. The diameter of the portal of **1** is approximately 4 Å and surrounded by the oxygen atoms of the carbonyl groups that protects a larger inner cavity of 5.8 Å. This cavity provided magnetic shielding for guests in NMR experiments that they performed later.[11,12] Mock's group also proposed the common name cucurbit[n]uril due to its likeness to a pumpkin and as the IUPAC nomenclature was somewhat of a mouthful: (dodecahydro-1*H*, 4*H*, 14*H*, 17*H*-2, 16:3, 15-dimethano-5*H*, 6*H*, 7*H*, 8*H*, 10*H*, 11*H*, 12*H*, 13*H*, 18*H*, 19*H*, 20*H*, 21*H*, 22*H*, 23*H*, 24*H*, 25*H*, 26*H*, 2, 3, 4a, 5a, 6a, 7a, 8a, 9a, 10a, 11a, 12a, 13a, 15, 16, 17a, 18a, 19a, 20a, 2la, 22a, 23a, 24a, 25a, 26a-tetracosaazabispentaleno[1''', 6''':5'', 6'', 7'']cycloocta[1'', 2'', 3'':3', 4']pentaleno(1', 6':5, 6, 7)cycloocta(1, 2, 3-*gh*: 1', 2', 3'-*g'h'*)cycloocta(1, 2, 3-*cd*:5, 6, 7-*c'd'*)dipentalene-1, 4, 6, 8, 10, 12, 14, 17, 19, 2 1, 23, 25-dodecone)!

2.2.2   Analogues of cucurbit[6]uril

Though hinted at in the PhD thesis of Shih, a student of Mock, the formal discovery of the first analogue of cucurbit[n]uril was not published until 1992. The treatment of a glycoluril analogue, dimethylglycoluril (**4**) with formaldehyde in acid led to the formation of the smaller decamethylcucurbit[5]uril (**5**) (Figure 2.2).[13] The extra methyl groups led to some steric strain, the crystal of the molecule having only C_2 symmetry for **5**; else the molecule in appearance was shown to be an analogue of **1**. As there was one less glycoluril (and associated methyl moieties from the formaldehyde precursor) the diameter of this analogue was smaller with the inner cavity only 4.4 Å in diameter and the carbonyl oxygen atoms making the entrance 2.4 Å, this somewhat restricting its use for guest encapsulation.[14]

The turn of the millennium brought the beginning of a deluge of research on cucurbit[n]uril, in particular the work performed in the laboratory of Kimoon Kim.[9] It was realized that like the macrocyclic calixarenes, the process of synthesis of cucurbit[n]uril was one of polymerization of long chains of methine linked glycolurils followed by cracking of the polymer to form the rings.[15] By lowering the temperature, it was shown that cucurbit[n]uril analogues could be synthesized. Kim's group managed to add three more cucurbit[n]urils to the library of macrocycles formed, their difference being only in ring size (Figure 2.2). The three, cucurbit[5]uril (**6**), cucurbit[7]uril (**7**) and cucurbit[8]uril (**8**), like the similarly shaped cyclodextrins have a range of differing properties with both the parent **1** and each other. It was noted from **6** that the external functionalization of external methyl groups of **5** had not had much of an effect on the dimensions of the cavity of the two cucurbit[5]urils (Table 2.1). **1**, **7** and **8** were shown to

be dimensionally similar to the cyclodextrins[16] and the existence of the latter two

revealed the possibility of expanded chemistry for this class of macrocycles.
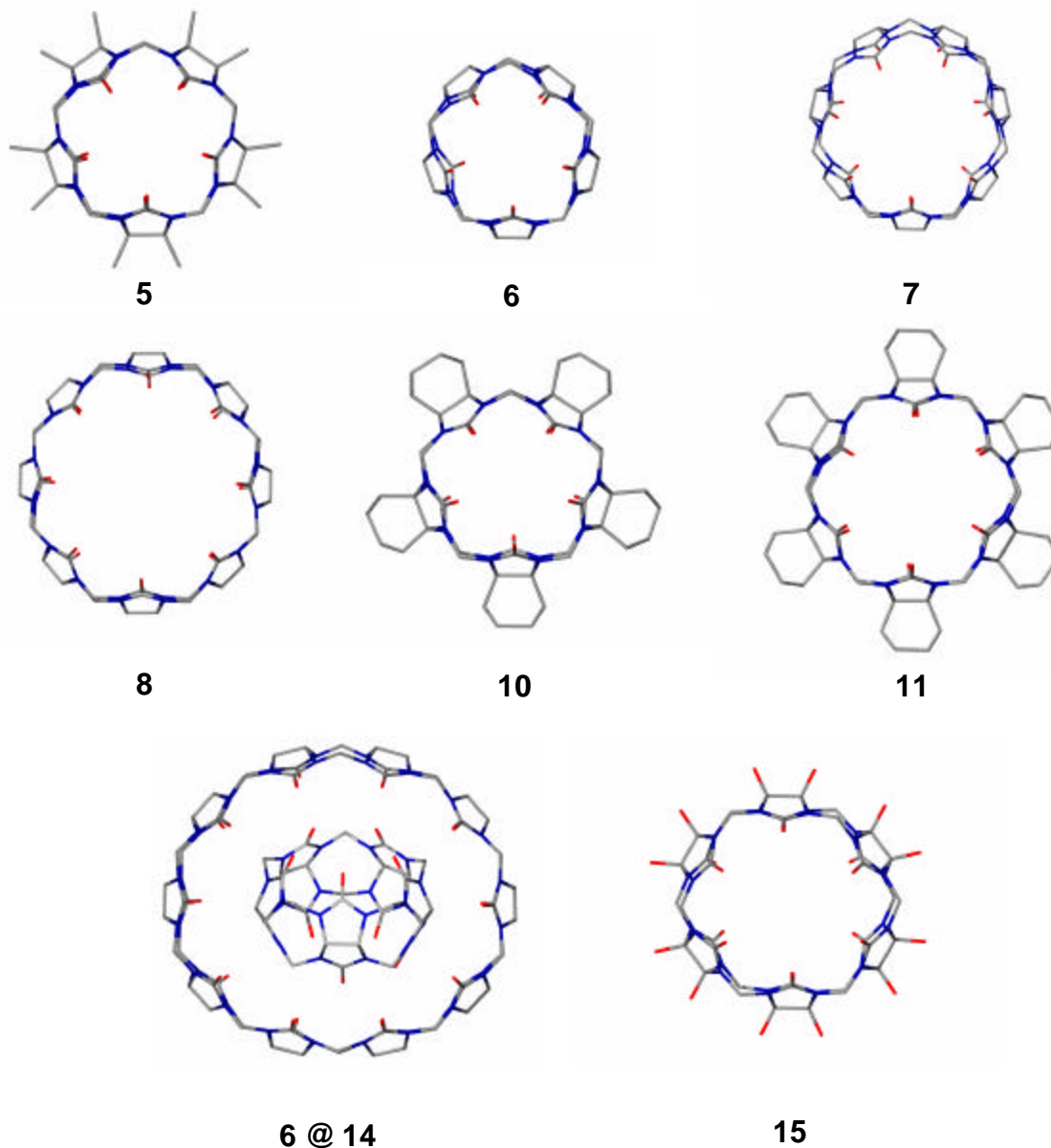
Figure 2.2. X-ray crystal structures of analogues of **1**.
5) Decamethylcucurbit[5]uril.   **6**) Cucurbit[5]uril.   **7**) Cucurbit[7]uril.
8) Cucurbit[8]uril.   **10**) Cyclohexanocurcurbit[5]uril.
11) Cyclohexanocurcurbit[6]uril.   **14**) Cucurbit[10]uril @ Cucurbit[5]uril.
(Hydrogen atoms and guest molecules not shown for clarity. **5** from Ref. 13,
6 – **8** from Ref. 9, **10** – **11** from Ref. 17, **6@14** from Ref. 20, **15** from Ref. 23.)

Relative to other macrocycles however, cucurbit[n]urils discovered up until this time still exhibited low solubilities in normal organic solvents or water. In 2001, the use of cyclohexanoglycoluril (**9**) as a substrate led to a cucurbit[n]uril analogue with vastly superior properties.[17] The resulting condensation product formed rings with either five or six units. Cyclohexanocucurbit[5]uril (**10**) and cyclohexanocucurbit[6]uril (**11**) was found to be readily soluble in organic and (somewhat surprisingly) aqueous solvents (Figure 2.2). In fact, **11** had similar solubility to α-cyclodextrin in water. The downside to this synthesis was the relatively low yield (**10**, yield: 16%; **11**, yield 2%). Despite this, the macrocycles were shown to be good ion sensors and acted as a neurotransmitter receptor mimic.

Table 2.1. Average dimensions of the various cucurbit[n]urils synthesized in comparison to the similar toroidal cyclodextrins.

Cucurbit[n]uril	n=	5	6	7	8		10
Diameters (Å)*							
Outer portal		2.4	3.9	5.4	6.9	1	13.
Inner cavity		4.4	5.8	7.3	8.8	1	14.

Cyclodextrin		α	β	γ
Diameters (Å)				
Upper portal		4.7	6.0	7.5
Lower portal		5.3	6.5	8.3

*Cucurbit[n]uril data (n = 5 – 8) from Ref. 9. Cucurbit[10]uril data from Ref. 20. Cyclodextrin data from Ref. 16.

The following year, a mixture of **2** and diphenylglycoluril (**12**) revealed the first asymmetrically formed cucurbit[n]uril (Figure 2.3).[18] Diphenyl cucurbit[6]uril (**13**) was synthesized so proving that the presence of large external functional groups such as two phenyl group did not completely restrict the ability to create cucurbit[n]uril molecules despite the known twisting of the precursor.[19] A molecule of **13** was able to form a

pseudorotaxane with the amine decorated spermine as per other cucurbit[n]urils. The NMR data indicated the existence of this host-guest complex *via* the shielding of both the spermine guest and the hydrogen atoms on the outer surface of **13** that were spatially close to the phenyl groups. Again, like **10** and **11**, the yield was quite low at only 30% (plus 30% cucurbit[6]uril synthesized along with **13**). The solubility of **13** was also similar to the original cucurbit[n]urils being quite insoluble in most solvents.

R =   CO$_2$Et,Phenyl,2-pyridyl,(CH$_2$)$_4$, Methyl, H
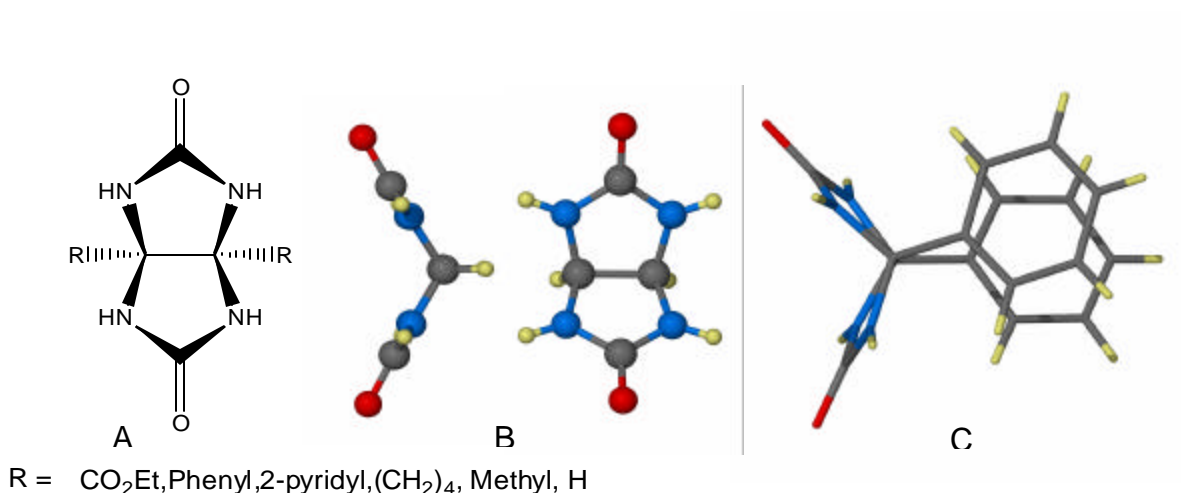
Figure 2.3. Glycoluril (**2**). A) Known compounds of glycoluril and analogues. B) Front and side view of **2** C) Crystal structure of diphenylglycoluril (**12**) that goes on to make **13,** the first asymmetric cucurbit[n]uril. Note how the large R groups can twist the parent compound (Crystal structure of **12** from Ref. 19, carbon = grey, hydrogen = yellow, nitrogen = blue, oxygen = red).

Working on the kilogram scale, Day and coworkers determined that the much larger cucurbit[10]uril (**14**) could be synthesized (Figure 2.2).[20] This, the largest cucurbit[n]uril "isolated" to date, was found to contain within its cavity cucurbit[5]uril (**6**) inclined at an angle of 64° with respect to the equator of **14**. In solution the inner molecule of **6** rotated fast enough on the NMR time scale such that the authors compared the overall system to a molecular gyroscope. Only in 2005 has a process to have **6** removed from **14** been successful.[21] This was achieved using a solution of a trifluroacetic acid salt thus showing the utility of different acidic conditions for synthesis of this class of macrocycle.

Day's group also investigated the synthesis of cucurbit[n]urils using a mixture of ratios of glycoluril and dimethylglycoluril and extensive use of electrospray mass spectrometry.[22] Not unexpectedly they found a range of differing cucurbit[n]urils from cucurbit[5]uril to cucurbit[7]uril, with cucurbit[n]urils consisting of a variable numbers of the precursor glycolurils **2** and **4**. The most common and isolated cucurbit[n]uril was that of the six membered ring with glycolurils alternating between **2** and **4** making a cucurbit[6]uril analogue. This was not unexpected, the synthesis of **13** revealing that steric considerations must be assessed in adding external functional groups to cucurbit[n]urils.

Even with the synthesis of **10** and **11**, up until 2003 analogues of cucurbit[6]uril either had low solubility and/or low yield. This was to change with the latest discovery of a way to functionalize the parent cucurbit[n]urils.[23] Cucurbit[n]urils (n = 5 – 8) were able to be completely hydroxylated at the hydrogen atom positions around the ring using potassium thiosulfate (Figure 2.2). While reasonable yields resulted for perhydroxycucurbit[5]uril (**15**) and the larger molecule perhydroxycucurbit[6]uril (**16**), the larger ring sizes produced anomalously low yields with this process. The access now to hydroxyl substituents on cucurbit[n]uril allowed for increasing solubility (in DMSO or DMF) and an easier functionalization to the parent compound. So for example it has been shown that **16** could be easily alkylated with an allyl halide or anhydride.

2.2.3   Analogues of cucurbit[n]uril *via* precursor modification

Another avenue of attack to improve the parent cucurbit[n]uril has been to completely change the structure and nature of the precursors. This has led to modification of the

overall cucurbit[n]uril structure that modifies its character. Research along these lines has given an insight into the process of synthesizing these toroidal structures.

Glycoluril (**2**) itself has been known for molecular recognition properties for some time (Figure 2.3).[24,25] The molecule of **2** formed as the backbone of one of the earlier molecular recognition tectons created by Rebek that could encircle up to two small guests.[26] They have also been investigated as building blocks for the construction of rigid host molecules designed to encapsulate both organic compounds and metals,[1] and to act as regioselective templates in crossed-Claisen condensations,[27] enzyme mimics,[28] and molecular clips.[29] The utility of **2** is in the rigidity of the structure, the angled surface resulting in an inner convex and outer concave region. While glycoluril itself is a well known for complexing guests such as small aromatic molecules,[26,30] the molecule itself has been little changed with further functionalization only occurring with methyl,[13] phenyl[31] or ester groups,[32] the majority of reactions occurring with the substitution of the proton atoms on the nitrogen atoms.

Produced from urea and 1,2-dione, diamino or diol compounds, a variety of glycoluril precursors have been formulated with an eye for supramolecular encapsulation including cucurbit[n]urils.[32,33] The investigation into cucurbituril analogues has shown that certain functional groups off the backbone of glycoluril have electron withdrawing capabilities that hinder the formation of cucurbit[n]uril analogues *via* destabilization of carbocation intermediates.[34]

A more mediated covalent approach has been to add the glycoluril units together in steps. Dimers of **2** have been the avenue in which to pursue these new cucurbit[n]uril analogues.[35] This research has to date been entirely conducted by the Isaacs group. Initial

research in 2002 by his group led to the realization of a mechanism for cucurbit[n]uril formation and an explanation for the difficulty in replacing the carbonyl oxygen atom with sulfur or amino moieties. Rather than a bystander to the reaction, the mechanism implicitly involves the carbonyl oxygen atoms in the intermediates between the parent glycoluril and the final cucurbit[n]uril. Replacement of the oxygen atom with a softer sulfur atom would result in differing chemistry and less likely binding between intermediates. An amino analogue at the carbonyl oxygen atom position would have difficulties in accepting a further proton and becoming $-NH_3^+$.

The dimers created by the Isaacs groups allow for a wide range of functional groups both off of the carbon backbone and the amine nitrogen atoms.[34] The dimers were shown to form in either a C- or S-shape with the former going on to form a cucurbit[n]uril while the latter would have to isomerize to the C-shape. Again it was realized by this group that considering the excellent yields of cucurbituril, then there must be facile rearrangement from S- to C-shape which would imply that the methine group connecting two molecules of **2** must not sterically hinder the transformation.

The dimers of glycoluril formed by the Isaac's group was an actual pursuit for something more ambitious; a step-wise approach to cucurbit[n]uril synthesis. Their synthesis was realized when they produced asymmetric analogues of cucurbit[n]uril, **17**, with aromatic spacers between some of the glycoluril units making up the ring (Figure 2.4).[36] The cucurbits as they have been called are more rectangular than ring shaped and due to the aromatic and other functional groups have differing properties to cucurbit[n]urils. The aromatic aspects of **17** were shown to produce fluorescence.[37] Both host and guest fluorescence was investigated while as a complex.

15
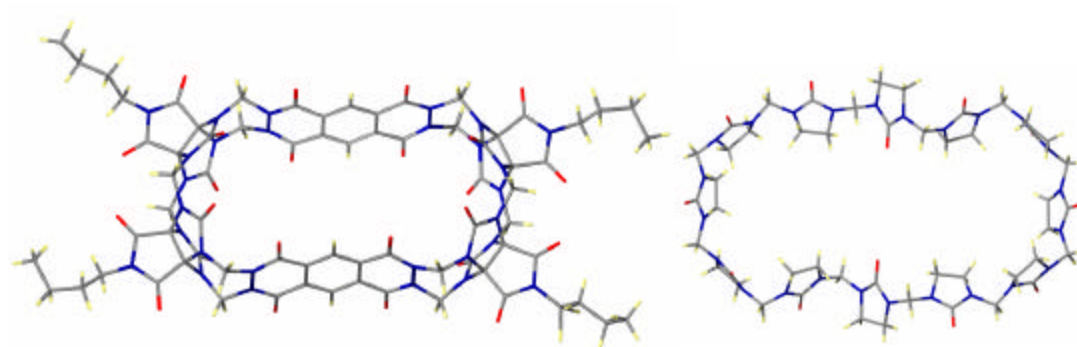
Figure 2.4. Crystal structures of cucurbit **17** (left) and hemicucurbit[12]uril **19** (right). **17** from Ref. 31, **19** from Ref. 33.

A more unusual approach was to split the glycoluril precursor in half.[38] Using ethylene urea it was possible to form hemicucurbit[6]uril, **18**. The macrocycle was quite floppy and the carbonyl head was found in all up or alternate position. These precursors also resulted in the largest characterized cucurbit[n]uril to date, the hemicucurbit[12]uril, **19** (Figure 2.4). These two analogues were soluble in organic solutions but could not take up metals, the preference going to small solvent or thiocyanate molecules. Also, water in the organic solutions would hydrogen bond to **19** leading to a figure of eight conformation, shrinking the cavity and further diminishing its utility for encapsulation.

To date, the only cucurbit[n]urils realized that don't have carbonyl portals have come from computational studies.[39] The investigation revealed the possibility of having sulfur atoms replace the oxygen carbonyl atoms. The computed structure was completely stable and showed promise for an opening up of cucurbit[n]uril chemistry. If the thio-cucurbit[n]urils could be successfully synthesized, metal-ligand tubes with soft metals such as mercury or gold linking adjacent cucurbit[6]uril could become a reality and further open up areas of chemistry.

2.2.4   Non-covalent constructs

After the characterization of cucurbit[6]uril (**1**), Mock and coworkers did a series of studies in regards to non-covalent encapsulation of guests.[11] They hit upon the fact that molecules with diamino substituents were tightly bound within the hydrophobic cavity, the nitrogen atoms sticking out of the portals and binding with the carbonyl oxygen atoms.[12] By increasing the length of the alkyl linker between the two amines it was deduced *via* NMR and binding studies that the facile complex formation between **1** and the diamines is an charge-dipole interaction between the protonated nitrogen atoms on the guest and the carbonyl oxygen atoms on the portals.

The most popular non-covalent construct of cucurbit[n]urils has been the production of pseudo-rotaxanes.[2] Pseudo-rotaxanes, ring structures that consist of at least one non-covalently bonded substructure (usually the guest) are structurally thought of as a way to create moving parts or an on/off switch (*via* a change in the environment) on a future nanomachine.[40]

In it's simplest form, Mock's studies of diaminoalkanes with cucurbit[6]uril constituted a fairly simple pseudo-rotaxane.[12] Generally this area of supramolecular chemistry has relied mostly but not entirely on **1**. The pseudo-rotaxanes are generally quite robust, in some cases even capable of being detected in the gas phase.[41] In other instances, platinum linkers, reminiscent of Fujita's panels,[42] have been used to form a large ring with three or four molecules of **1** entwined.[43] Changing transition metals has allowed for a variety of shapes to be formed from the pseudo-rotaxanes, including hexamers, linear chains, squares and helicies.[44] Adjusting the linker allows for structural modification of the overall supermolecule so for instance that the use of a L-shaped alkyl

amino chain allowed for a one dimensional square-shaped coordination pseudo-rotaxane.[45]

Other pseudo-rotaxanes of **1** have been attached to gold surfaces.[46] A thioalkyl chain with appropriate amino groups on the end was attached to the gold surface (Figure 2.5). In a solution of **1** and $[Fe(CN)_6]^{3-}$ it was shown *via* cyclic voltammetry that when the **1** was attached as a pseudo-rotaxane the iron was prevented from getting to the gold surface. These pseudo-rotaxanes were formed using pH as a control mechanism for possible future use as a biomarker. It was shown also that with addition of a guest with differing redox properties, longer chains could be built up from out of the gold surface using **1** as a linker.[47] This mechanism was shown to be quite general, it being also possible to thread **1** on when the amino alkyl chains was part of a polymer.[48]
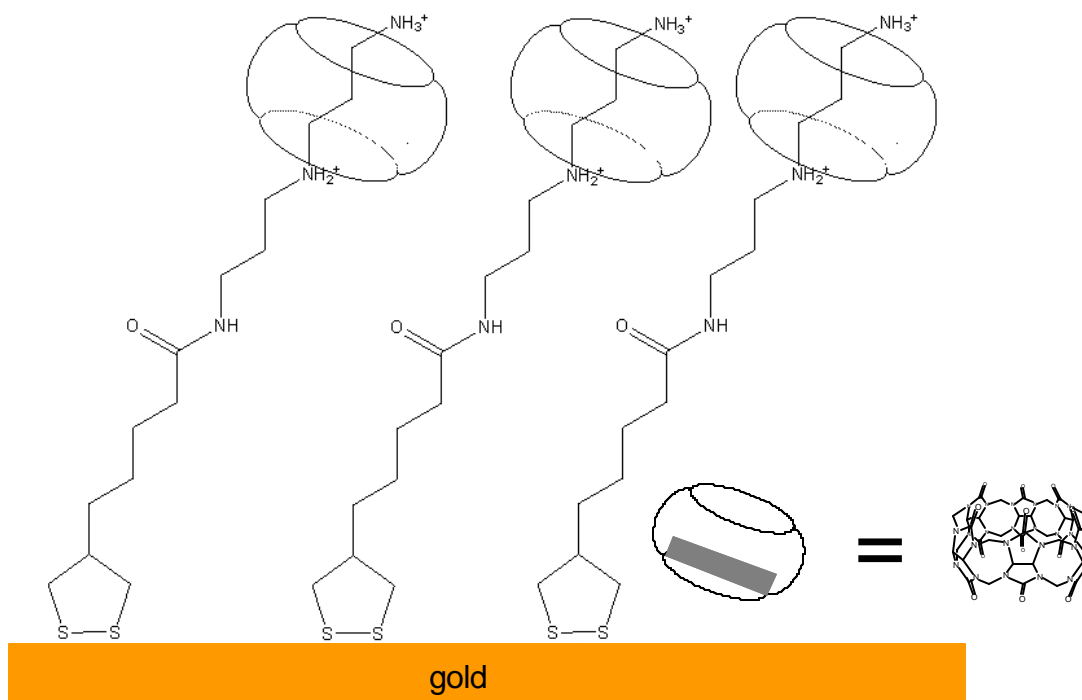
Figure 2.5. Pseudo-rotaxanes on gold such as this structure can have cucurbit[6]uril threaded and dethreaded depending on solvent conditions (from Ref. 46).

Another use of cucurbit[n]uril pseudo-rotaxanes was to form a much longer poly-rotaxane using the catalytic properties within the hydrophobic cavity of **1** (Scheme 2.2).[49] Two separate pseudo-rotaxanes were formed with "bulky" stoppers of protonated amines stopping movement of **1**. An extension of the amino groups on both sides where attached to one of two precursors capable of a 1,3-cycloaddition reaction.[50] Using the catalytic ability of **1** it was possible for the two separate pseudo-rotaxanes to covalently bind within the hydrophobic cavity of the macrocycle and so produce a polyrotaxane. The surprising aspect of this research was that the "bulky" stopper required for pseudo-rotaxane formation was nothing more than a protonated amine, it both attracting the carbonyl oxygen atoms of two adjacent cucurbit[n]urils and stopping its host from leaving coming off the alkyl chain.

Rotaxanes (like pseudo-rotaxanes but with covalently linked blocking molecules) of **1** were also examined for their association constants with cyclodextrins in solution.[51] **1** and a diaminoalkyl chain were used to form a pseudo-rotaxane and then the bulky aromatic groups benzene or naphthalene were added to form a rotaxane. The rotaxane was added to an aqueous solution of β-cyclodextrin and it was possible to determine the association constant for the whole system *via* the UV-Visible spectrum. This was the first instance of complex formation of cucurbituril rotaxanes that could be measured and the only published case of cyclodextrin and cucurbituril interaction.
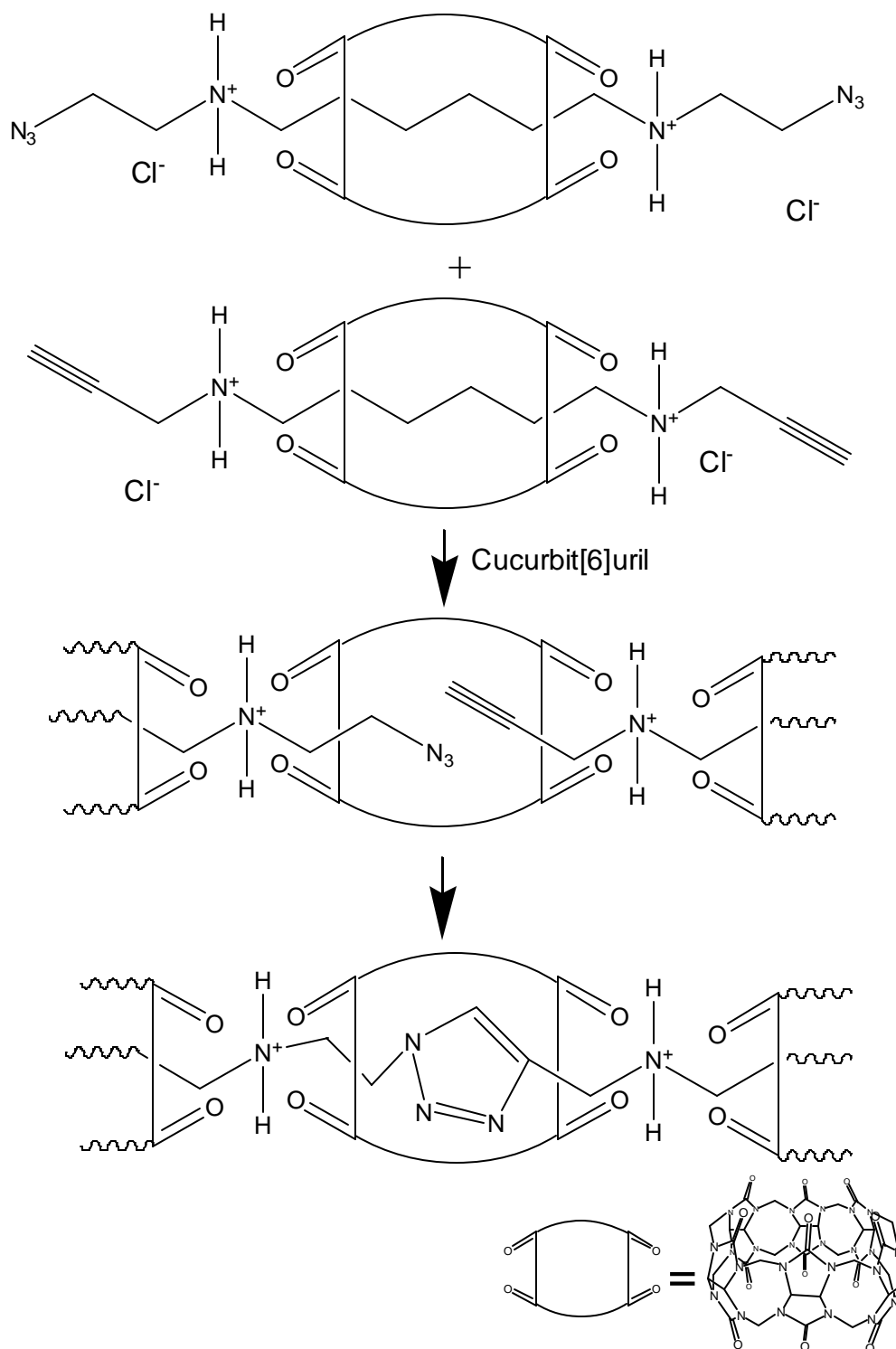
Scheme 2.2. Pseudorotaxane polymers are catalysed with cucurbit[6]uril from two smaller pseudorotaxanes of diamino alkylchains with cucurbit[6]uril and the appropriate precursor functionalities (from Ref. 49).

The molecule 4,4'-bipyridinium (viologen, **20,** Figure 2.6) is a common guest

molecule used in the literature for complexation within the cavity of cucurbit[n]urils.[52,53]

The nitrogen atoms of **20** are in the perfect position to coordinate with the carbonyl

portals of cucurbit[n]uril for ion-dipole bonding. An association constant between

cucurbit[7]uril (**7**) and **20** of 1.03 ± 0.03 x 10^5 L/mol is comparatively high in aqueous

solution and is attributed to both the ion-dipole interaction and the tight fit of the

aromatic groups. This affinity for viologens led to cucurbit[7]uril being non-covalently

bound to a dendrimer.[54] This dendrimer consisted of one of three successive generations

of carboxylic acid groups making up the dendrimer with the viologen moiety attached.

The dendrimer was then shown to non-covalently bind with cucurbit[7]uril *via* the

viologen. It was also shown that as a dendrimer-cucurbit[n]uril complex, DNA could be

entangled within to make a large aggregate capable of acting as a gene delivery vehicle.[55]
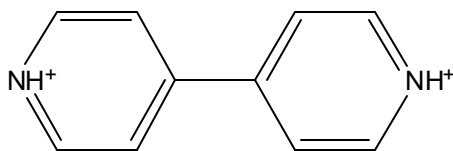
Figure 2.6. A common guest for cucurbituril is the molecule 4,4'-bipyridinium

(viologen, **20**).

By using a guest with a electron donating and electron accepting sections,

cucurbit[8]uril (**8**) has been shown to lock the guest into a position resulting in a charge

transfer complex.[56] Using a flexible molecule consisting of both **20** and naphthalene

connected together *via* a small, flexible alkyl chain it was shown by both color change

(from colorless to violet) and by proton NMR that the molecule had gone from being

linear to doubled over itself within the internal cavity of **8**, something unlikely to occur in

solution. A similar redox system was used to create a photochemical redox cascade system with ruthenium bypyridine.[57]

Dihydroxynaphthalene and analogues of **20** unattached by an alkyl chain this time were also found to form large vesicles with **8** (Scheme 2.3).[58] The redox properties of the two could be controlled, leading to both guests leaving **8** and disrupting the vesicles. By attaching alkyl chains directly to the cucurbit[n]uril, the Kim's group has also managed to form vesicles though the mechanism by which they form is still unclear.[59] By rigidly locking an angled, fixed spacer between the electron donating and electron accepting molecules, it is possible to form a molecular necklace with **8**.[60] Using **8**, the supermolecule was a pentameric ring with five each of cucurbit[8]uril and guest.

R= -CH$_3$,-(CH$_2$)$_{11}$CH$_3$,-(CH$_2$)$_{15}$CH$_3$,
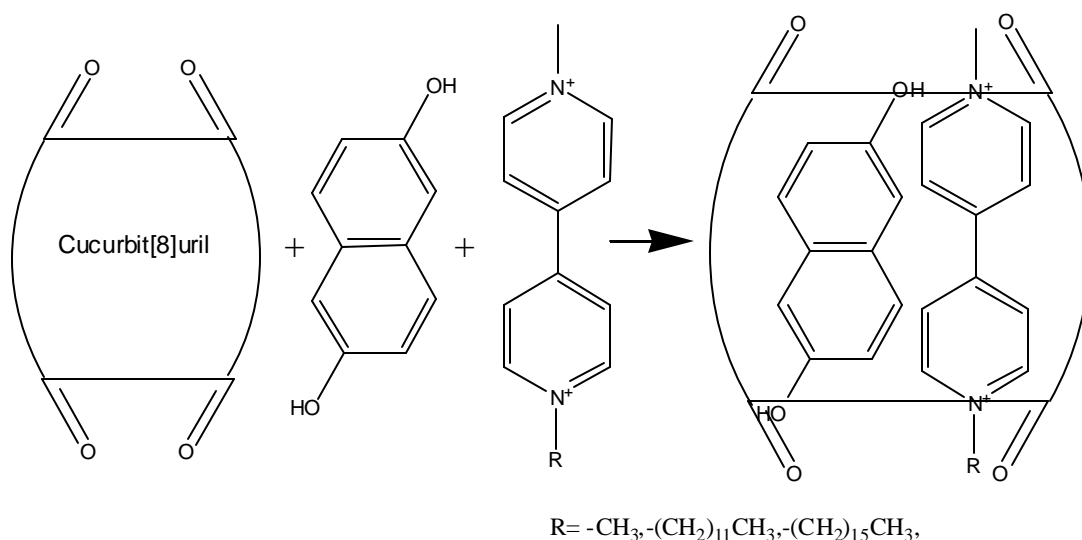
Scheme 2.3. The ternary complex of cucurbit[8]uril, alkylviologens and dihydroxynaphthalene produce large vesicles (Ref. 58).

Using the analogous methylviologen and **8**, it was discovered that redox chemistry could be used to tune the host:guest stoichiometry.[61] Reduction of the cationic guest to a radical moved the methylviologen from one molecule of **8** to another and complex within

22

the cavity with another methylviologen. To the authors this appeared to be the first case of a host:guest complex being controlled by redox chemistry.

Cucurbit[7]uril (**7**) has also been shown to shield sensitive compounds from isomerization (Scheme 2.4).[62] *Cis*-stilbene with the cavity of **7** has been shown to have a reduced tendency to transform to the *trans*-isomer. Normally at room temperature *cis*- to *trans*- isomerism occurs relatively quickly yet NMR studies showed the *cis*-isomer remained unchanged after one month with **7** present. The cavity of **8** was also used to stabilize a tetrathiafulvalene cation radical dimer at room temperature, unheard of previously except at very low temperatures.[63]
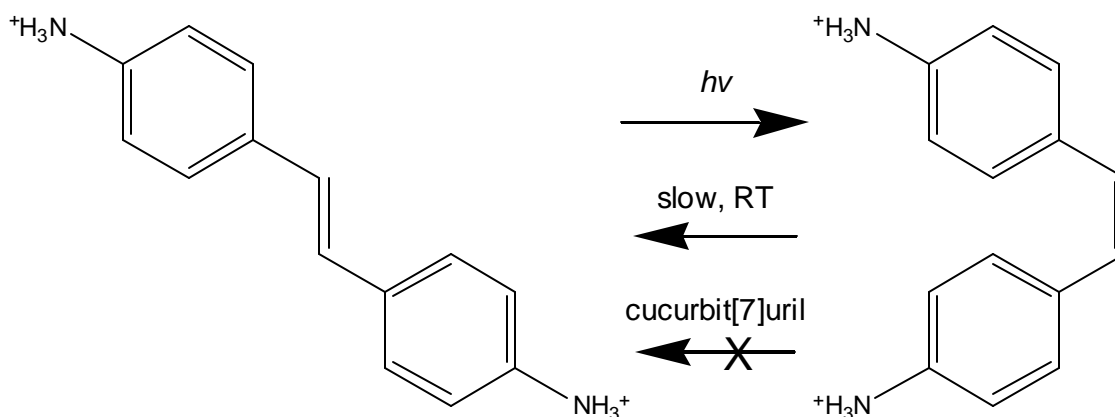
Scheme 2.4.. Cis-stilbene will slowly return to trans-stilbene but will remain indefinitely in the cis- position in the presence of cucurbit[7]uril.

The ammonium cation, a byproduct of cucurbit[n]uril formation seen as a decomposition product of the synthesis has also been deliberately introduced as the salt NH_4Cl.[3] This guest has led to some misunderstanding with characterization of cucurbit[n]uril, especially with cucurbit[5]uril in the early years of its discovery. The ammonium cation hindered encapsulation of other molecules but was also found to be act somewhat usefully as a lid for cucurbit[5]uril. The ammonium ion lies in the portals of

this smallest of cucurbit[n]urils and when removed, the opening of the macrocycle allows for the selective entrapment of gases such as carbon dioxide and NO_x. The ammonium lids have been shown to keep the gases and small solvent molecules within the cavity for much longer than without them.[14] Neutral gases such as xenon also had some affinity for the cavity.[64]

One of the more unusual supramolecular structures occurred when *o*-carborane was added to the precursors of cucurbit[n]uril to see if it could act as template.[4] Surprisingly, the resulting mixture of cucurbit[n]urils also produced *o*-carborane within cucurbit[7]uril. The fit was tight enough such that *o*-carboranes could not be released and this supramolecular construct was promoted as a molecular ball-bearing. Another spherical molecule which has been shown to interact with **7** was fullerene C_{60}. A complex of cucurbit[7]uril:fullerene C_{60} was shown to have been formed through ball-milling or in solution.[65] The ratio of cucurbit[7]uril to fullerene could be controlled between 2:1 to 1:2 depending on the conditions used.

Finally another macrocycle, cyclam, has also been inserted into **8**.[66] This "macrocycle within macrocycle" was able to coordinate to copper or zinc ions.

2.2.5   Metal-ligand compounds

The large electronegative portals above and below the bulk of cucurbit[n]uril makes it a natural for metal binding. Size discrimination has been shown, with metals binding from one to six carbonyl portals depending on charge and the metal's atomic radius. As per much of the extended chemistry of cucurbit[n]urils much of this research has focused on cucurbit[6]uril (**1**).

Alkali metals have been used extensively for coordinate with cucurbit[n]uril. Sodium[67] and potassium[68] are too small to form with all the carbonyl functional groups of **1**. Two each of these metal atoms bind to a portal. Cesium is used to solubilize cucurbit[n]uril complexes such that mass spectrometry information can be obtained[69]. This metal appears to be large enough to cover the portal, requiring only one cesium atom to bind to **1**; it is positioned squarely in the center of the portal. Rubidium too forms two atoms per portal and produces the most interesting and potentially useful structure (Figure 2.7).[70] The solid state structure has large 10 Å voids between rows of columnar rubidium cucurbit[6]uril complexes and looking down the c axis of the crystal produces a hollow honeycomb pattern.
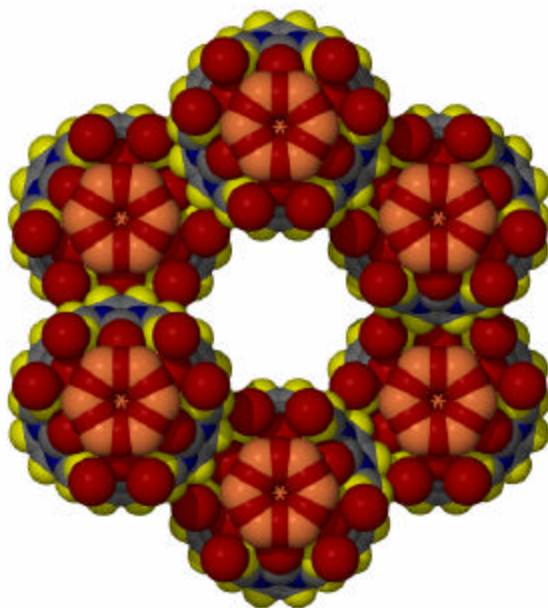
Figure   2.7.   Catena-((μ6-Cucurbit[6]uril)-bis(μ2-hydroxo)-(μ2-methanol)-aqua-rubidium heptadecahydrate). This arrangement of rubidium and cucurbit[6]uril forms water channels of 10 Å diameter. (Rubidium and attached water is disordered over 3 positions, water in cavity not shown for clarity. Rubidium = orange, carbon = grey, hydrogen = yellow, oxygen = red, nitrogen = blue).

Calcium can form a direct complex with two molecules of **1**, coordinating with one and two carbonyls of adjacent macrocycles, the portal able to accommodate two calcium atoms.[71] This was an isomer of the original structure discovered by Mock and coworkers that finally confirmed the structure of **1**.[1] The larger strontium atom has one of the higher binding constants with **1** among metals of the first two columns of the periodic table.[72] It is also one of the few metals to be examined with two different cucurbit[n]urils, cucurbit[6]uril and cucurbit[8]uril (**8**).[73] While in both structures the cucurbit[n]urils where found to bind to two strontium atoms per portal, **1** produced an angled coordination polymer with the metals and **8** resulting in a more columnar looking structure.

Trans-[InCl$_2$.(H$_2$O)$_4$]$^+$ and *trans*-[InCl$_4$.(H$_2$O)$_2$]$^-$ produces channels of **1**, the metal chloride lying in the interstitial spaces between the cucurbit[n]urils.[74] The symmetry for the channels was the highest possible for a cucurbit[n]uril system, D_{6h}. Tungsten and molybdenum, like sodium or cesium, has been used to act as a lid on the portals of **1**.[75] The lid can be on either one or both sides of the macrocycle and protects a pyridine within the cavity as shown by single crystal x-ray diffraction. A chalcogenide-bridged cluster, [Cl$_3$InW$_3$S$_4$(H$_2$O)$_9$]$^{2+}$, also acted as lids for **1**.[76]

In one of the more complex structures initiated with cucurbit[6]uril, one dimensional columns of cucurbit[6]uril with sodium chloride where turned to helical structures *via* anion exchange with aromatic copper complexes and the association with iodine (Figure 2.8)[77] Depending on the aromatic ligand it was discovered that chiral or meso-helices could be produced. Helices have also been formed using silver aromatic guests for cucurbit[6]uril.[78]
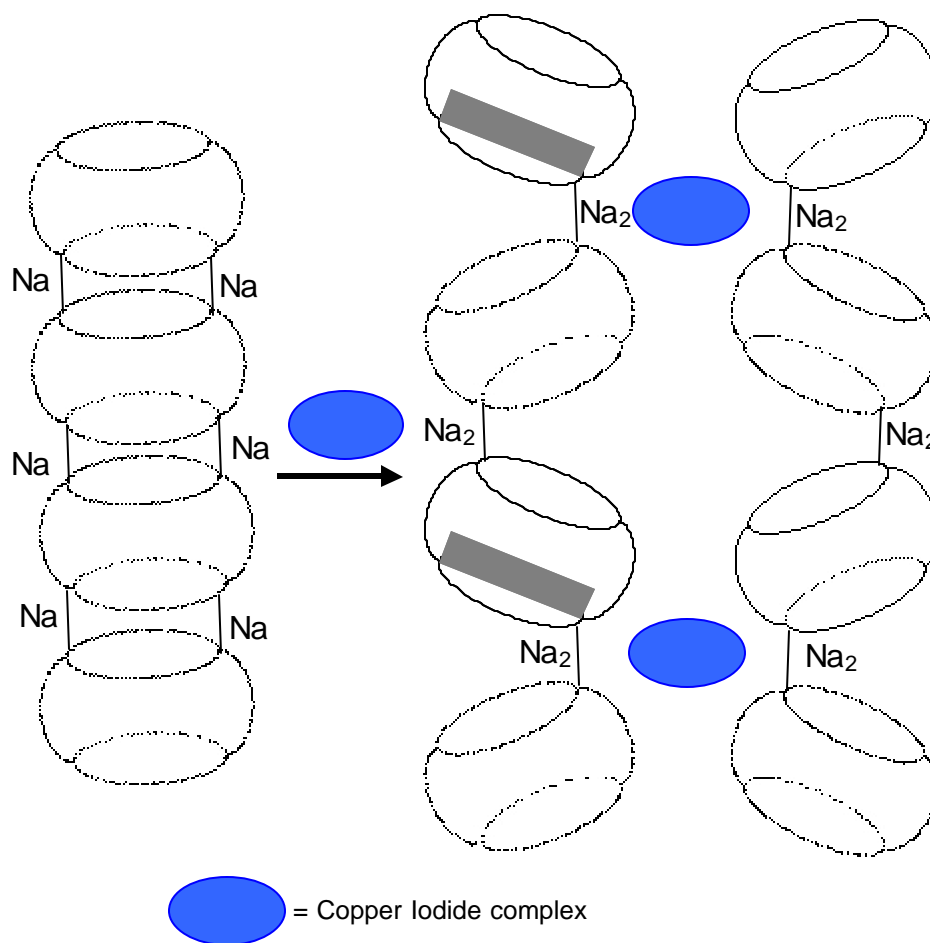
Figure 2.8. With the addition of a copper iodine anion exchange agent Na$_2$.cucurbit[6]uril changes from a columnar to a helical structure.

Lanthanides have been shown to form a range of structures with **1**. For example with gadolinium, the portal is taken up by a complexed gadolinium nitrate and water.[79] The overall structure is bidentate with the adjacent **1**. At the extreme of atomic radii, the actinides have been shown to not fit into or near the portal of cucurbit[n]uril at least in the case of uranium.[80] Rather water molecules are required to interface between the open portals of the cucurbit[n]uril and the large metals.

2.3 Synthesis of Cucurbit[n]uril analogues

2.3.1 Retrosynthetic analysis to functionalize cucurbit[n]uril.

This project began in 2000 with the search for analogues of cucurbit[n]uril that would improve on its solubility characteristics. The hypothesis was that the functionalization of cucurbit[n]urils would lead to enhanced solubility. Retrosynthetically, the avenue of attack to create analogues came from two directions (Scheme 2.5):
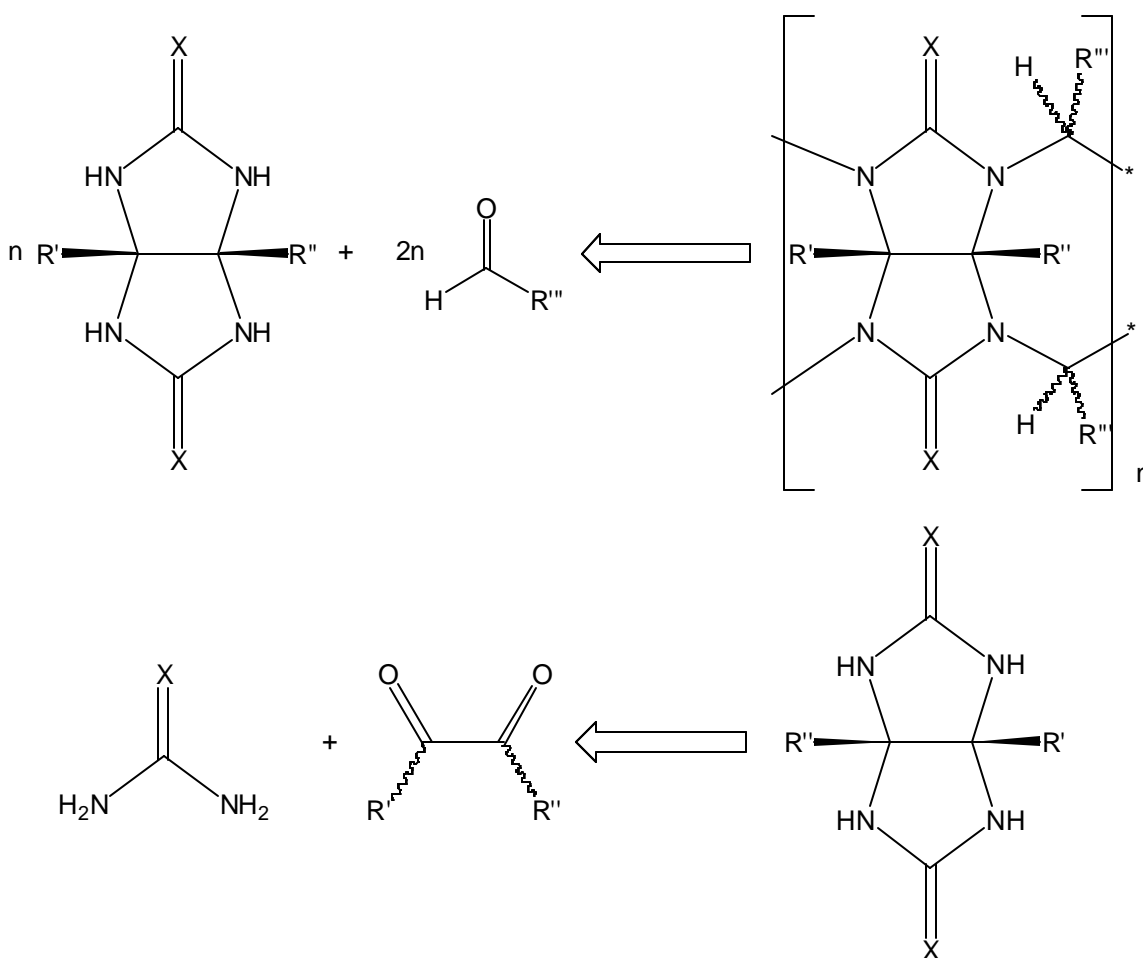
Scheme 2.5. Retrosynthetic analysis for cucurbit[n]uril analogue synthesis.

In particular, by adding alkyl chains to the structure it would be possible to improve the solubility of the compound in organic solvents. Conversely functionalizing with ionic

or sulfonated functional groups would improve the solubility of cucurbit[n]urils in aqueous solutions.

Formaldehyde is a useful precursor in that its small size and reactivity has allowed it to be one of the more common substrates for macrocycle synthesis as for example the calix[n]arenes discussed in the next chapter.[15] However the hypothesis was that by using larger, functionalized aldehydes it would be possible to change the properties of the resultant cucurbit[n]uril (Scheme 2.6). Given the steric constraints imposed by the larger R group, this would lead to a symmetrical structure with the larger group (orange, Scheme 2.6) in the axial positions and the hydrogen atoms (yellow, Scheme 2.3) in the equatorial position.
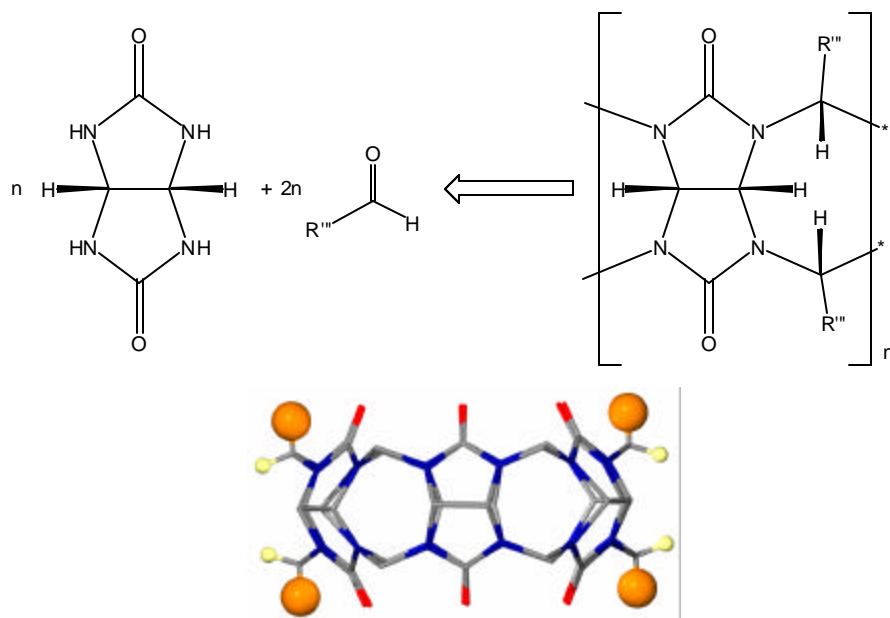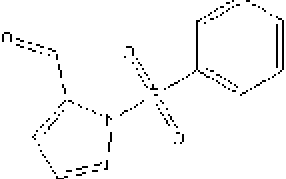
Scheme 2.6. Visualization of hypothesis for using different aldehydes. Due to steric constraints it was thought that the protons (yellow) will be equatorial and the larger R''' (orange) groups in axial positions to reduce steric hindrance. Other hydrogen atoms not shown for clarity.
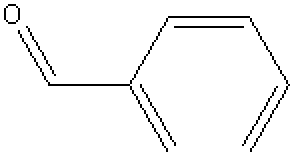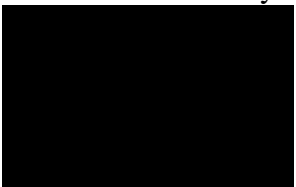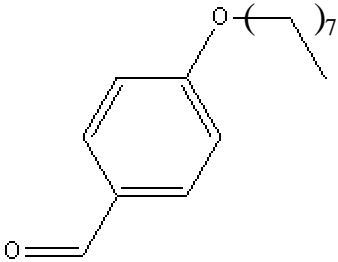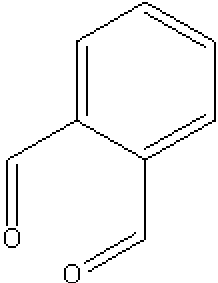
The other major constituent that could be changed in regards to the precursors is the glycoluril moiety. The parent molecule **2** is itself synthesized *via* the reaction of urea with glyoxal. One of the problems associated with the synthesis of glycolurils is their limited solubility in normal organic and/or polar solvents.[74] Functionalization of the glycoluril at one or both of the carbonyls, or at the nitrogen positions, has been investigated with mixed results.[81] Using retrosynthetic analysis this molecular clip could have synthesized analogues either by substituting the urea or the glyoxal for a molecule with more useful functionality (Scheme 2.2).
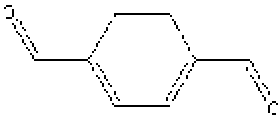
2.3.2   Using formaldehyde analogues to improves solubility

At this stage of the PhD project it was envisioned to examine both precursors by adjusting all three of these molecules in a step-wise fashion. Initially attempted synthesizes of cucurbiturils using different aldehydes was performed (Table 2.2):

Table 2.2. Aldehydes and outcome of reactions with glycoluril

	Aldehyde	Expected R''' group	Outcome
21	2-furaldehyde	-furan	Decomposition
22	1-(phenylsulfonyl)-2-pyrrole carboxaldehyde	-1-(phenylsulfonyl)-1H-pyrrole	Decomposition of aldehyde

	Aldehyde	Expected R'" group	Outcome
23			
	acetaldehyde	-methyl	Polymerization of aldehyde
24	benzaldehyde	-phenyl	No reaction
25	2-formylbenzenesulphonic acid, sodium salt hydrate	-sodium benzenesulfonate hydrate	No reaction
		-1-(octyloxy) benzene	
26	4-octyloxybenzaldehyde		No reaction
27	phthalic dicarboxyaldehyde	-phthalaldehyde-	No reaction

	Aldehyde	Expected R''' group	Outcome
28	benzene-1,4-dicarboxaldehyde	-1,4-benzene-	No reaction
29	glutaric dialdehyde	-1,3-butane-	Polymerization of aldehyde

The aldehydes were chosen for various reasons. **21**, **22** and **25** were chosen due to their hydrogen bonding abilities with the idea that they would make the resulting cucurbituril soluble in aqueous solutions. **23, 24** and **26** were chosen for the opposite reason in that their lipophilic aromatic and alkyl groups would allow the cucurbituril to have improved solubility in organic solvents. Precursors **27** – **29** were chosen for determination into whether cucurbiturils could have further cross bonding within the toroid and the addition of aromatic moieties to improve organic solvent solubilities.

The reactions as a group were rather unsuccessful. Two of the compounds (**23**, **29**) seem to go for preferential polymerization rather than form aminal bonds with glycoluril.[82,83] Another two reactions (**21**, **22**) seemed to decompose completely and the reaction mixture was returned as a black carbonaceous looking substance, only the glycoluril moiety recognizable by ^{1}H NMR. The others appeared to produce no reaction even in by varying the acid reaction medium.

Approximately the time this research was being conducted Day and coworkers released their theory on cucurbit[n]uril formation.[84] It is their belief that formaldehyde condenses onto all the amines of the glycoluril (Scheme 2.7). The formaldehyde then

becomes methoxy functionalities off the amine or the formaldehyde may link to another amine on the same glycoluril moiety leading to a cyclic ether.

They believed that condensation of formaldehyde occurred at all nitrogen atoms on the glycoluril. This intermediate step, with two methoxy moieties so close to each other would seem to preclude any larger R''' group than formaldehyde on the grounds of steric hindrance.
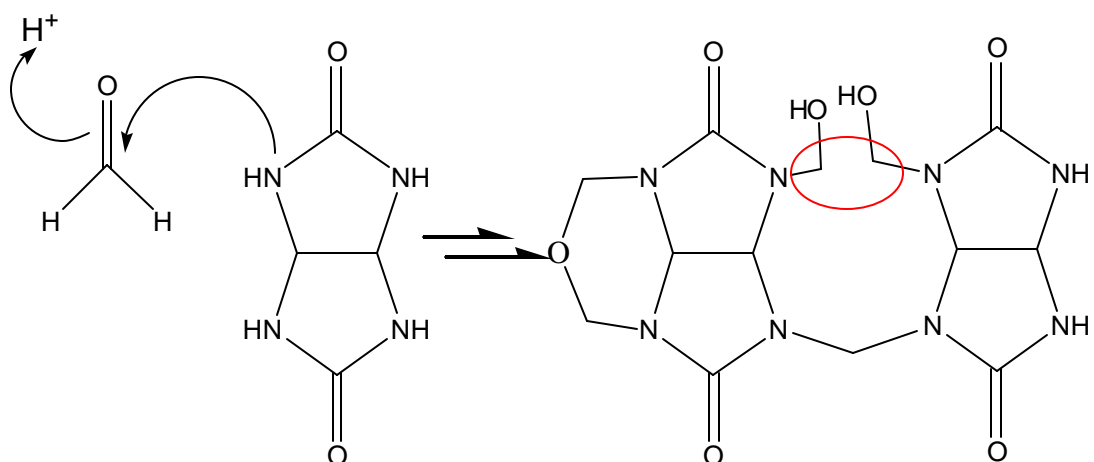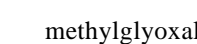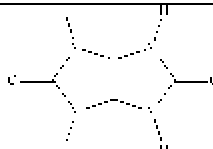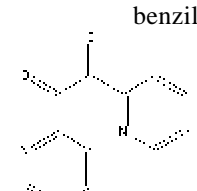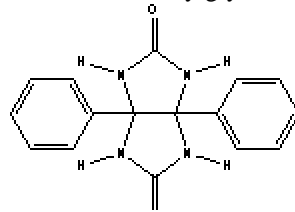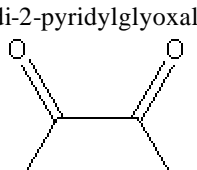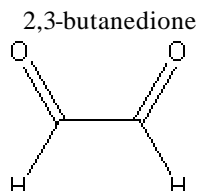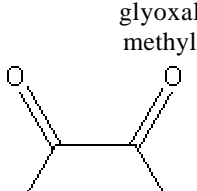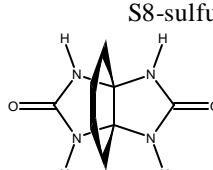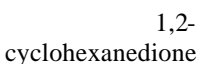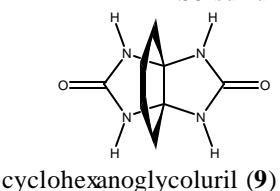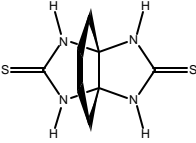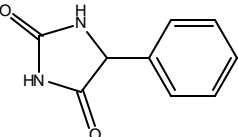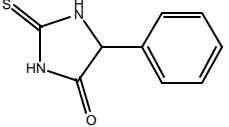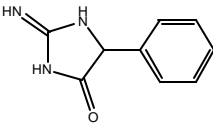
Scheme 2.7. Key step in cucurbituril formation from Day *et al.* (Ref. 84) that would imply difficulties in attaching aldehyde with large R''' group due to steric hindrance (circled in red).

2.3.3   Derivatives of glycoluril explored

Glycoluril analogue synthesis proceeded more smoothly than aldehyde substitution though some unexpected side reactions occurred. Again a range of glycolurils were synthesized and characterized (Table 2.3):

Table 2.3. Precursors, expected and actual products formed for glycoluril analogues

Precursor	"Urea" molecule	Product	Expected Product
methylglyoxal	urea	methylglyoxal ...	methylglycoluril
benzil	urea	diphenylglycoluril (**12**)	diphenylglycoluril
di-2-pyridylglyoxal	urea	decomposed	dipyridineglycoluril
2,3-butanedione	urea	decomposed	dimethylglycoluril
glyoxal	thiourea	unreacted	thioglycoluril
methyl glyoxal	thiourea	S8-sulfur	methylthioglycoluril
1,2-cyclohexanedione	urea	cyclohexanoglycoluril (**9**)	cyclohexanoglycoluril

Precursor	"Urea" molecule	Product	Expected Product
1,2-cyclohexanedione	thiourea	cyclohexanothioglycoluril	cyclohexanothioglycoluril
phenylglyoxal	urea	5-phenyl-imidazolidine-2,4-dione	phenylglycoluril
phenylglyoxal	thiourea	5-phenyl-2-thioxo-imidazolidin-4-one	phenylthioglycoluril
phenylglyoxal	guanidine hydrochloride	2-imino-5-phenylimidazolidin-4-one	phenylaminoglycoluril

In various cases the requisite condensation occurred and the glycoluril was formed. So for **30**, **31**, **36** and **37** glycolurils were formed from a simple condensation reaction. It should be noted though that with thiourea instead of urea the yield of **37** was low (26%). It appeared that thiourea was not as robust as urea so for instance in the case of **35** crystals of the sulphur polymorph S_8 appeared to be the dominant product; not exactly the most efficient way to produce such a compound!

2.3.4   Unexpected formation of hydantoins

Though unexpected, potentially more useful was the formation of hydantoins (**38** – **40**, Scheme 2.8). Hydantoins are the common name of a wide and varied class of compounds called imidazolidin-4-ones that feature in many areas of science and their derivatives have medical applications. The earliest known imidazolidin-4-one,

synthesized in 1938, is the active ingredient of the commercial compound Dilantin (5,5-diphenyl-hydantoin) which has antiepileptic activity.[85] The urea moiety of this hydantoin has been implicated in its biological activity. Derivatives of hydantoins have activity over a wide range of ailments from antiarrhymthmia[86] to anticonvulsant activity[87] and even the ability to stop cell division.[88] In addition, they show fungicidal and herbicidal activity, either created synthetically[89] or by nature.[90]
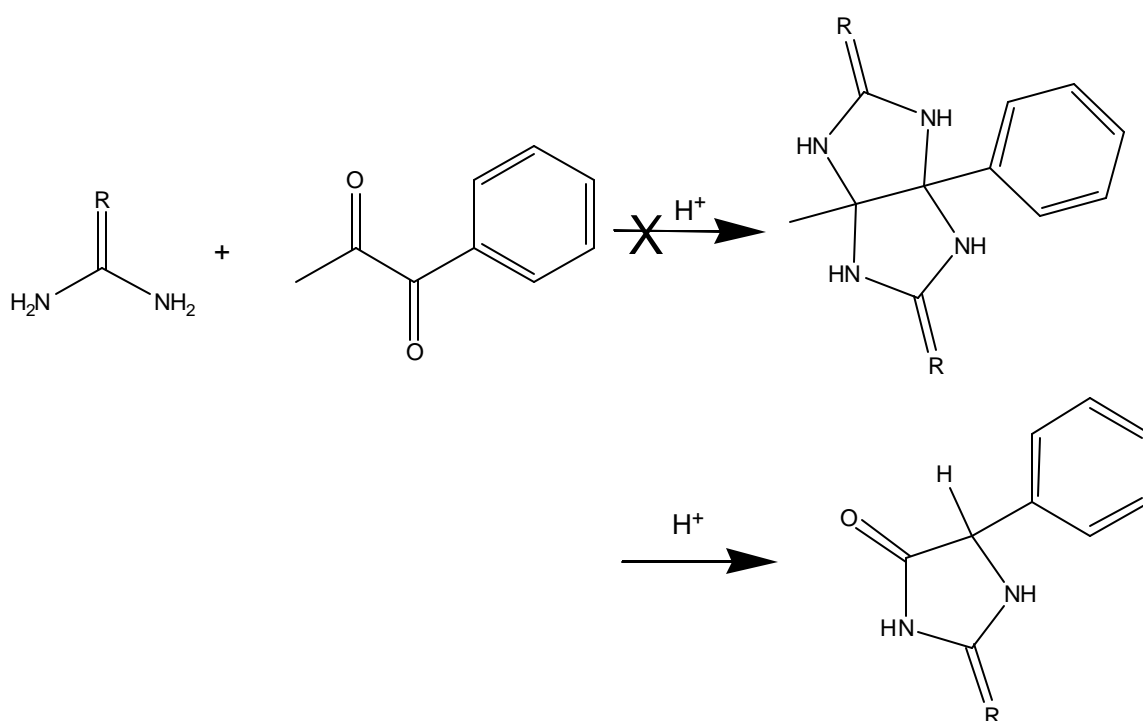
Scheme 2.8. Unexpected reaction of **38** – **40** resulted in only one urea or urea-like molecule reacting with phenylglyoxal to form a hydantoin (R = O, S, NH).

The formation of 5-aryl-hydantoins has been of interest in their use as precursors to the synthesis of peptides and amino acids,[91] especially δ-arylglycines.[92] Their synthesis usually involves strong organic acids[93,94] and/or toxic cyanide precursors.[95,96] While there are many synthetic methods for the production of such compounds, there is no literature method involving reaction of phenylglyoxal in the formation of phenylhydantoins. The condensation reactions conducted in the search for glycolurils analogues have allowed us

36

to find that for phenylglyoxal, not only is 5-phenyl-hydantoin, **38**, and 5-phenyl-2-thiohydantoin, **39**, formed but also that this synthesis allows for the formation of the newly discovered analogue 5-phenyl-2-iminohydantoin, **40**. By using an approach that avoids using organic solvents we have shown that there is a minimization of the amount of toxic waste generated and overall develop a more benign, green, protocol. This is then more likely to lead to down stream applications.

Trifluroacetic acid (TFA) is soluble in both organic and polar solvents and was used to initiate the condensation of the two substrates. The use of catalytic amounts of TFA involving slow addition and monitoring the pH is a more benign alternative than traditional methods where quantitative amounts have been used to condense urea and urea-type molecules with glyoxals.[81]

In recent papers the synthesis of hydantoins *via* the 'green' technique of microwave irradiation has emerged.[97,98] The use of water, as a benign solvent, rather than more commonly used organic solvents such as toluene or benzene has minimal effect on the yields of all hydantoins (Table 2.4), and indeed for **37** it was beneficial with an approximate 12% increase in yield. The results also show that the similarity in the yields for **39** mean that organic solvents are unnecessary and the use of cheaper water is more economical as well as more benign.

Table 2.4. Yields of each product using different solvents

| | Yield (%) | | |
	Water	Toluene	Benzene
37	71	59	36
38	52	54	52
39	77	70	75

Comparison of adding catalytic amount (3 or 4 drops) of the acid versus a quantitative amount (approximately 10 mL) resulted in the same yields for the products. Due to the low boiling point of trifluroacetic acid (boiling point = 74 °C) it is easy to retrieve the desired product *via* evaporation of the acid and solvent. This is a lot simpler than the practical inconvenience of removing large amounts of organic acids *via* neutralization with base that is prevalent with other traditional methods.

Surprisingly the solid state structures of the three hydantoins which in a search of the literature[99-104] and CSD[105,106] have not been established despite the importance of such compounds.

All three compounds were readily recrystallized from water, methanol or ethanol and single crystals suitable for x-ray diffraction were deposited over one week (diffraction data in Experimental section at end of chapter). All three compounds form in the solid state as layered structures that form one-dimensional sheets *via* hydrogen bonding between carbonyl and amino groups in a plane but not perpendicular to the sheets. This is where the similarities end for the change in substituent has quite a varied effect on the arrangement.

In **38**, sheet formation involves hydrogen bonding (Figure 2.9). Extensive bonding between the water of crystallization acts as the 'glue' between opposing sides of each layer of **38** while adjacent molecules also network *via* hydrogen bonding between both nitrogen and carbonyl oxygen centers. Furthermore, each sheet interacts via the phenyl groups. Adjacent sheets non-covalently bonds with the sheet above and below in a herring-bone formation.
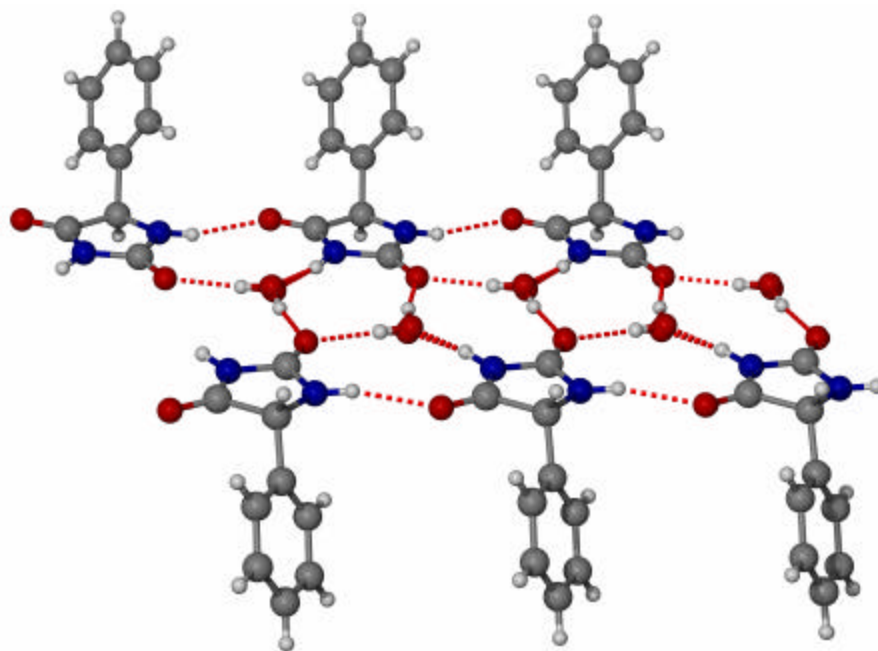
Figure 2.9. The multiple hydrogen bonding arrangement between water and **38** resulting in a ribbon-like structure (Carbon = grey, hydrogen = white, oxygen = red, nitrogen = blue).

It was found that with compound **39** the larger thionyl groups precluded any solvent from interacting with the hydantoin. Instead, a straight non-covalent dimerization occurs between two of the molecules (Figure 2.10). There is no interaction between the dimers and other molecules of **39** parallel or perpendicular in the solid state, leading to each residing adjacent to each other. The lack of such non-covalent interactions in **39,** in contrast to both **38** and **40,** leads to the phenyl group being capable of more rotational mobility which is manifested in them being disordered over two positions involving a rotation around the principle axis of the phenyl ring of 47°. Despite this disorder, the packing structure for the rest of the molecule remains unchanged.
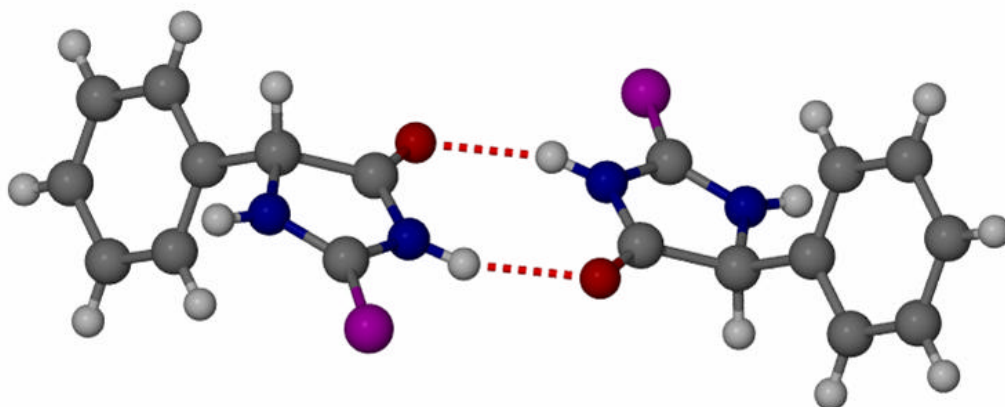
Figure 2.10. Non-covalent dimerization between two molecules of **39**. Phenyl rings shown are from one of two disordered positions (Atom colors as per Figure 2.5 plus sulfur = purple).

In contrast for compound **40**, there are substantially more opportunities for hydrogen bonding, and the compound co-crystallized with trifluroacetic acid. The trifluroacetic acid moiety acts as a blocker for what would have resulted in more extensive hydrogen bonding between amino and carbonyl groups on adjacent molecules of **40**. As such, the hydrogen bonding network only occurs once between each hydantoin and once between a hydantoin and the trifluroacetic substrate.

The extended structure consists of one-dimensional, hydrogen-bonded ribbons (Figure 2.11). Each ribbon contains the repeating unit of both **40** and trifluoroacetate in a 1:1 ratio, and the molecules are tethered to one another by hydrogen bonds, four of which are crystallographically unique. Neighboring molecules of **40** are directly linked to one another via an intermolecular N-H•••O hydrogen bond. These molecules are also indirectly linked by hydrogen bonds to the acid group of the anion, the parent hydantoin being the cation due to the protonated imine. The amino group shares a proton to hydrogen bond with the oxygen of another trifluoroacetate anion within the ribbon.
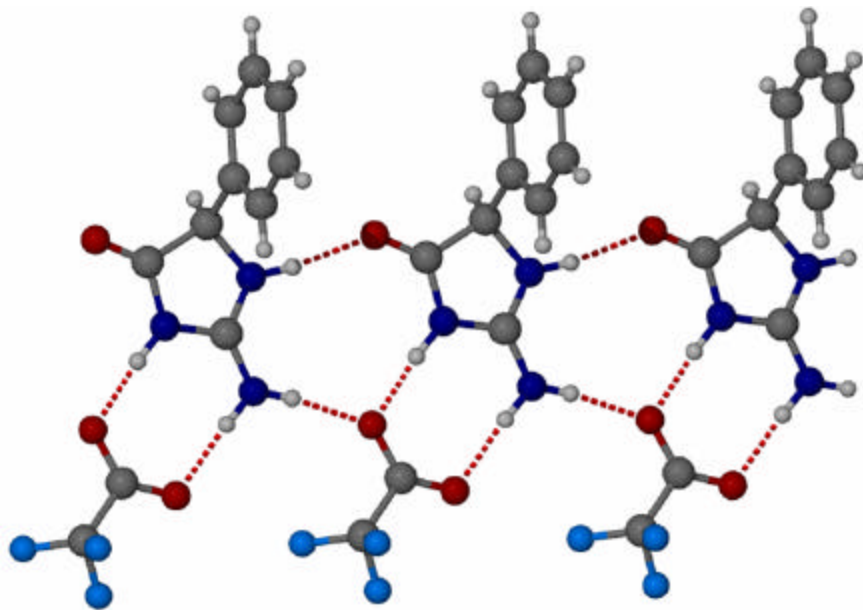
Figure 2.11. View of the one-dimensional, hydrogen bonded ribbon structure of **40** (Atom colors as per Figure 2.5 with fluorine = blue).

An extended study of the inter-hydantoin interplay afforded intriguing results. Surprisingly when attemps to co-crystallize with other hydantoins **38** or **40**, 5-phenyl-2-thiohydantoin dimerizes to form **41**, 4,4'-Diphenyl-2,2'-dithioxo-[4,4']biimidazolidinyl-5,5'-dione (Figure 2.12, Table 2.5). This compound was further characterized by ^{1}H, ^{13}C, and DEPT NMR. A further NMR study of **39** that had been left in storage for six months showed that the dimerization was also occurring at very slow rate with a small but characteristic peak at 73 ppm on the ^{13}C NMR spectrum. This is assigned to the carbon where dimerization occurs as the peak disappears on the DEPT NMR spectra. Initial NMR of compound **39** at the time of reaction shows no sign of **41** being present. ^{1}H NMR shows that the yield of **41** formed via dimerization of **39** is 13% after six months.

Table 2.5. Solid state Structure from solution[a] of ratio's of hydantoins.

Hydantoins	Ratio 1:3	Ratio 1:1	Ratio 3:1
38:39	41	41	41
38:40	40	38	38
39:40	41	41	39

[a] Solvent: 1:1 Methanol: Ethanol
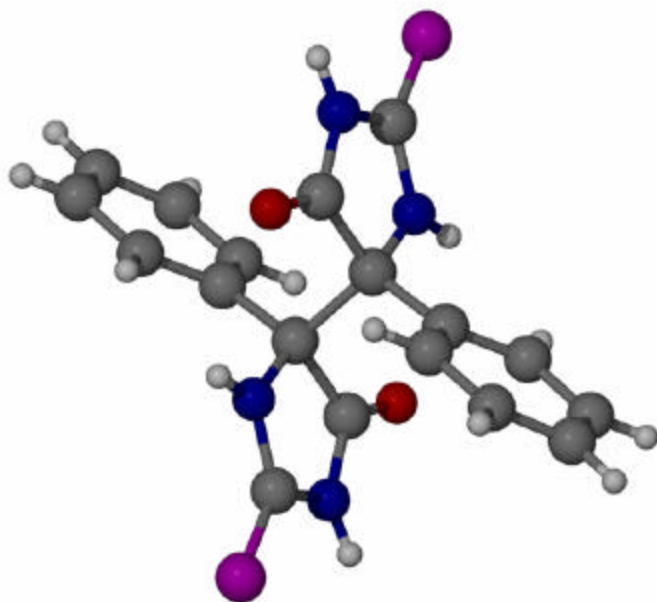
Figure 2.12. A single molecule of **41** showing dimerization at the carbon connecting the phenyl group to the hydantoin moiety (Carbon = grey, hydrogen = white, oxygen = red, nitrogen = blue, sulfur = purple).

This compound had been alluded to being formed previously after some controversy over the characterisation of the compound.[107] Even as a minority component in the solution, **39** or **41** preferentially crystallizes from solution over crystallisation of **38** or **40**. However in a solution of just the monomer, only **39** crystallizes out. The other hydantoins must be accelerating the formation of **41** as witnessed by the crystallisation of the thio derivative undimerized when on its own or with a small amount of the imino derivative in

solution. No evidence has been found for the dimerization of **38** or **40** under similar conditions.

In solution, the lone pair of electrons from either oxygen or nitrogen from any of the monomers can attack the acidic proton of **39**. This proton is acidic due to well known tautomerism between the α carbon and the carbonyl group.[108] Due to the lower electronegativity of sulphur versus nitrogen or oxygen,[109] it appears from the co-crystallization results that the lone pair of electrons on the oxygen atom of **38** or imino nitrogen atom of **40** is responsible for abstracting the proton. Removal of the proton at this position could then lead to dimerization. The molecule might then undergo some radical rearrangement that allows for dimerization to take place, possibly *via* some modification of the Gomberg reaction.[110] On the other hand, it is possible that through the conjugated network of the **39** the carbon may become comparatively positive allowing for an attack by a protonless negatively charged molecule of **39**.

The extended structure for **41** is a similar one-dimensional ribbon (Figure 2.13) as per **38** and **40**. However, the dimers act as hydrogen bond acceptors on opposite sides of the molecule. Due to the bulkiness of **41**, alternate molecules form hydrogen bonds *via* the oxygen atoms while the next molecule along hydrogen bonds involves nitrogen atoms. For each row, adjacent rows are tied packed together by π…π stacking at 4.4 Å distance in a face-to-face motif.
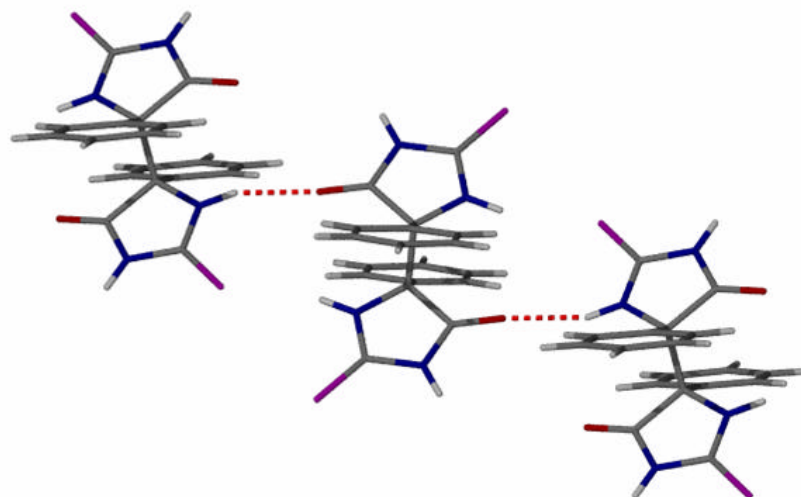
Figure 2.13. The staircase formation of **41** showing alternate nitrogen/oxygen hydrogen bonding arrangement between each molecule ((Carbon = grey, hydrogen = white, oxygen = red, nitrogen = blue, sulfur = purple).

2.3.5 Successful glycoluril formation

Synthesis of the two cyclohexanedione derived glycolurils (**36**, **37**) resulted in two novel structures (Figure 2.14). The former had been synthesized and it seems forgotten about since its production in the former Soviet Union.[111] The structure has a typical carbonyl-oxygen bond distance of 1.24 Å found in the parent glycoluril. However, the cyclohexane section of the molecule has closed the bite angle to 110° from 121° for glycoluril. Like the hydantoins, extensive hydrogen bonding occurs throughout the crystal structure (Figure 2.15). Each oxygen atom on the carbonyl group is found to hydrogen bond with two separate amine protons on different molecules of **36**. The cyclohexane functionality, like the phenyl moiety on the hydantoins, causes the crystal structure to form layers consisting of the hydrogen bonded sheet of the main glycoluril and the lipophilic layer made up of the cyclohexane.

For quite some time it has been considered that a glycoluril with sulfur at both ends was not possible, the closest structure being that with one thionyl and one carbonyl moiety.[27] Thioglycoluril **37** is only the second case of one pot formation of such a class of product and the first involving acid catalyzed condensation (Figure 2.14).[112] As was found in this case, the yields are not high and generally lead to many side products. This is the first thioglycoluril structurally characterized by X-ray crystal diffraction. While only different to **36** in the exchange of oxygen for sulfur, **37** produced a very different crystal motif. The carbon¨sulfur bond of 1.73 Å as would be expected is longer than for the carbon¨oxygen 1.24 Å. Combined with the softness of the sulfur atom in comparison to the oxygen completely change the long range packing (Figure 2.15). Whereas the bite angle for **36** had closed up in comparison to the parent molecule **37** has a bite angle of 142.1°. The sulfur molecule appears to be only weakly hydrogen bonding[40] with adjacent molecules and it seems more likely in this case that a S¨HN bond length of 3.01 Å has more to do with packing effects that what is seen for **36**.[113,114]
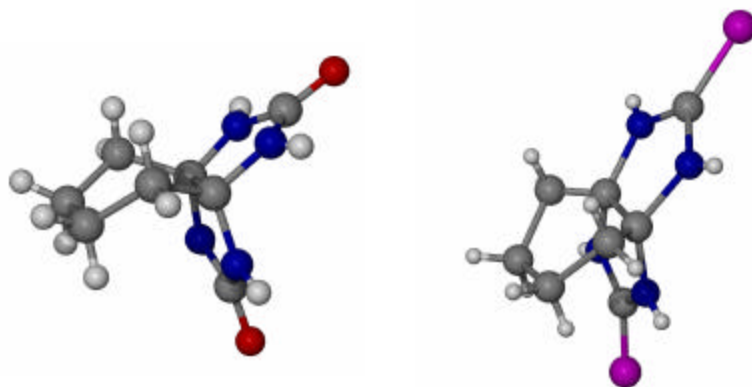
Figure 2.14. Crystal structure of cyclohexanoglycoluril (**36**) and cyclohexanothioglycoluril (**37**) (Carbon = grey, hydrogen = white, nitrogen = blue, oxygen = red, sulfur = purple).
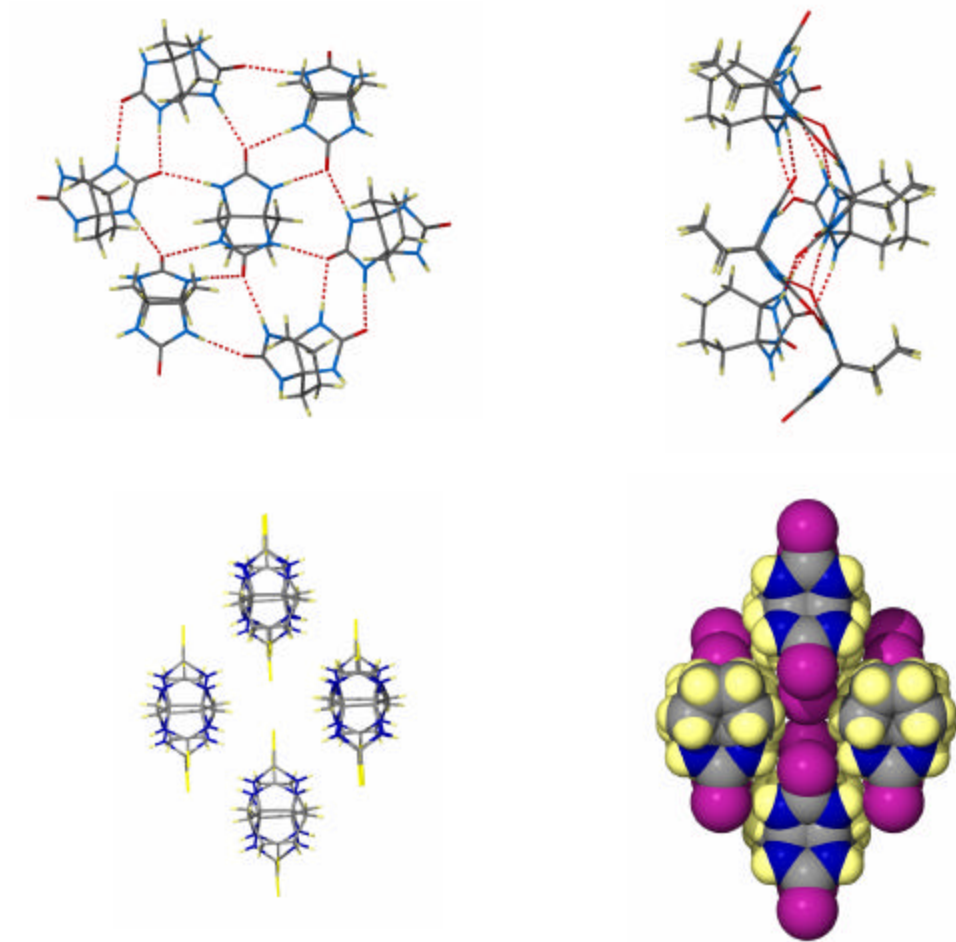
Figure 2.15. Solid state comparisons between glycolurils **36** and **37**. Top left: **36** undergoes extensive hydrogen bonding, each carbonyl oxygen bonding two protons on two adjacent molecules of **36**. Top right: Side view of coordinated molecules of **36** showing alternate layers of hydrogen bonded and lipophilic regions. Bottom left: **37** does not hydrogen bond at all and the molecules are arranged in zig-zag columns. Bottom right: Space-fill packing structure looking down the (100) plane (Carbon = grey, hydrogen = yellow, nitrogen = blue, oxygen = red, sulfur = purple).

2.4   Formation of "new" cucurbituril

The successful synthesis of the other glycolurils methylglycoluril (**30**), diphenylglycoluril (**31**), cyclohexanoglycoluril (**36**) and cyclohexanothioglycoluril (**37**) allowed for examination into their ability to become tectons for cucurbituril synthesis.

Mass spectral evidence revealed that for **30** and **36**, cucurbiturils had been synthesized using the procedure of Kim.[9] However in the case of (methyl)$_6$cucurbit[6]uril it was found to be as insoluble as the parent cucurbit[6]uril. Diphenylcucurbit[6]uril (**13**) was not completely characterized in this lab. However from a mixture of glycoluril and **31, 13** was eventually isolated in by others where it was shown to require an intensive dialysis to work up the 30% yield from the major "contaminant", cucurbit[6]uril.[18]

The thio analogue **37** showed mass spectral evidence for formation of a glycoluril dimer but no evidence for any ring or even a trimer. In light of the later evidence published by Isaacs that implies that dimerization and extension to the intermediate oligomers would require the essential functionality of the carbonyl oxygen, it would appear that **37** was not a suitable precursor for cucurbituril synthesis.[35] As can be seen below the longer C=S double bond (c.f. C=O bond) also appears to be a steric hindrance for the smaller ring size cucurbiturils at least (Figure 2.13).

Cyclohexanoglycoluril (**9**) was also a successful precursor for the formation of a new cucurbituril. The compound was surprisingly soluble in water and ^{1}H NMR revealed two structures in solution (i.e.: two sets of doublets from the ring locked methine protons). Recrystallization in water using acetone vapor led to the single crystal X-ray diffraction pattern of cyclohexanocucurbit[5]uril (**10**) (Figure 2.16). Unfortunately the elucidation of this structure in our group occurred simultaneously with the publication of the same structure from Kimoon Kim's lab.[17]
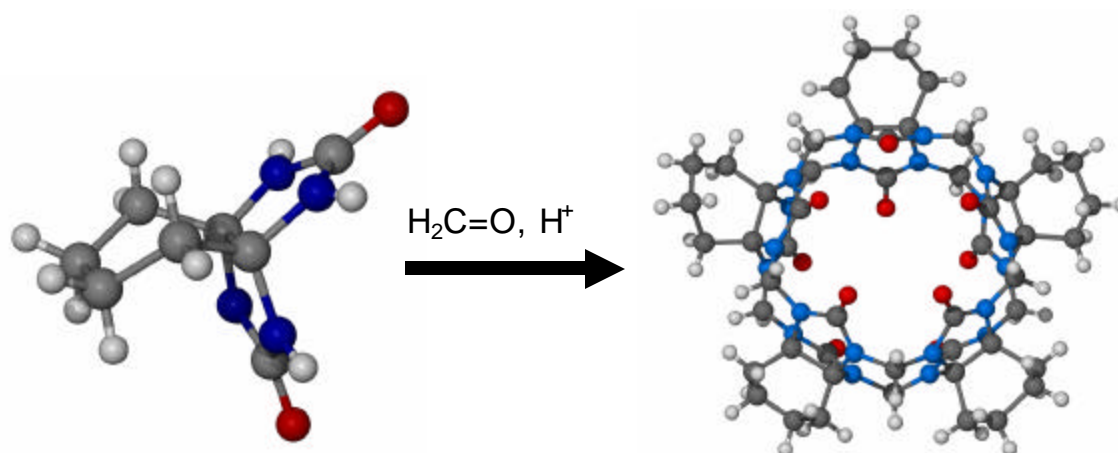
Figure 2.16. The reaction of **36** with formaldehyde under acidic conditions led to the creation of "new" cucurbituril **10** (Carbon = grey, hydrogen = white, nitrogen = blue, oxygen = red).

2.5 Cucurbit[n]uril potassium complex

2.5.1 New metal coordinated cucurbit[6]uril stucture

As mentioned, while cucurbituril is relatively insoluble in most solvents it is readily dissolved in an aqueous solution of alkaline salts. In an investigation of the improvement of the solubility for the macrocycle we discovered that it was possible to produce a new solid state structure when using complexing potassium with cucurbit[6]uril (**1**). While this crystallographic motif has been found previously for the larger cesium cation,[69] this example shows that polymeric structures with different bonding characteristics can form *via* different conditions using the same reagents. Furthermore, this is the first example of a metal-cucurbituril complex that is non-covalently bonded between three carbonyl portals of the cucurbituril. There is only one previous example of this metal-cucurbituril feature involving more than two carbonyls of a single cucurbituril. In that case the cesium ion was linked to four carbonyls on two cucurbiturils.[69]

In the solid state and with the absence of directional interactions, **1** can take on D_{6h} symmetry. With this present structure, it has been distorted by the potassium cation such that the structure has been reduced to C_{2h} symmetry with the molecule now forming a more ellipsoid shape (Figure 2.17). Each potassium ion is disordered over two sites on the face formed by the portal, and complexes to three carbonyls at one of the 'pointy' ends of the ellipse made by the plane of the carbonyls. This structure was compared to the average found from twenty one cucurbituril crystal structures taken from CCDC database. The longest distance between carbonyls is 7.69 Å (Average: 7.00 Å) while the other four carbonyls are squashed closer together at 6.58 Å (Average: 6.61 Å). This is the largest distortion imposed on cucurbit[6]uril found in the solid state on inspection of the CCDC crystallographic database.
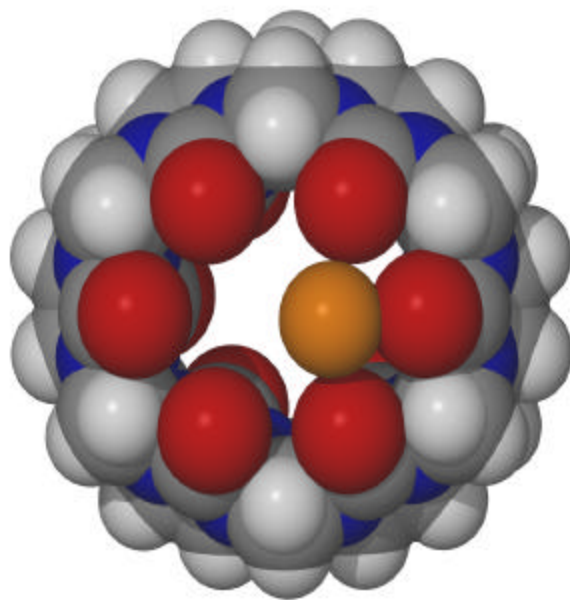
Figure 2.17. Space filling view of complex looking through portals of cucurbituril (Carbon = grey, hydrogen = white, nitrogen = blue, oxygen = red, potassium = orange. Other oxygen atoms and potassium cation not shown for clarity).

The oxygen atoms around the potassium atom form a distorted octahedral pattern, Figure 2.18. In addition to bonding to three of the carbonyl oxygen atoms on **1**, the potassium atom is attached to three oxygen atoms, presumably from three water molecules (O4-6), one of which is disordered over two positions (O4a,b). Oxygen atom O6 is located in the cavity of **1** just below the plane formed by the carbonyl oxygen atom. This oxygen also has only half occupancy over two positions such that it is located on the opposite side of the ellipse to where the potassium is. It cannot be on the same side as the potassium due to otherwise unfavorable non-bonding interactions with K··O length of 1.61 Å. This seems to fix the position of O10 which due to steric restrictions must be directly below the potassium atom. O10 was also found in one of two positions but must be below the potassium since the other position would be too close to O6. Due to symmetry constraints of the crystal, this fixes the positions of the potassium and other two waters found on the other side of the cavity as seen in Figure 2.18. The final oxygen O4 is also disordered over two positions. No doubt the majority of the oxygen atoms found are water molecules though refinement revealed a complicated electron density
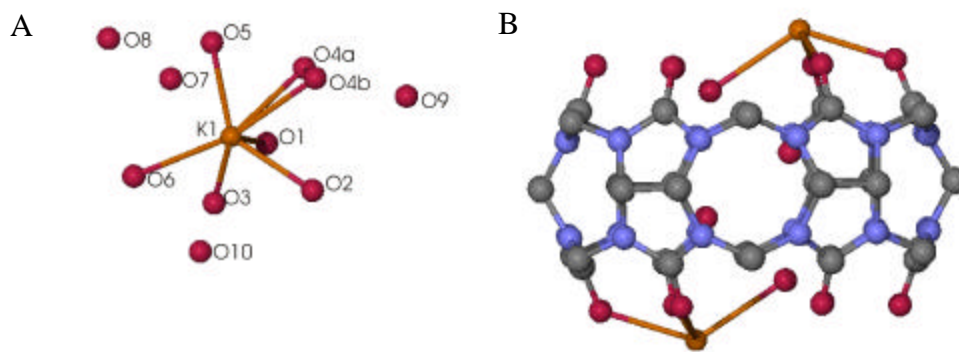
Figure 2.18. (A) Position of oxygen atoms in relation to potassium atom. (B) Showing how the position of the potassium cation fixes the position of the oxygen atoms within the cavity (Carbon = grey, nitrogen = blue, oxygen = red, potassium = orange, hydrogen atoms not shown for clarity).

that didn't allow for identification of the protons. The nitrate anion sits on a special position 6.2 – 6.8 Å away from the disordered potassium ions, it fitting snuggly between the side walls of two other molecules of **1**.

2.5.2   Extended packing of one dimensional coordination solid.

This K···O···K bonding is part of a one-dimensional coordination solid. Due to the symmetry of the bonding between **1** and potassium it makes little difference which half of the face the potassium is situated. This structure appears to be a consequence of the packing arrangements of the adjacent chain. Each individual column is staggered due to the position of the bonding arrangement between the oxygen linking the two adjacent complexes of **1**. These columns form a sheet into which an alternate row of one dimensional polymers dovetail between alternate columns. Projected down the *ab* plane, each column is skewed left or right ~15°, Figure 2.16. The other oxygen atom which in theory can also bind the two potassium atoms on adjacent molecules of **1** is congested by the close proximity of the alternate one dimensional columnar sheets. Between each column forming a single sheet, two nitrate anions reside. Water fills the space between the alternate rows of the polymer.

Just recently, a potassium complex with cucurbit[6]uril in a completely different environment was reported.[68] Kim *et al.* found that a one dimensional polymer is formed by two potassium atoms forming the metal "cement" between each molecule of **1**, with each potassium bonded to two carbonyl oxygen atoms. This coordination was also found for rubidium bound to the same cucurbituril.[70] Rather our structure conforms to a similar situation in which molecular barrels and polymers are formed with cesium in place of

potassium.[69] When the cucurbituril cavity is devoid of organic molecules, the cesium binds asymmetrically to four of the carbonyls on the face of the cucurbituril and link to a cesium on the adjacent complex. Only by introducing THF into the cavity of the cucurbituril does the overall system become more symmetrical with **1** now lining up in columns. However, the polymeric nature would break down with only one cesium able to bind to each molecule of **1**.
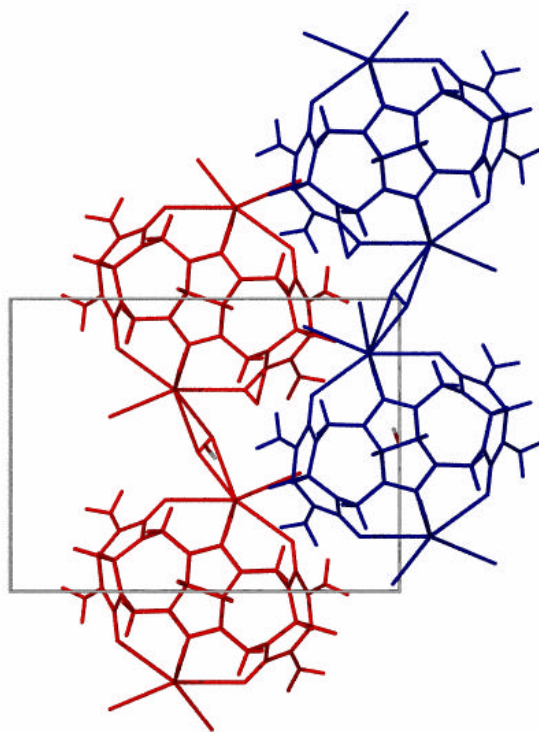
Figure 2.19. Looking down the *ab* plane of the unit cell at how two adjacent chains of cucurbit[6]uril.(potassium)$_2$.(H$_2$O)$_8$ dovetail into each other (Grey square is unit cell).

Our new structure also follows closely to the cesium model. However due to the smaller size of the metal ion it appears it can fit in closer into the portal of **1** than has

been previously found for alkali metals. The price to pay though is that the cucurbituril moiety is now found to be quite strained, more so than has been found for any other molecule of **1** thus far. This can be seen in the reduced symmetry of **1**. Potassium complexed structures then seem to be able to take on the arrangements of both rubidium and cesium based cucurbituril complexes depending on the choice of guest. It may be that potassium is just the right size to produce a variety of structures. Cesium cucurbituril of course, have been shown to lose their polymeric ability upon introduction of THF. By introducing a guest molecule or different anion, it appears the coordination structure can be changed or disrupted.

2.6   Conclusion

In conclusion, the investigation of cucurbit[n]uril tectons has resulted in the discovery of a greener synthesis of hydantoins and the possibilities of sulfur based cucurbit[n]urils *via* the use of cyclohexanothioglycoluril. It has also been shown that with judicious choice of cation or guest it is possible to vary the bonding characteristics between the metal and cucurbituril. Such a situation allows for more deliberate design approach to crystal engineering of such systems. This is also the first example of metal-cucurbituril complex requiring a non-metal to act as a mediator between adjacent cavitands and the first example that shows polymeric formation may occur in more than one fashion with the same building blocks. This allows for structures with more interesting properties such as swapping the oxygen bonding the two potassium atoms with other non-metals such as sulphur or nitrogen containing groups. Probably the strongest point ironically of this project was that publishing results in a swift time frame will reduce the frustration of being scooped!

2.7   *Experimental*

Unless stated all chemicals came from either Sigma-Aldrich, Acros or were available in-house.

Glycoluril plus 2-furaldehyde (**21**)
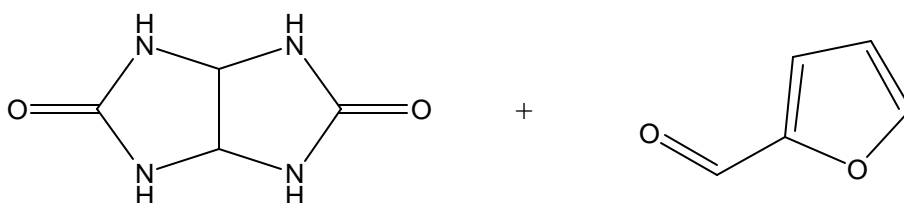
In round bottom flask covered with aluminum foil, glycoluril (7.04 x 10^{-3} mol) was dissolved up in 100 mL water with 5 mL of 9M sulfuric acid. 2-furaldehyde (0.0281 mol) was added and the light brown solution was refluxed overnight. The mixture by this time had become a dark yellow solution with black precipitate. TLC indicated that there was no 2-furaldehyde left in solution. Attempts to dissolve the black precipitate in acidic or organic solutions proved futile with NMR showing no peaks in the aromatic region or the region for glycoluril.

Glycoluril plus 1-(phenylsulfonyl)-2-pyrrole carboxaldehyde (**22**)
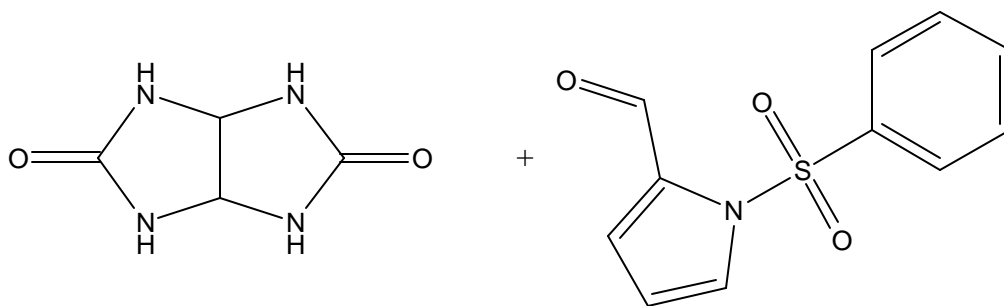
Glycoluril (2.13 x 10^{-6} mol) was dissolved up in water with trifluroacetic acid added drop wise until pH ~ 1. 1-(phenylsulfonyl)-2-pyrrole carboxaldehyde (4.25 x 10^{-6}) was added to afford a purple solution. The solution was refluxed for two hours whereupon it

had turned into a brown solution. Proton NMR of the solution revealed no sign of aromatic compounds and only the glycoluril moiety left.

Glycoluril plus acetaldehyde (**23**)
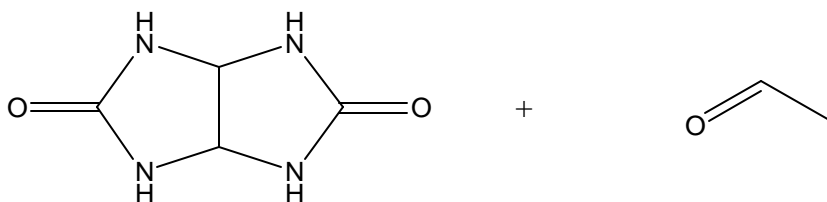
Glycoluril (8.41×10^{-4} mol) was added to a) ionic liquid N^{644} Amide or; b) placed in a mortar and pestle or c) added to 9M sulfuric acid. a) and b) had toluene-4-sulphonic acid added. Acetaldehyde (1.68×10^{-3} mol) was added drop wise which in all cases caused some bubbling to occur in the reaction mixture. Both a) and c) were heated to approximately 80°C for 12 hours. b) was ground in the mortar and pestle for 10 minutes upon which the white powder and clear liquid had turned into a gooey blob which then turned pale orange after leaving to set for six hours. All experiments where then washed with acetone, a precipitate forming for a) and c) and to remove the acid for b). No indication of cucurbituril formation was detected by NMR or MS. For the ionic liquid the precipitate was white and glycoluril was detected by NMR. For b) and c) the precipitate was brown or orange and only peaks in the alkane and alkene area were visible and were unable to be interpreted.

Glycoluril plus benzaldehyde (**24**)
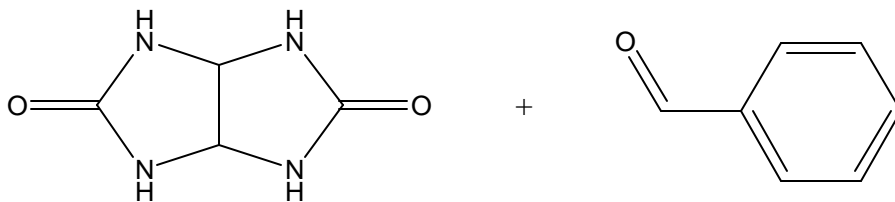
Glycoluril (6.93 x 10^{-4} mol) was dissolved in 9M sulfuric acid and benzaldehyde (1.39 x 10^{-3} mol) was added drop wise. The solution was heated to approximately 90°C and left stirring overnight. After cooling pale white crystals were filtered off and subjected to X-ray crystal analysis. This revealed them to be crystals of glycoluril. Further reactions at 100°C also showed no reaction as measured by ^{1}H NMR.

Glycoluril plus 2-formylbenzenesulphonic acid, sodium salt hydrate (**25**)
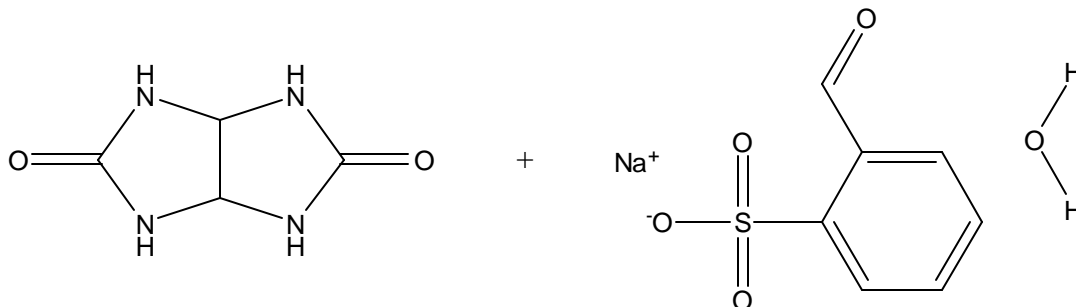
Glycoluril (6.80 x 10^{-3} mol) and 2-formylbenzenesulphonic acid, sodium salt hydrate was added to 9M sulfuric acid and under nitrogen the dissolved solution was stirred at 95°C overnight. The yellow solution was added to acetone where upon an orange precipitate formed and was filtered off and washed with acetone. An examination of the precipitate using ^{1}H NMR revealed only starting materials.

Glycoluril plus 4-octyloxybenzaldehyde (**26**)

To a solution of glycoluril (4.51 x 10^{-4} mol) in 9M sulfuric acid was added drop wise
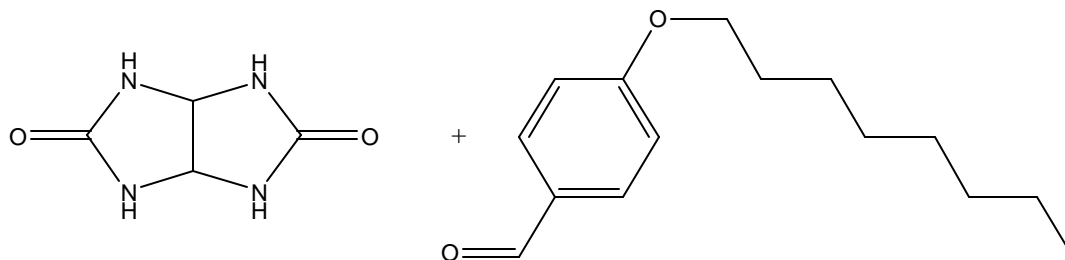
a yellow solution of 4-octyloxybenzaldehyde (9.01 x 10^{-4}). The solution was stirred vigorously due to the aldehyde's immiscibility in aqueous solutions which was refluxed overnight. Upon cooling a biphasic solution (orange, top later; clear, bottom layer) was present. Aliquots of both layers revealed unreacted precursors *via* ^{1}H NMR analysis.

Glycoluril plus phthalic dicarboxyaldehyde (**27**)
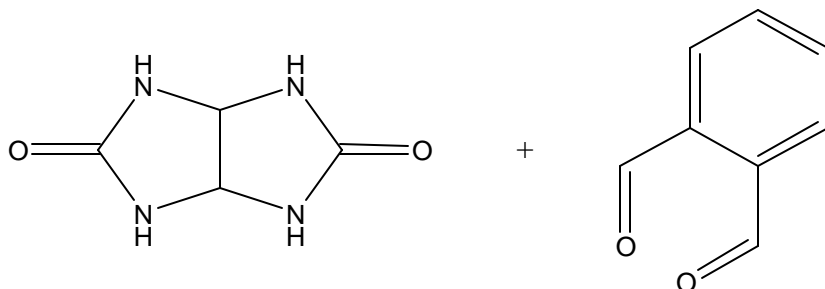
White, crystalline glycoluril (7.00 x 10^{-3} mol) and the pale yellow solid phthalic dicarboxyaldehyde were added to a solution of 9M sulfuric acid and refluxed with stirring overnight. Despite reflux the solution never at any stage seem to go clear. At the end of the reflux the solution was cooled and no sign of reaction occurred as examined *via* ^{1}H NMR.

Glycoluril plus benzene-1,4-dicarboxaldehyde (**28**)
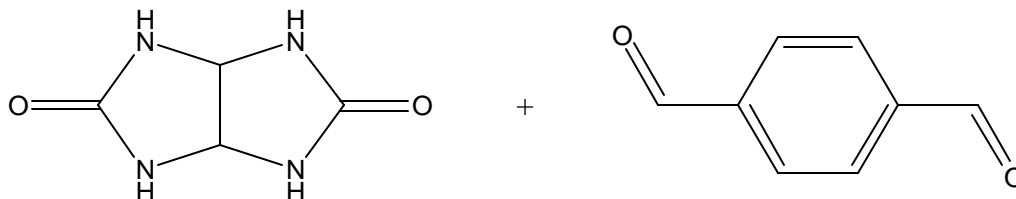
Glycoluril (1.55×10^{-3} mol) and phthalic dicarboxyaldehyde (1.55×10^{-3} mol) was added to a solution of 9M sulfuric acid. The phthalic dicarboxyaldehyde did not seem to be very soluble in the acidic aqueous solution. The mixture was stirred vigorously and refluxed overnight. Upon cooling a white precipitate crashed out of solution along with two types of crystals; long thin needles and hexagonal prisms. X-ray analysis revealed them to be the precursors. ^{1}H NMR of the white precipitate also backed this up.

Glycoluril plus glutaric dialdehyde (**29**)
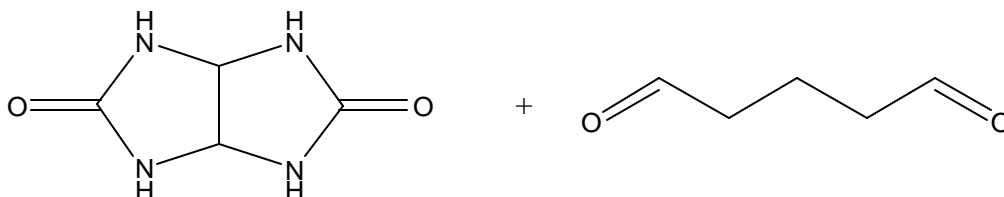
To a solution of glycoluril (0.110 mol) in a) 9M sulfuric acid or b) acetic acid was added drop wise glutaric dialdehyde (50% weight in water, 0.110 mol). Each drop of the aldehyde would result in an exothermic reaction and the solution quickly became a dark orange. The reaction was heated at 80°C and stirred overnight. Upon addition of acetone a white precipitate formed and sank to the bottom. Also red-brown, rubbery looking lumps floated at the top of the solution or in the case of acetic acid remained at the bottom. ^{1}H NMR of white precipitate and rubbery bits revealed glycoluril and an

unknown compound with peaks in the alkane and alkene part of the spectrum. From these observations it appears the aldehyde had polymerized.

Methylglycoluril (**30**)
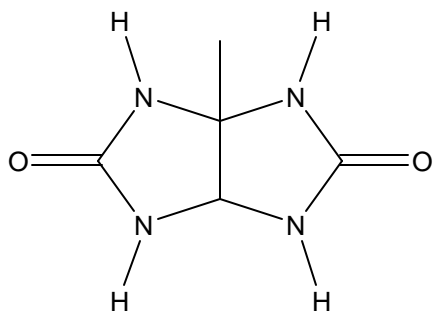
A mixture of methylglyoxal (40% in water, 0.277 mol) and urea (0.554 mol) were added to water where upon the urea dissolved and the solution became yellow. The solution was stirred and acidified to pH of 1 by adding trifluroacetic acid or hydrochloric acid drop wise to the solution. The solution temperature was set at 40°C and left to stir. After approximately six hours the solution had become orange with white precipitate. The solution was left to cool, the precipitate collected and left to dry in air (Yield: trifluroacetic acid, 23%; HCl 81%).

IR (nujol, NaCl plate): 1695.7 cm^{-1} C=O, 3253.7, 3168.5 cm^{-1} N–H; ^{1}H NMR (D$_2$O, d_4-MeOH, 300 MHz): 5.097 (s, 1H), 1.58 (s, 3H); ^{13}C NMR (D$_2$O, d_4-MeOH, 300 MHz): 174.5, 63.3, 50.8, 27.7; EI-MS *m/z* 156.

Diphenylglycoluril (**31**)
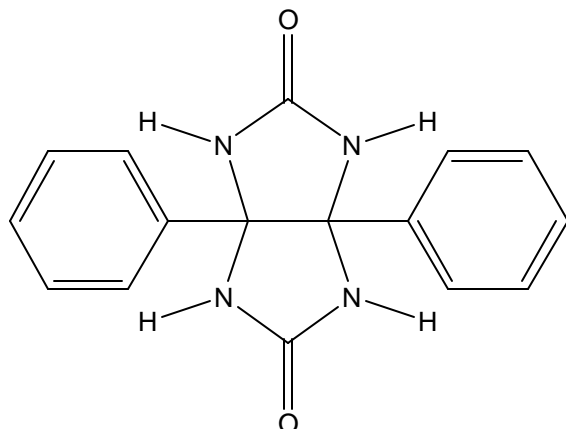
A yellow solution of benzil (0.0476 mol) dissolved in methanol was added to a clear solution of urea (0.0952 mol) in methanol (an alternate solvent of toluene was also used). trifluroacetic acid was added drop wise until the pH of solution was approximately 1.5. The solution was refluxed and the reaction left stirring overnight upon which white precipitate had formed in the yellow solution. The precipitate was filtered and washed with methanol upon which it had developed a yellow impurity. Sonication of the yellow precipitate in methanol and further filtering resulted in a white precipitate. The precipitate was filtered and allowed to dry. (Yield: 54%)

^{1}H NMR (d_6-DMSO, 300 MHz): 7.24 – 7.09 (m, 10H), 4.14 (br, 4H); ^{13}C NMR (d_6-DMSO, 300 MHz): 160.71, 127.0, 126.98, 126.98, 81.78 (Note: a quaternary carbon did not appear to show up); EI-MS *m/z* 294 (M+).

Urea plus di-2-pyridilglyoxal (**32**)
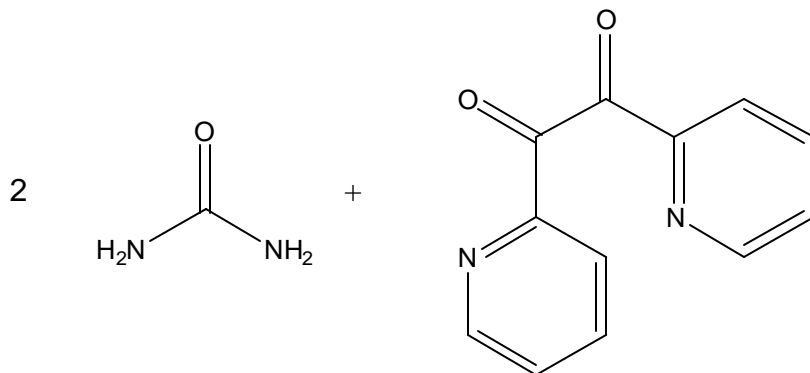
Urea (0.0472 mol) and di-2-pyridilglyoxal (0.0236) was dissolved into methanol and trifluroacetic acid added drop wise until the pH of the solution was approximately one. The solution quickly turned an opaque red upon refluxing. After approximately 12 hours the solution had turned brown/black and no precipitate was present. Addition of acetone had no effect. Rotary evaporation of liquid resulted in gooey, black, tar-like solid.

Urea plus 2,3-butanedione (**33**)
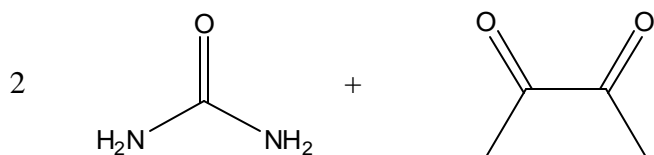
Urea (8.33 x 10^{-3} mol) was dissolved into water and a yellow solution of 2,3-butanedione (4.17 x 10^{-3} mol) was added drop wise into the solution. Upon addition of trifluroacetic acid the solution became a darker yellow and eventually a layer of black oil formed on top of the water. The oil was decanted off and heating of the solution while stirring began. This was stopped quickly when the solution had darkened to a brown color. Removal of solvent led to a brown goo that was resistant to analysis.

61

Thiourea plus glyoxal (**34**)
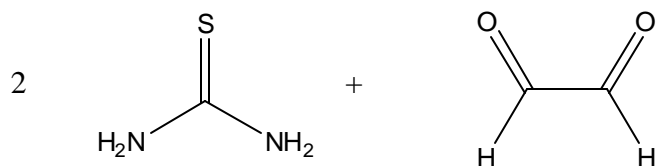
Thiourea (0.131 mol) was dissolved in water and glyoxal (0.0655 mol) added drop wise. trifluroacetic acid was added drop wise until the solution had pH = 1. The clear, orange solution was stirred and heated to 30°C. The solution was cooled after 24 hours and the solution removed by rotary evaporation. Red-orange crystals had formed from the product mixture and were examined by ^{1}H NMR which revealed no carbons or protons! Examination by single crystal X-ray determination revealed the crystals to be S_8 sulphur.

Thiourea plus methylglyoxal (**35**)
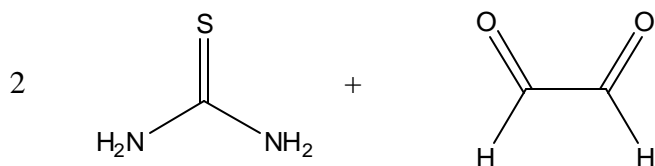
Thiourea (0.131 mol) was dissolved in methanol and methylglyoxal (0.0655 mol) added drop wise. Hydrochloric acid was added until the solution was approximately 1 (only a few drops). The solution was refluxed for seven hours upon which the orange solution had turned a brown yellow color. The solvent and acid were rotary evaporated off leaving a red powder. Recrystallization in methanol led to thin red crystals. These were examined and were found to be thiourea.

Cyclohexanoglycoluril (**36**)
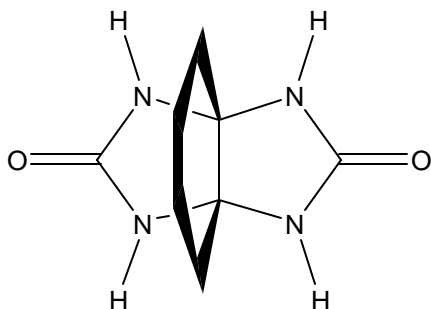
Cyclohexanedione (0.0446 mol) and urea (0.0892 mol) was dissolved into water and trifluroacetic acid added drop wise until pH reached 1. The solution was refluxed for 24 hours and once cooled the yellow solution contained yellow precipitate. The precipitate was filtered off, washed with water, upon which the precipitate was now white and dried in air. Leaving the yellow solution in the refrigerator produced more precipitate which was filtered, washed and dried as above. The structure of the product was confirmed by NMR and single crystal X-ray diffraction (Yield: 32%)

^{1}H NMR (DMSO, 300 MHz): 1.69 (t, 4H), 1.39 (t, H); EI-MS m/z 196 (M$^+$); Found: C, 49.5; H, 6.1; N, 28.05. $C_8H_{12}N_4O_2$ requires C, 48.91; H, 6.16; N, 28.56.

Crystal Data for **36**

Crystal data for: $C_8H_{12}N_4O_2$, $M = 196.22$, colorless parallelepiped, $0.40 \times 0.30 \times 0.25$ mm^3, orthorhombic, space group $Pca2_1$ (No. 29), $a = 11.919(3)$, $b = 6.5868(2)$, $c = 11.623(3)$ Å, $V = 912.5(4)$ Å^3, $Z = 4$, $D_c = 1.428$ g/cm^3, $F_{000} = 416$, Nonius KappaCCD diffractometer (? scan mode, M radiation MoKα, ? = 0.71073 Å), $T = 173(2)$ K, $2q_{max} = 54.3°$, 4753 reflections collected, 1529 unique (R$_{int}$ = 0.0894). Final $GooF = 0.918$, $R1 = 0.0548$, $wR2 = 0.1079$, R indices based on 943 reflections with I >2sigma(I) (refinement

on F^2), 143 parameters, 1 restraint. Lp and absorption corrections applied, $\boldsymbol{m} = 0.106$ mm^{-1}.

Cyclohexano thio glycoluril (**37**)
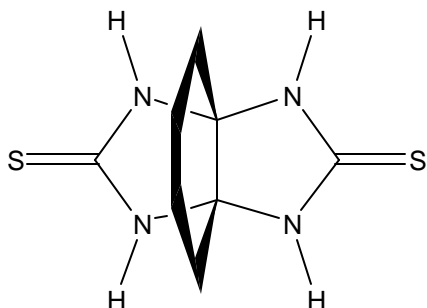
Thiourea (0.135 mol) and 1,2-cyclohexanedione (0.045 mol) was added to a solution of toluene and trifluroacetic acid added (10 mL). The yellow solution was stirred and refluxed overnight upon which it could be seen that white precipitate had formed in the now brown solution. A Dean-Stark trap was attached and water was allowed to collect in the trap. Once no more water was found to come off, the solution was cooled. Adding methanol to the solution resulted in more precipitate crashing out. This was filtered off and dried. Recrystallization from acetone gave crystals of **37**. (Yield: 26%)

^{1}H NMR (DMSO, 300 MHz): 1.73 (t, 4H), 1.35 (t, H); ^{13}C NMR (d_6-DMSO, 75 MHz): 181.6 (CO), 82.1 (CR$_4$), 29.4 (CH$_2$), 16.8 (CH$_2$); EI-MS m/z 228 (M$^+$)

Crystal Data for **37**

Crystal Data for $C_{32}H_{48}N_{16}S_8$ M = 913.35 , colorless rectangular prism, 0.5 x 0.2 x 0.2 mm^3, orthorhombic, space group *Pna2$_1$* (No. 33) $a = 8.5029(17)$, $b = 12.5324(25)$, $c = 10.0140(2)$Å $V = 1067.11(2)$ Å^3, $Z = 4$ $D_c = 1.4211$ g/cm^3, F$_{000}$ = 480, Nonius KappaCCD diffractometer (? scan mode, M radiation MoKα, ? = 0.71073 Å), 1516 reflections collected, 1381 unique, *R1* = 0.0694, *wR2* = 0.0797, *R* indices based on 1189 reflections

with I >2sigma(I) (refinement on F^2), 127 parameters, 1 restraint. $T = 173(2)$ K, $2q_{max} = 54.3°$, $\mu = 0.47$ mm^{-1}

General Synthetic Procedure: 5-Phenyl-imidazolidine-2,4-dione (**38**).
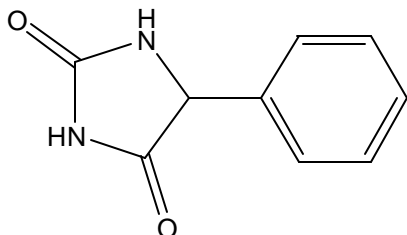
Phenylglyoxal (6.57 x 10^{-3} mol) and urea (13.1 x 10^{-3} mol) was added to 40 mL of water in a 100 mL round bottom flask fitted to a condenser. trifluroacetic acid was added until pH of the solution was approximately 1, generally only 3 to 4 drops was required. This amount of acid was then also applied to the reaction with toluene or benzene as solvent. For water, the murky yellow solution was refluxed for 5 hours. Using toluene or benzene as solvent resulted in an orange and white precipitate that was separated from the solution *via* filtration. The product in all cases can be recrystallized from water. Unit cells were identical for all compounds in all solvents.

Urea and phenylglyoxal in water (**38**).

Mp: 180-181 °C (from water); IR (nujol, NaCl plate): 1718, 1752 cm^{-1} (C=O); ^{1}H NMR(300 MHz; DMSO) 5.16 (1H, s, CH), 7.31-7.43 (5H, m, ArH), 8.41 (1H, s, NH), 10.8 (1H, s, NH); ^{13}C NMR (75 MHz; DMSO) 61.5 (CH), 127.1 (Ar), 128.6 (Ar), 129.0 (Ar), 136.4 (Ar), 157.8 (CO), 174.6 (CO); *m/z* (EI) 176.1(M$^+$); Found: C, 61.35; H, 4.8; N, 15.05. $C_9H_8N_2O_2$ requires C, 61.4; H, 4.6; N, 15.9; O, 18.2%.

Urea and phenylglyoxal in toluene (**38**).

Mp: 180-181 °C (from water); IR (nujol, NaCl plate): 1699, 1783 cm^{-1} (C=O); 1H NMR(300 MHz; DMSO) 5.11 (1H, s, CH), 7.33-7.45 (5H, m, ArH), 8.38 (1H, s, NH), 10.83 (1H, s, NH); 13C NMR (75 MHz; DMSO) 61.5 (CH), 127.1 (Ar), 128.6 (Ar), 129.0 (Ar), 136.4 (Ar), 157.8 (CO), 174.6 (CO); *m/z* (ESI) 177.1 (M + H$^+$, 100%); Found: C, 61.9; H, 5.4; N, 15.1. $C_9H_8N_2O_2$ requires C, 61.4; H, 4.6; N, 15.9; O, 18.2%.

Urea and phenylglyoxal in benzene (**38**).

Mp: 180-181 °C (from water); IR (nujol, NaCl plate): 1699, 1783 cm^{-1} (C=O); ^{1}H NMR (250 MHz; DMSO) 5.18 (1H, s, CH), 7.35-7.47(5H, m, ArH), 8.38 (1H, s, NH), 10.73 (1H, s, NH); ^{13}C NMR (250 MHz; DMSO) 61.5 (CH), 127.1 (Ar), 128.6 (Ar), 129.0 (Ar), 136.5 (Ar), 157.6 (CO), 174.6 (CO); *m/z* (EI) 175(M$^+$, 100%; Found: C, 61.4; H, 5.11; N, 15.8. $C_9H_8N_2O_2$ requires C, 61.4; H, 4.6; N, 15.9; O, 18.2%.

Crystal data for **38**

$C_{36}H_{40}N_8O_{12}$, *M* = 156.15, colorless parallelepiped, 0.40 × 0.30 × 0.25 mm^3, monoclinic, space group *P2$_1$/c* (No. 14), *a* = 18.717(3), *b* = 6.3273(9), *c* = 7.9632(12) Å, *b* = 99.679(3)°, *V* = 929.6(2) Å^3, Z = 6, D_c = 1.395 g/cm^3, F_{000} = 410, Bruker SMART 1000 CCD diffractometer, MoKα radiation, λ = 0.71073 Å, *T* = 173(2)K, 2*q*$_{max}$ = 54.2°, 5446 reflections collected, 2029 unique (R$_{int}$ = 0.0214). Final *GooF* = 1.093, *R1* = 0.0397, *wR2* = 0.1121, *R* indices based on 1535 reflections with I >2σ (I) (refinement on F^2), 143 parameters, 0 restraints. Lp and absorption corrections applied, *m* = 0.111 mm^{-1}.

General Procedure: 5-Phenyl-2-thioxo-imidazolidin-4-one (**39**).
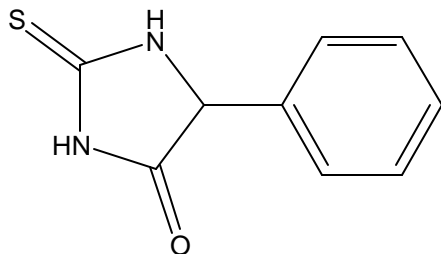
Phenylglyoxal (6.57×10^{-3} mol) and thiourea (13.1×10^{-3} mol) was added to 40 mL of water in a 100 mL round bottom flask fitted to a condenser. Trifluroacetic acid was added until pH solution of water was approximately 1, generally only 3 to 4 drops was required. The amount used was then also applied to the reaction with toluene or benzene as solvent. For water, a clear yellow solution formed upon refluxing which was continued for 5 hours and the solvent then taken off. Using toluene or benzene, the solution quickly became a red-purple solution. Pale orange precipitate was removed upon cooling and the filtrate left to evaporate which led to more precipitate forming. The product was recrystallized in all cases from ethanol. Unit cells were identical for all compounds in all solvents.

Thiourea and phenylglyoxal in water (**39**).

Mp: 223-224 °C (from EtOH); IR (nujol, NaCl plate): 1743 cm^{-1} (C=O); ^{1}H NMR(300 MHz; DMSO) 5.40 (1H, s, CH), 7.26-7.44 (5H, m, ArH), 10.52 (1H, s, NH), 11.88 (1H, s, NH); ^{13}C NMR (75 MHz; DMSO) 64.2 (CH), 127.1 (Ar), 129.0 (Ar), 129.3 (Ar), 134.9 (Ar), 175.2 (CS), 183.3 (CO); m/z (ESI) 193.1(M + H$^+$, 100%). Found: C, 56.05; H, 4.2; N, 14.65; S, 16.8. $C_9H_8N_2OS$ requires C, 56.2; H, 4.2; N, 14.6; S, 16.7%.

Thiourea and phenylglyoxal in toluene (**39**).

Mp: 223-224 °C (from EtOH); IR (nujol, NaCl plate): 1742 cm^{-1} (C=O); ^{1}H NMR (300 MHz; DMSO) 5.41 (1H, s, CH), 7.27-7.44 (5H, m, ArH), 10.52 (1H, s, NH), 11.88 (1H, s, NH); ^{13}C NMR (75 MHz; DMSO) 64.3 (CH), 127.1 (Ar), 128.9 (Ar), 129.3 (Ar), 134.9 (Ar), 175.2(CS), 183.3(CO); *m/z* (EI) 193.1(M + H^{+}, 100%; Found: C, 56.15; H, 4.4; N, 14.5; S, 17.6. C$_9$H$_8$N$_2$OS requires C, 56.2; H, 4.2; N, 14.6; S, 16.7%.

Thiourea and phenylglyoxal in benzene (**39**).

Mp: 223-224 °C (from EtOH); IR (nujol, NaCl plate): 1742 cm^{-1} (C=O); ^{1}H NMR (250 MHz; DMSO) 5.41 (1H, s, CH), 7.29-7.45 (5H, m, ArH), 10.50 (1H, s, NH), 11.83 (1H, s, NH); ^{13}C NMR (63 MHz; DMSO) 64.3 (CH), 127.4 (Ar), 129.0 (Ar), 129.8 (Ar), 134.5 (Ar), 175.1(CS), 183.3(CO); *m/z* (EI) 192(M^{+}, 100%; Found: C, 56.02; H, 4.24; N, 14.47; S, 16.42. C$_9$H$_8$N$_2$OS requires C, 56.2; H, 4.2; N, 14.6; S, 16.7%.

Crystal Data for **39**.

C$_{18}$H$_{16}$N$_4$O$_2$S$_2$, M = 180.22, colorless parallelepiped, 0.40 × 0.30 × 0.25 mm^3, triclinic, space group P-1 (No. 2), a = 4.8302(5), b = 8.9683(9), c = 10.4938(10) Å, $\boldsymbol{a}$ = 80.228(2), $\boldsymbol{b}$ = 82.325(2), $\boldsymbol{g}$ = 79.387(2)°, V = 437.86(8) Å^3, Z = 2, D_c = 1.367 g/cm^3, F_{000} = 188, Bruker SMART 1000 CCD diffractometer, MoKα radiation, λ = 0.71073 Å, T = 173(2)K, $2\boldsymbol{q}_{max}$ = 54.2°, 2764 reflections collected, 1885 unique (R$_{int}$ = 0.0196). Final $GooF$ = 1.088, $R1$ = 0.0878, $wR2$ = 0.2464, R indices based on 1496 reflections with I >2σ (I) (refinement on F^2), 130 parameters, 0 restraints. Lp and absorption corrections applied, $\boldsymbol{m}$ = 0.320 mm^{-1}.

General Procedure: 2-Imino-5-phenyl-imidazolidin-4-one (**40**).
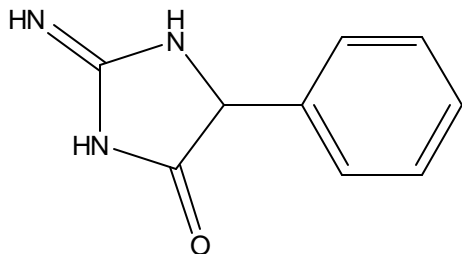
Phenylglyoxal (6.57 x 10^{-3} mol) and guanidine hydrochloride (6.57 x 10^{-3} mol) was added to 40 mL of water in a 100 mL round bottom flask fitted with a condenser. Water, benzene or toluene (50 mL) was used as solvent. In the case of water, trifluroacetic acid was added drop wise until pH solution of water was approximately 1, requiring only 3 to 4 drops (approximately 0.15 – 0.2 mL). The amount used was then also applied to the reaction with toluene or benzene as solvent for comparison. The solution was refluxed for 5 hours. For water, a small amount of yellow precipitate formed upon cooling. In toluene or benzene, the precipitate formed as a viscous material during reflux without really dissolving. Crystals for analysis were the trifluroacetic acid salt of the compound recrystallized from water. Unit cells were identical for all compounds in all solvents.

Guanidine hydrochloride and phenylglyoxal in water (**40**).

Mp: 184-186 °C (from water); IR (nujol, NaCl plate): 1759 cm^{-1} (C=O); ^{1}H NMR (300 MHz; DMSO) 5.44 (1H, s, CH), 7.30-7.43 (5H, m, ArH), 9.32 (2H, s, NH), 10.28 (1H, s, NH); ^{13}C NMR (75 MHz; DMSO) 62.4 (CH), 127.4 (Ar), 129.2 (Ar), 129.3 (Ar), 134.4 (Ar), 158.4 (CN), 174.6 (CO); *m/z* (ESI) 176.1 (M - CF$_3$COOH + H$^+$, 100%; Found: C, 44.60; H, 3.65; N, 15.45. C$_{11}$H$_{10}$F$_3$N$_3$O$_3$ requires C, 45.7; H, 3.5; F, 19.7; N, 14.5; O, 16.6.

Guanidine hydrochloride and phenylglyoxal in toluene (**40**).

Mp: 184-186 °C (from water); IR (nujol, NaCl plate): 1758 (C=O); ^{1}H NMR (300 MHz; DMSO) 5.38 (1H, s, CH), 7.34-7.43 (5H, m, ArH), 9.34 (2H, s, NH), 10.32 (1H, s, NH); ^{13}C NMR (75 MHz; DMSO) 62.3 (CH), 127.5 (Ar), 129.3 (Ar), 134.2 (Ar), 158.4 (CN), 174.0 (CO); m/z (ESI) 176.2 (M - CF3COOH + H$^+$, 100%; Found: C, 44.6; H, 3.65; N, 15.45. $C_{11}H_{10}F_3N_3O_3$ requires C, 45.7; H, 3.5; F, 19.7; N, 14.5; O, 16.6.

Guanidine hydrochloride and phenylglyoxal in benzene (**40**).

Mp: 184-186 °C (from water); IR (nujol, NaCl plate): 1759 (C=O); ^{1}H NMR (250 MHz; DMSO) 5.41 (1H, s, CH), 7.38-7.53 (5H, m, ArH), 9.34 (2H, s, NH), 10.31 (1H, s, NH); ^{13}C NMR (62 MHz; DMSO) 62.2 (CH), 127.8 (Ar), 129.3 (Ar), 134.2 (Ar), 158.1 (CN), 174.0 (CO); m/z (EI) 175(M$^+$, 100%); Found: C, 45.1; H, 3.60; N, 13.93. $C_{11}H_{10}F_3N_3O_3$ requires C, 45.7; H, 3.5; F, 19.7; N, 14.5; O, 16.6.

Crystal Data for **40**.

$C_{11}H_{10}F_3N_3O_3$, M = 289.22, colorless parallelepiped, 0.50 × 0.40 × 0.40 mm^3, monoclinic, space group $C2$ (No. 5), a = 27.894(3), b = 6.2616(7), c = 7.1989(8) Å, b = 93.176(2)°, V = 1255.4(2) Å^3, Z = 4, D_c = 1.530 g/cm^3, F_{000} = 592, Bruker SMART 1000 CCD diffractometer, MoKα radiation, λ = 0.71073 Å, T = 173(2)K, 2q_{max} = 54.2°, 3997 reflections collected, 2585 unique (R$_{int}$ = 0.0252). Final $GooF$ = 0.947, $R1$ = 0.0395, $wR2$ = 0.0848, R indices based on 2063 reflections with I >2sigma(I) (refinement on F^2), 222 parameters, 1 restraint. The three fluorine atoms where disordered around the carbon and were modeled in two positions with occupancy of 0.5 each. Lp and absorption corrections applied, m = 0.141 mm^{-1}. Absolute structure parameter = -0.1(9) (Flack, H.

D. *Acta Cryst*. **1983**, *A39*, 876-881).

General Synthetic Procedure: 4,4'-Diphenyl-2,2'-dithioxo-[4,4']biimidazolidinyl-5,5'-dione (**41**).
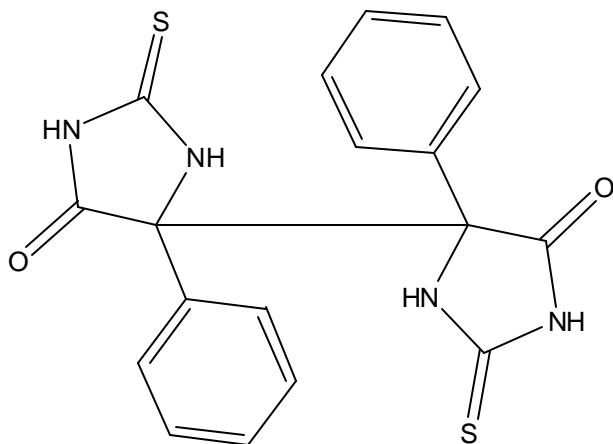
A solution of **39** and either **38** or **40** was dissolved in methanol was slowly evaporated until rectangular crystals formed. Compound **41** was also found to form slowly from **39**. Compound **41** due to it's formation *via* mixing with **38** or **40** with **39** was not completely analyzed due to difficulty in separation of the monomers.

^{1}H NMR (500 MHz; DMSO) 7.38-7.53 (5H, m, ArH), 9.34 (2H, s, NH), 10.31 (1H, s, NH); ^{13}C NMR (125 MHz; DMSO) 73.0 (CC), 127.5 (Ar), 127.7 (Ar), 131.0 (Ar), 172.3 (CS), 182.2 (CO).

Crystal data for **41**

$C_{36}H_{28}N_8O_4S_4$, M = 764.11, colorless parallelepiped, 0.40 × 0.30 × 0.25 mm^3, triclinic, space group P-1 (No. 2), a = 8.5993(14), b = 9.4751(16), c = 11.766(2) Å, $\boldsymbol{a}$ = 112.985(3), $\boldsymbol{b}$ = 97.862(3), $\boldsymbol{g}$ = 90.568(3)°, V = 872.1(3) Å^3, Z = 11, D_c = 1.456 g/cm^3, F_{000} = 396, Bruker SMART 1000 CCD diffractometer, MoKα radiation, λ = 0.71073 Å,

T = 173(2)K, $2q_{max}$ = 46.6°, 5602 reflections collected, 2504 unique (R_{int} = 0.0479). Final *GooF* = 1.027, *R1* = 0.0486, *wR2* = 0.1036, *R* indices based on 1681 reflections with I >2sigma(I) (refinement on F^2), 236 parameters, 0 restraints. Lp and absorption corrections applied, m= 0.326 mm^{-1}.

Experimental for Cucurbit[6]uril-Potassium nitrate structure

Cucurbit[6]uril (**1**) was formed *via* a similar method to Kim *et al.* using standard reagents.[9] ESI-MS and ^{1}H NMR confirmed the formation of **1**. A few milligrams of cucurbituril was then placed in a vial and dissolved in approximately 3 mL of a stock solution of 0.5 *M* potassium nitrate. The opaque white suspension was then heated until a clear pale yellow solution resulted. Slow evaporation of the solvent led to the formation of a large clear, cubic, crystal, a fragment of which was cut off (0.2 x 0.2 x 0.2 mm^3) for crystallographic studies. Crystals formed from the diffusion of methanol into potassium nitrate with dissolved cucurbituril resulted in the same structure.

Crystal Data: $C_{72}H_{74}N_{52}O_{64}K_4$, M = 1424.04 g mol^{-1}, orthorhombic, Pnnm, a = 15.7846(9)Å, b = 11.8105(7)Å, c = 14.9146(9)Å, V = 2780.44 Å^3, Z = 2, d_{calcd} = 1.7007 g cm^{-3}, T = 173 K,

Data were collected on a Bruker SMART CCD diffractometer (ω scan mode Mo-K$_\alpha$ radiation, λ = 0.7107 Å). Data was corrected for absorption using the program SADABS[115]. Structure solution and refinement proceeded similarly for all structures (SHELX-97 software[116] using the X-Seed[117] interface). Direct methods yielded all non-hydrogen atoms of the asymmetric unit. These atoms were refined anisotropically (full-matrix least-squares method on F^2). Hydrogen atoms were placed in calculated positions

with their isotropic thermal parameters riding on those of their parent atoms. Two oxygen atoms and the potassium atom were found to be disordered and were modeled at occupancy rates of 0.5. All X-ray structure figures were prepared with X-Seed and POV-Ray (http://www.povray.org).

(1) Freeman, W. A.; Mock, W. L.; Shih, N.-Y. *J. Am. Chem. Soc.* **1981**, *103*, 7367-7368.

(2) Kim, K. *Chem. Soc. Rev.* **2002**, *31*, 96-107.

(3) Miyahara, Y.; Abe, K.; Inazu, T. *Angew. Chem. Int. Ed.* **2002**, *41*, 3020-3023.

(4) Blanch, R. J.; Sleeman, A. J.; White, T. J.; Arnold, A. P.; Day, A. I. *Nano Lett.* **2002**, *2*, 147-149.

(5) Karcher, S.; Kornmüller, A.; Jekel, M. *Water Sci. Technol.* **1999**, *40*, 425-433.

(6) Kolbel, M.; Menger, F. M. *Advanced Materials* **2001**, *13*, 1115-1119.

(7) Wheate, N. J.; Day, A. I.; Blanch, R. J.; Arnold, A. P.; Cullinane, C.; Collins, J. G. *Chem. Commun.* **2004**, 1424-1425.

(8) Marquez, C.; Hudgins, R. R.; Nau, W. M. *J. Am. Chem. Soc.* **2004**, *126*, 5806-5816.

(9) Kim, J.; Jung, I.-S.; Kim, S.-Y.; Lee, E.; Kang, J.-K.; Sakamoto, S.; Yamaguchi, K.; Kim, K. *J. Am. Chem. Soc.* **2000**, *122*, 540-541.

(10) Behrend, R.; Meyer, E.; Rusche, F. *Liebigs Ann. Chem.* **1905**, *339*, 1-37.

(11) Mock, W. L.; Shih, N.-Y. *J. Org. Chem.* **1986**, *51*, 4440-4446.

(12) Mock, W. L.; Shih, N.-Y. *J. Am. Chem. Soc.* **1988**, *110*, 4706-4710.

(13) Flinn, A.; Hough, G. C.; Stoddart, J. F.; Williams, D. J. *Angew. Chem. Int. Ed.* **1992**, *31*, 1475-1477.

(14) Kellersberger, K. A.; Anderson, J. D.; Ward, S. M.; Krakowiak, K. E.; Dearden, D. V. *J. Am. Chem. Soc.* **2001**, *123*, 11316-11317.

(15) Gutsche, C. D. In *Calixarenes: A Versatile Class of Macrocyclic Compounds*; Vicens, J., Böhmer, V., Eds.; Kluwer Academic Publishers: Dordrecht, 1991; Vol. 3, p 264.

(16) Lagona, J.; Mukhopadhyay, P.; Chakrabarti, S.; Isaacs, L. *Angew. Chem. Int. Ed.* **2005**, *44*, 4844-4870.

(17) Zhao, J.; Kim, H.-J.; Oh, J.; Kim, S.-Y.; Lee, J. W.; Sakamoto, S.; Yamaguchi, K.; Kim, K. *Angew. Chem. Int. Ed.* **2001**, *40*, 4233-4235.

(18) Isobe, H.; Sato, S.; Nakamura, E. *Org. Lett.* **2002**, *4*, 1287-1289.

(19) Moon, K.; Chen, W.-Z.; Ren, T.; Kaifer, A. E. *CrystEngComm* **2003**, *5*, 451-453.

(20) Day, A. I.; Blanch, R. J.; Arnold, A. P.; Lorenzo, S.; Lewis, G. R.; Dance, I. *Angew. Chem. Int. Ed.* **2002**, *41*, 275-277.

(21)   Liu, S.; Zavalij, P. Y.; Isaacs, L. *J. Am. Chem. Soc.* **2005**, *127*, in press.

(22)   Day, A. I.; Arnold, A. P.; Blanch, R. J. *Molecules* **2003**, *8*, 74-84.

(23)   Jon, S. Y.; Selvapalam, N.; Oh, D. H.; Kang, J.-K.; Kim, S.-Y.; Jeon, Y. J.; Lee, J. W.; Kim, K. *J. Am. Chem. Soc.* **2003**, *125*, 10186-10187.

(24)   O'Leary, B. M.; Szabo, T.; Svenstrup, N.; Schalley, C. A.; Lutzen, A.; Schafer, M.; Julius Rebek, J. *J. Am. Chem. Soc.* **2001**, *123*, 11519-11533.

(25)   Kölbel, M.; Menger, F. M. *Adv. Mater.* **2001**, *13*, 1115-1119.

(26)   Meissner, R. S.; Rebek, J., Jr.; Mendoza, J. d. *Science* **1995**, *270*, 1485-1488.

(27)   Cow, C. N.; Harrison, P. H. M. *J. Org. Chem.* **1997**, *62*, 8834-8840.

(28)   Sun, S.; Britten, J. F.; Cow, C. N.; Matta, C. F.; Harrison, P. H. M. *Can. J. Chem.* **1998**, *76*, 301-306.

(29)   Mock, W. L.; Manimaran, T.; Freeman, W. A.; Kuksuk, R. M.; Maggio, J. E.; Williams, D. H. *J. Org. Chem.* **1985**, *50*, 60-62.

(30)   Rebek Jr., J. *Angew. Chem. Int. Ed.* **2005**, *44*, 2068-2078.

(31)   Jansen, R. J.; Rowan, A. E.; Gelder, R. d.; Scheeren, H. W.; Nolte, R. J. M. *Chem. Commun.* **1998**, *1998*.

(32)   Burnett, C. A.; Lagona, J.; Wu, A.; Shaw, J. A.; Coady, D.; Fettinger, J. C.; Day, A. I.; Isaacs, L. *Tetrahedron* **2003**, *59*, 1961-1970.

(33)   Butler, A. R.; Leitch, E. *J. Chem. Soc., Perkin Trans. 2* **1980**, *1*, 103-105.

(34)   Wu, A.; Chakraborty, A.; Witt, D.; Lagona, J.; Damkaci, F.; Ofori, M. A.; Chiles, J. K.; Fettinger, J. C.; Isaacs, L. *J. Org. Chem.* **2002**, *67*, 5817-5830.

(35)   Chakraborty, A.; Wu, A.; Witt, D.; Lagona, J.; Fettinger, J. C.; Isaacs, L. *J. Am. Chem. Soc.* **2002**, *124*, 8297-8306.

(36)   Lagona, J.; Fettinger, J. C.; Isaacs, L. *Org. Lett.* **2003**, *5*, 3745-3747.

(37)   Wagner, B. D.; Boland, P. G.; Lagona, J.; Isaacs, L. *J. Phys. Chem. B* **2005**, *109*, 7686-7691.

(38)   Miyahara, Y.; Goto, K.; Oka, M.; Inazu, T. *Angew. Chem. Int. Ed.* **2004**, *43*, 5019-5022.

(39)   Pichierri, F. *Chem. Phys. Lett.* **2005**, *403*, 252-256.

(40)   Steed, J. W.; Atwood, J. L. *Supramolecular Chemistry*; John Wiley & Sons: Chichester, 2000.

(41)   Zhang, H.; Paulsen, E. S.; Walker, K. A.; Krakowiak, K. E.; Dearden, D. V. *J. Am. Chem. Soc.* **2003**, 9284-9285.

(42)   Fujita, M.; Tominaga, M.; Hori, A.; Therrien, B. *Acc. Chem. Res.* **2005**, *38*, 369-378.

(43)   Park, K.-M.; Kim, S.-Y.; Heo, J.; Whang, D.; Sakamoto, S.; Yamaguchi, K.; Kim, K. *J. Am. Chem. Soc.* **2002**, *124*, 2140-2147.

(44)   Park, K.-M.; Whang, D.; Lee, E.; Heo, J.; Kim, K. *Chem. Eur. J.* **2002**, *8*, 498-508.

(45)   Park, K.-M.; Roh, S.-G.; Lee, E.; Kim, J.; Kim, H.-j.; Lee, J. W.; Kim, K. *Supramol. Chem.* **2002**, *14*, 153-158.

(46)   Kim, K.; Jeon, W. S.; Kang, J.-K.; Lee, J. W.; Jon, S. Y.; Kim, T.; Kim, K. *Angew. Chem. Int. Ed.* **2003**, *42*, 2293-2296.

(47)   Kim, K.; Kim, D.; Lee, J. W.; Ko, Y. H.; Kim, K. *Chem. Commun.* **2004**, 848-849.

(48)   Tan, Y.; Choi, S.; Lee, J. W.; Ko, Y. H.; Kim, K. *Macromolecules* **2002**, *35*, 7161-7165.

(49)   Tuncel, D.; Steinke, J. H. G. *Macromolecules* **2004**, *37*, 288-302.

(50)   Mock, W. L.; Irra, T. A.; Wepsiec, J. P.; Manimaran, T. L. *J. Org. Chem.* **1983**, *48*, 3619-3620.

(51)   Buschmann, H.-J.; Cleve, E.; Mutihac, L.; Schollmeyer, E. *Microchem. J.* **2000**, *64*, 99-103.

(52)   Ong, W.; Gomez-Kaifer, M.; Kaifer, A. E. *Org. Lett.* **2002**, *4*, 1791-1794.

(53)   Kim, H.-J.; Jeon, W. S.; Ko, Y. H.; Kim, K. *PNAS* **2002**, *99*, 5007-5011.

(54)   Ong, W.; Kaifer, A. E. *Angew. Chem. Int. Ed.* **2003**, *42*, 2164-2167.

(55)   Lim, Y.-b.; Kim, T.; Lee, J. W.; Kim, S.-m.; Kim, H.-J.; Kim, K.; Park, J.-s. *Bioconjugate Chem.* **2002**, *13*, 1181-1185.

(56)   Lee, J. W.; Kim, K.; Choi, S.; Ko, Y. H.; Sakamoto, S.; Yamaguchi, K.; Kim, K. *Chem. Commun.* **2002**, 2692-2693.

(57)   Jeon, W. S.; Ziganshina, A. Y.; Lee, J. W.; Ko, Y. H.; Kang, J.-K.; Lee, C.; Kim, K. *Angew. Chem. Int. Ed.* **2003**, *42*, 4097-4100.

(58)   Jeon, Y. J.; Bharadwaj, P. K.; Choi, S.; Lee, J.; Kim, K. *Angew. Chem. Int. Ed.* **2002**, *41*, 4474-4476.

(59)   Lee, H.-K.; Park, K. M.; Jeon, Y. J.; Kim, D.; Oh, D. H.; Kim, H. S.; Park, C. K.; Kim, K. *J. Am. Chem. Soc.* **2005**, *127*, 5006-5007.

(60)   Ko, Y. H.; Kim, K.; Kang, J.-K.; Chun, H.; Lee, J. W.; Sakamoto, S.; Yamaguchi, K.; Fettinger, J. C.; Kim, K. *J. Am. Chem. Soc.* **2004**, *126*, 1932-1933.

(61)   Jeon, W. S.; Kim, H.-J.; Lee, C.; Kim, K. *Chem. Commun.* **2002**, 1828-1829.

(62)   Choi, S.; Park, S. H.; Ziganshina, A. Y.; Ko, Y. H.; Lee, J. W.; Kim, K. *Chem. Commun.* **2003**, 2176-2177.

(63)   Ziganshina, A. Y.; Ko, Y. H.; Jeon, W. S.; Kim, K. *Chem. Commun.* **2004**, 806-807.

(64)   El Haouaj, M.; Young, H. K.; Luhmer, M.; Kim, K.; Bartik, K. *J. Chem. Soc., Perkin Trans. 2* **2001**, *11*, 2104-2107.

(65)   Constabel, F.; Geckeler, K. E. *Tetrahedron Letters* **204**, *45*, 2071-2073.

(66)   Kim, S.-Y.; Jung, I.-S.; Lee, E.; Kim, J.; Sakamoto, S.; Yamaguchi, K.; Kim, K. *Angew. Chem. Int. Ed.* **2001**, *40*, 2119-2121.

(67)   Jeon, Y.-M.; Kim, J.; Whang, D.; Kim, K. *J. Am. Chem. Soc.* **1996**, *118*, 9790-9791.

(68)	Heo, J.; Kim, J.; Whang, D.; Kim, K. *Inorg. Chim. Acta* **2000**, *297*, 307-312.

(69)	Whang, D.; Heo, J.; Park, J. H.; Kim, K. *Angew. Chem. Int. Ed.* **1998**, *37*, 78-80.

(70)	Heo, J.; Kim, S.-Y.; Whang, D.; Kim, K. *Angew. Chem. Int. Ed.* **1999**, *38*, 641-643.

(71)	Samsonenko, D. G.; Sharonova, A. A.; Sokolov, M. N.; Virovets, A. V.; Fedin, V. P. *Russian Chemical Bulletin, International Edition* **2001**, *27*, 10-15.

(72)	Buschmann, H.-J.; Jansen, K.; Meschke, C.; Schollmeyer, E. *Journal of Solution Chemistry* **1998**, *27*, 135-140.

(73)	Gerasko, O. A.; Gerasko, O. A.; Virovets, A. V.; Samsonenko, D. G.; Tripol´skaya, A. A.; Fedin, V. P.; Fenske, D. *Russ. Chem. Bull., Int. Ed.* **2003**, *52*, 585-593.

(74)	Samsonenko, D. G.; Sokolov, M. N.; Virovets, A. V.; Pervukhina, N. V.; Fedin, V. P. *Eur. J. Inorg. Chem.* **2001**, *2001*, 167-172.

(75)	Sokolov, M. N.; Dybtsev, D. N.; Fedin, V. P. *Russian Chemical Bulletin, International Edition* **2003**, *52*, 1041-1060.

(76)	Sokolov, M. N.; Dybtsev, D. N.; Virovets, A. V.; Clegg, W.; Fedin, V. P. *Russ. Chem. Bull., Int. Ed.* **2001**, *50*, 1144-1147.

(77)	Zhang, F.; Yajima, T.; Li, Y.-Z.; Xu, G.-Z.; Chen, H.-L.; Liu, Q.-T.; Yamauchi, O. *Angew. Chem. Int. Ed.* **2005**, *44*, 3402-3407.

(78)	Whang, D.; Heo, J.; Kim, C.-A.; Kim, K. *Chem. Commun.* **1997**, 2361-2362.

(79)	Samsonenko, D. G.; Lipkowski, J.; Gerasko, O. A.; Virovets, A. V.; Sokolov, M. N.; Fedin, V. P.; Platas, J. G.; Hernandez-Molina, R.; Mederos, A. *Eur. J. Inorg. Chem.* **2002**, 2380-2388.

(80)	Gerasko, O. A.; Samsonenko, D. G.; Sharonova, A. A.; Virovets, A. V.; Lipkowski, J.; Fedin, V. P. *Russ. Chem. Bull., Int. Ed.* **2002**, *51*, 346-349.

(81)	Butler, A. R.; Hussain, l.; Leitch, E. *J. Chem. Soc., Perkin Trans. 2* **1980**, 106-109.

(82)	Hnizda, V.; Brown, D. J. *J. Phys. Chem.* **1932**, *36*, 2842-2843.

(83)	Hardy, B. P. M.; Nicholls, A. C.; Rydon, H. N. *J. Chem. Soc., Perkin Trans. 2* **1972**, 2270-2278.

(84)	Day, A.; Arnold, A. P.; Blanch, R. J.; Snushall, B. *J. Org. Chem.* **2001**, *66*, 8094-8100.

(85)	Kleinpeter, E. *Struct. Chem.* **1997**, *8*, 161-173.

(86)	Havera, H. J.; Strycker, W. G.; Miles Laboratories, Inc.: USA, 1976, p 14.

(87)	Cortes, S.; Liao, Z.-K.; Watson, D.; Kohn, H. *J. Med. Chem.* **1985**, *28*, 601-606.

(88)	Hotha, S.; Yarrow, J. C.; Yang, J. G.; Garrett, S.; Renduchintala, K. V.; Mayer, T. U.; Kapoor, T. M. *Angew. Chem. Int. Ed.* **2003**, *42*, 2379-2382.

(89)	Marton, J.; Enisz, J.; Hosztafi, S.; Tímár, T. *J. Agric. Food. Chem.* **1993**, *41*, 148-152.

(90)   Nakajima, M.; Itoi, K.; Takamatsu, Y.; Kinoshita, T.; Okazaki, T.; Kawakubo, K.; Shindo, M.; Honma, T.; Tohjigamori, M.; Haneishi, T. *J. Antibiotics* **1991**, *44*, 293-300.

(91)   Bodanszky, M. *Principles of Peptide Synthesis*; 2nd ed.; Springer-Verlag: Berlin, 1993.

(92)   Beller, M.; Eckert, M.; Moradi, W. A.; Neumann, H. *Angew. Chem. Int. Ed.* **1999**, *38*, 1454-1457.

(93)   Yamada, M.; Takahashi, S.; Kogyo, K. K.; Kaisha, K.: USA, 1991, p 4.

(94)   Hendel, W.; Leonding, A. T.; Kloistein, E.; Klaus, L.; Viehböck, A.; Haidinger, K.; Linz, A. T.: Germany, 1994, p 6.

(95)   Woodbury, R. P.; Clarke, R.; Dow, 2005; Vol. 2005.

(96)   Sarges, R.; Howard Jr., H. R.; Kelbaugh, P. R. *J. Org. Chem.* **1982**, *47*, 4081-4085.

(97)   Muccioli, G. G.; Wouters, J.; Poupaert, J. H.; Norberg, B.; Poppitz, W.; Scriba, G. K. E.; Lambert, D. M. *Org. Lett.* **2003**, *5*, 3599-3602.

(98)   Muccioli, G. G.; Poupaert, J. H.; Wouters, J.; Norberg, B.; Poppitz, W.; Scriba, G. K. E.; Lambert, D. M. *Tetrahedron* **2003**, *59*, 1307-1307.

(99)   Kinoshita, T.; Sato, S.; Tamura, C. *Tetrahedron Lett.* **1971**, *12*, 3695-3696.

(100)   Koningsveld, H. v. *Tetrahedron* **1976**, *32*, 2121-2122.

(101)   Hoffmann, R. W.; Hagenbruch, B.; Smith, D. M. *Chem. Ber.* **1978**, *110*, 23-36.

(102)   Thieme, P. C.; Haedicke, E. *Justus Liebigs Annalen der Chemie* **1978**, *2*, 227-237.

(103)   Iwata, M.; Bruice, T. C.; Carrell, H. L.; Glusker, J. P. *J. Am. Chem. Soc.* **1980**, *102*, 5036-5044.

(104)   Cameron, A. F.; Cameron, I. R.; Duncanson, F. D. *J. Chem. Soc., Perkin Trans. 2* **1981**, *5*, 789-793.

(105)   Allen, F. H. *Acta. Cryst.* **2002**, *B58*, 380-388.

(106)   Bruno, I. J.; Cole, J. C.; Edgington, P. R.; Kessler, M.; Macrae, C. F.; McCabe, P.; Pearson, J.; Taylor, R. *Acta. Cryst.* **2002**, *B58*, 389-397.

(107)   Schulte, K. E.; von Weissenborn, V.; Kwon, S. K. *Arch. Pharm.* **1976**, *309*, 1016-1019.

(108)   McMurry, J. *Organic Chemistry*; 4th ed.; Brooks/Cole Publishing Company: Pacific Grove, 1996.

(109)   Pauling, L.; Allen, L. C.; Allred, A. L. In *CRC Handbook of Chemistry and Physics*; Lide, D. R., Ed.; CRC Press LLC: Boca Raton, 2003, pp 9-74.

(110)   Gomberg, M. *J. Am. Chem. Soc.* **1900**, *22*, 757-771.

(111)   Kutepov, D. F.; Potashnik, A. A.; Khokhlov, D. N.; Tuzhilkina, V. A. *Zhurnal Obshchei Khimii* **1959**, *29*, 855-858.

(112)   Broan, C. J.; Butler, A. R.; Reed, D.; Sadler, I. H. *J. Chem. Soc., Perkin Trans. 2* **1989**, 731-740.

(113)   Smith, J. N.; Hoffman, J. T.; Shirin, Z.; Carrano, C. J. *Inorg. Chem.* **2005**, *44*, 2012-2017.

(114)   Ueyama, N.; Nishikawa, N.; Yamada, Y.; Okamura, T.; Oka, S.; Sakurai, H.; Nakamura, A. *Inorg. Chem.* **1998**, *37*, 2415-2421.

(115)   Blessing, R. H. *Acta Cryst.* **1995**, *A51*, 33-38.

(116)   Sheldrick, G. M.: Göttingen, 1997.

(117)   Barbour, L. J. *J. Supramol. Chem.* **2003**, *1*, 189-191.

Chapter 3: Fullerene-Calixarene solid state structures; manipulating solid state from the liquid phase

Abstract

It has been determined that the fullerene C_{70}, a minor product in the normal formulation of fullerenes, can have a profound effect on the solid state structure of fullerene C_{60} when combined with calix[5]arene in toluene.[1] A complicated sheet of fullerenes is formed when pure C_{60} and calix[5]arene form crystals.[2] However with the addition of a small amount of C_{70} (among other globular molecules) the structure is simplified so that the C_{60} now forms a one dimensional helical strand surrounded by a network of calix[5]arene molecules.

A tentative hint of the C_{70}:calix[5]arene complex was found when pure C_{70} is co-crystallized with calix[5]arene in a solution of *p*-xylene resulting in another structure.[3] Calix[5]arene and C_{70} in *p*-xylene form a ball-and-socket supramolecular complex with the C_5 axis of the fullerene tilted 40° relative to the symmetry axis of the calixarene, the extended structure comprising of well-separated zigzag sheets of C_{70} molecules. The solvent has been ruled out as a possible reason for this change in solid state character for C_{60} since with *p*-xylene instead of toluene as solvent, similar crystals are formed (as determined by the unit cells). This effect seems to involve not only the host-guest properties of the larger fullerene as it was found that C_{84} and carboranes can also induce the C_{60}:Calix[5]arene:toluene structure. Further conformation of the differences in the three structures was determined by examining the bulk compounds using powder x-ray

diffraction and HPLC. The unique ability of the fullerene:calix[5]arene system was determined when investigating calix[6]arene and mixed fullerene compounds.

3.1   *Impetus for project*

In the quest for structural archetypes that can act as tectons or devices on future nanomachinery, the arena of fullerene research is one that shows much promise. Fullerenes are quite recent discoveries, only fully characterized since 1990. Yet since their discovery they have gone on to be one of the most researched molecules ever. This class of molecule has been a dominant interest in both the Raston and Atwood groups for many years now and fullerenes where an impetus for both this project and to a lesser extent the research in Chapter 4.

An important aspect of building structures on the nanoscale level is the ability to manipulate the process such that the required conformations can be mediated, preferably by simple and efficient means and little post processing. To this end it was decided to investigate how it may be possible to affect the structural characteristics of supramolecular constructs of fullerenes and calixarenes. This aim was to develop an understanding of what are the general aspects of the solid state structures that we have managed to develop between the fullerenes C_{60} and C_{70} with calix[5]arenes.

The impetus of this project was the unusual formation of five fold linear chains of C_{60} that crystallized out with calix[5]arene (denoted the "Z-array") . Surprisingly we found subtle changes of fullerene ratios will lead to vastly different structures. *The hypothesis for this project is that while C_{70} interrupts the structural conformation of the calixarene with C_{60}, the smaller fullerene has a stronger interaction with the calixarene and so falls out of solution in preference to C_{70} fullerene.*

3.2   *Fullerene background*

3.2.1   Discovery and characterization of C_{60} and C_{70}.

In 1984, E. A. Rohlfing and co-workers were laser ablating carbon rods to determine gas phase carbon cluster masses.[4] The bimodal structure of the spectrum they obtained showed clusters forming in multiples of one carbon atom per cluster up to ~C_{30} and another overlapping series of carbon atom clusters building up in groups of two atoms from ~ C_{20} up to C_{90}. Unnoticed by them among the spectrum they obtained was two carbon cluster peaks relatively higher than those around them. These relatively larger peaks were at m/z = 720 (C_{60}) and a smaller, less distinguishable peak at m/z = 840 (C_{70}). They attributed the characteristics of the spectra as belonging to a triply bonded ethyne phase of carbon, a theoretical construct considered at the time to be the likely suspect.

It took another year for the true elucidation of the structure of fullerene C_{60}.[5] In 1985, Smalley, Kroto and coworkers at Rice University, Texas, were trying to interpret interstellar gas molecular signatures. To do this they were attempting to compare the unknown signatures with the mass spectra of carbon clusters from laser ablation of carbon rods. Again, the mass spectrum showed a stable structure for sixty and seventy carbon atoms though because of the differing conditions compared to that performed by Rohlfing *et al.* the peaks at the m/z for C_{60} and C_{70} were a lot more prevalent.

They realized that the only way a molecule of sixty carbon atoms could be stable without any dangling reactive valence electrons was through the three dimensional enclosed space of the sphere-like Archimedean solid, the truncated icosahedron. Using a simple molecular model kit and the constraints of carbon chemistry they determined that the sphere was made from twenty hexagonal rings surrounding twelve pentagonal rings

(Figure 3.1). The larger cluster molecule C_{70} was similarly theorized as an elongated C_{60} with an extra ring of benzene substituents around the centre. The authors gave these clusters the name buckminsterfullerene after realization that the geometrical shape and construction of C_{60} had already been visualized by the architect Buckminster Fuller.[6]

This amazing realization based solely on peaks on a mass spectrograph (which gives information on both mass and stability) and the group's proposed theoretical structures electrified the scientific community. It took five years however to prove the hypothetical
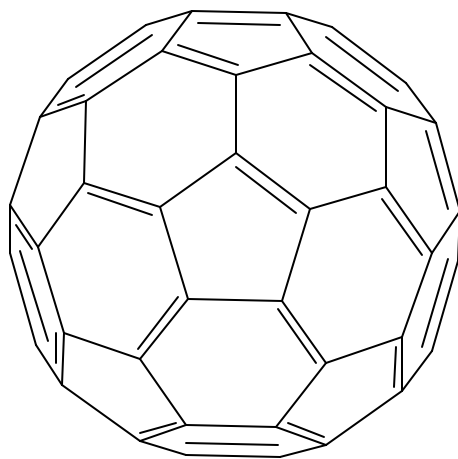
Figure 3.1. The elucidated structure of C_{60} by Kroto *et al.*

structures. In 1990, a process was discovered whereby milligram amounts of fullerenes could be isolated and the prediction could be assessed.[7] Analysis *via* ^{13}C NMR spectroscopy[8] and eventually crystal structures of C_{60} and C_{70} proved that the structures visualized by Kroto and Smalley's group was correct.[9] The third allotrope of carbon (after graphite and diamond) has been intensively researched ever since and led to Kroto, Smalley and coworker R. F. Curl getting the Nobel Prize in 1996.

3.2.2   Formation and isolation of fullerenes.

Unfortunately the initial method of laser ablation of carbon rods was not a high yielding one for fullerenes. The product mixture, called fullerite, consists of a variety of products which besides amorphous carbon includes larger fullerenes and other similar structures such as bucky onions, bucky horns and most likely even carbon nanotubes (though they were not known to be there at the time). Until 1990 when Kraetschmer *et al.* found a method for producing large amounts of C_{60} and C_{70}, fullerite was too difficult a mix to do any more than analytical chemistry.[7] The method to produce milligram amounts of fullerenes was simple enough. It consisted of merely heating a carbon rod up in an inert argon atmosphere. The resulting smoke contained a relatively appreciable amount of the two most common fullerenes.

Even at this point there was still an "impurity" within C_{60}, there being approximately 1% of C_{70}. So chromatography[10] or complexation[11] has been used to further separate the two fullerenes. The former method involved a neutral alumina column and hexane eluent. The latter method involves using the cup shaped *tert*-methyl-calix[8]arene. The first method led to enough material to be isolated for single crystal studies to be conducted and in 1991 the structural determination of C_{60} proved beyond doubt the truncated icosahedron shape of buckminsterfullerene.[9] Since then, several other types of fullerenes ($C_{70}, C_{76}, C_{78}, C_{84}$) have become commercially available.

3.2.3   Variety of fullerenes.

Besides the two major fullerenes C_{60} and C_{70}, there are a whole range of fullerene "analogues" containing both larger and smaller amounts of carbon atoms. The structures possible from both actual and theoretical studies have followed "the pentagonal rule".

Simply put, for a surface comprising of pentagons and hexagons, the only way a structure can combine together without leaving irregular gaps is by surrounding each pentagon with hexagons. In fact, because successively larger fullerenes are formed by adding rings of hexagons around the waist of C_{60}, there are always only 12 pentagons.[12]

From a synthetic viewpoint, once macroscopic gram scale amounts of fullerenes could be created, ^{13}C NMR spectroscopy revealed fullerenes all the way up to C_{102}.[13] Owing to the intrinsic stability of C_{60} and C_{70}, the next larger and most common fullerenes are C_{76} and C_{78}.[10] There are various reasons why the structures have not been quantified by solid state structures. First, their low yield (< 1% versus yields of C_{60} and C_{70}) has made it difficult to produce enough material so that single crystal studies can be conducted. The major complication however is that fullerenes higher than C_{70} become chiral which results in isomers are (e.g.: C_{76}, two; C_{78}, five[6]) possible and indeed have been detected *via* spectroscopic techniques.[14,15] The isomers come about because that while each pentagonal ring of carbons must be surrounded by hexagonal rings, the hexagonal rings do no require to be attached to a pentagonal ring. Therefore the placement of the pentagons can be changed and so structural isomers form.

3.2.4   Properties of fullerenes.

The majority of the studies of the properties of fullerenes have been on C_{60} and to a lesser extent, C_{70}. Fullerenes are quite soluble in many solvents, though the aromatic or halogenated solvents are generally the best.[16] Since fullerenes are electron deficient, solvents capable of electron pair donation and polarizability also allowed for enhanced solubility.[17] Though they are soluble in solvents the time to actually dissolve into solution can be upwards of twenty four hours.

In the typical solvent systems of benzene or toluene, pure C_{60} is a deep purple color and C_{70} a darker red color. This therefore means that mixtures of C_{60} and C_{70} result in the solution being a deep red. However it had been reported that the color of C_{60} in solution varies depending on the solvent. This is attributed to charge transfer between fullerene and solvent rather than aggregation of the fullerene.[18] It is thought that the electron deficient fullerene accepts some electron density from the surrounding solvent and the absorption produces the complementary color that is viewed. The change in color in different solvents was shown *via* UV-Vis spectroscopy to be an optical illusion due to differences in solubility (and so concentration) giving the impression of a different color. While this research had determined that in solution the fullerenes are generally monomeric, there has been evidence for aggregation in benzonitrile.[19,20]

Due to their electron deficiency, fullerenes will readily acquire electrons to become fullerides, even picking up electrons from less than 1% impurities in toluene-acetonitrile solutions.[21] The fullerene anion has increased solubility but also leads to side reactions that can end in degradation of the fullerene. While adding electrons to the electron deficient fullerenes is relatively easy, more difficult routes are required to produce a fullerene cation. Reaction of C_{60} with the superacid $H(CB_{11}H_6X_6)$ (X = Cl, Br) resulted in the first fullerene cation HC_{60}^+.[22] The binding energy of this cation has been somewhat controversial due to the difficulties in analysis before decomposition or side reactions occur.[23]

Fullerenes, like benzene generally undergo addition reactions in preference to other classes of reaction.[12] The only proviso in using C_{60} is that due to symmetry concerns the entire molecule acts as a single giant atom of approximately 10 Å diameter and so steric

considerations must be recognized before undertaking regular synthetic chemistry. However the addition of substituents to fullerenes is usually found to be regioselective with additions usually occurring on a hexagonal carbon ring in a 1,2 or 1,4 conformation.

3.2.5   Interfullerene bonding.

In regards to the research of structural supramolecular chemistry, one of the more intriguing aspects of fullerenes is using them as substrates for molecular polymers or wires. As will be explored in Chapter 4, carbon nanotubes are interesting and useful macromolecules that unfortunately are synthesized with a vast array of diameters and chiralities.[24] As one avenue of attack to controlling the size and length of carbon nanotubes, it would be convenient to be able to preorganize the carbon precursors. Starting with the known dimensions of fullerenes, it has been theorized that it could be possible to condense them into nanotubes.

Using organic molecules to position fullerenes so that interfullerene bonding can occur allows for a range of fullerene polymers to form. High pressure techniques had been used to form C_{60} dimers, with the two C_{60} molecules bonded with a simple carbon-carbon bond on adjacent carbons.[25] After five GPa of pressure at 200°C and removing the organic spacer it was found that this could be achieved in 80% yield. By using a co-crystallizing technique from research in our group, it became possible to take linear preorganized rows of fullerenes and polymerize them into even longer chains.[26] Their ability as wires was questioned however due to the fragility of the polymer and that the inter-fullerene linkage, a single carbon-carbon bond is not conducive to electron conduction.

Using alkali metals, some control has also been obtained with interfullerene bonding when using fullerides rather than neutral fullerenes. It has been shown that the size of the metal is important in the overall interfullerene structure formed. For instance when lithium is the counter ion during [2 + 2] cycloaddition reactions of C_{60}, a two dimensional polymer is formed with two bonds between two fullerene and a single bond between fullerenes orthogonal to the first two.[27] Other larger cations disrupt the two dimensional polymerization and C_{60} forms dimers or one dimensional chains with the counterions lying between the adjacent chains in the spaces formed by the bulky fullerene.[28-31]

In comparison, it has been quite difficult to find a method whereby C_{70} could be polymerized.[32] However, using a high pressure piston-and-cylinder on a crystal of C_{70} at 300°C it was found that much like C_{60} molecules, the larger fullerene can also form covalent bonds between spheres. Noteworthy though is that unlike the linear chains of C_{60}, the use of C_{70} results in a two dimensional zigzag conformation. This is due to the ovaloid shape of the larger fullerene, the regioselective 1,2 carbon-carbon bonding and the symmetrical constraints of producing C···C on a six-fold axis of a molecule with five-fold symmetry along its center.

Another method in an attempt to create nanotubes was to use a sol-gel method to form wires from fullerenes.[33] A batch of C_{70} was reduced which then allowed them to be solubilized in an aqueous solution, and after further processing, a sol-gel. The sol-gel was then added to an alumina template and the system was annealed at 500°C. Some success was found with this experiment with crystalline wires being produced which were both parallel and not bundled like carbon nanotubes. However, their diameters also covered a large range (100 – 300 nm) as well attenuating their usefulness.

3.2.6   Halogenated fullerene solid state chemistry.

Part of the impetus of the creation of this project was that fullerenes were on the verge of an exciting discovery in regards to superconductivity at the turn of the millennium. Our group was investigating solid state structures of fullerenes with an eye to controlling the spatial position of fullerenes using calix[n]arenes[34] or bromoform.[35]

The spacing between fullerenes was considered an intrinsic parameter of superconductivity until fraud tainted the results.[36,37] Crystals of C_{60} co-crystallized with alkali metals were shown to increase their temperature at which superconductivity ceased, from 20.1 K with K_3C_{60} to 32.5 K with Rb_2CsC_{60}.[37,38,39] Then it was discovered in 1995 that small halogenated methane analogues were also found to readily co-crystallize with fullerenes.[40] These structures were determined in 2001 to produce an amazingly high superconductivity transition temperature of 117 K when tribromomethane was the spacing counterion.[35] By increasing the interfullerene distance in the crystal structure with the introduction of inert haloforms, the authors and others reasoned that this therefore also increased the density of states allowing for increased electron and hole doping.[37] This result sent superconductivity researchers scratching their heads somewhat as it did not follow the expected theory of superconductivity.

Unfortunately all the work was put into disrepute when it was found by co-workers that some of the results had been copied and presented as original data even though they had been found to be from completely different chemical systems. The density of states argument was also uncertain, others finding that the crystal structure showed that differing haloforms produced similar structures with little change in the spacing between

fullerenes as would've been expected.[41] The copied data put the whole area of their research into disrepute.

Anecdotally it was also noted that only 1 in 100 of these crystals would perform as expected. The cracking of single crystals is still a problem for superconducting research to this day, superconductivity stopping at the crystal boundary and effectively reducing the coherence length. Since then the focus on superconductivity with C_{60} molecules has, like with polymers, been based on a metal-fullerene rather than a halogen-fullerene framework. Other parts of the periodic table have been explored as well; for instance the use of lanthanum.[42] Again, showing the difficulty of this research the authors found that the superconductivity of the lanthanum-fullerene compound was actually from a lanthanum-carbide phase.

3.3   Calix[n]arenes

Along with C_{60} and C_{70} fullerenes, this project focuses on the supermolecular interactions of calix[n]arenes. The calix[n]arenes are macrocyclic compounds synthesized from a mixture of formaldehyde and phenols (Figure 3.2).[43] They come in a range of sizes and the yields are condition dependent. Generally, a base induced condensation reaction between *p-tert*-butyl-phenol produces a range of *p-tert*-butyl-calix[n]arenes (Scheme 3.1).

Like cucurbiturils in Chapter 2, the initial formation is thought to form as long acyclic oligomers that then separate or "crack" and cyclize into the macrocycle. The *p-tert*-butyl-calix[n]arenes are then turned to calix[n]arenes using aluminum chloride.[43] This general synthesis produces calix[n]arenes from n = 4 – 8. Even numbered calixarenes are fairly simple to make with methods available to produce a majority

product that is the tetramer, hexamer or octamer. However, production of calix[n]arenes consisting of odd numbered quantities of the precursors is quite difficult.
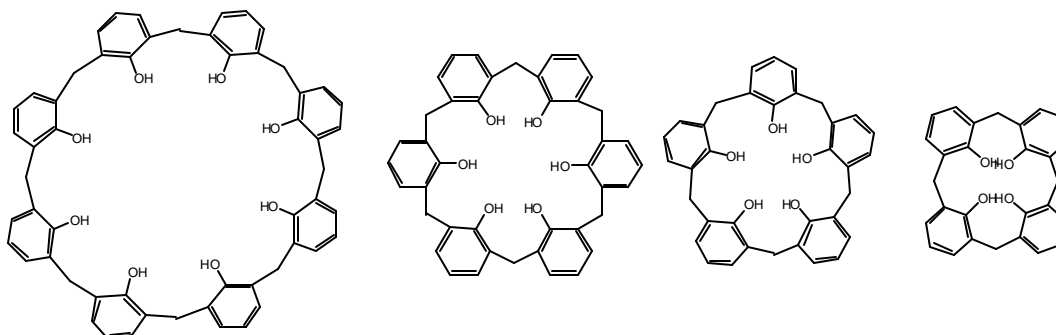
Figure 3.2. Structure of the most common calix[n]arenes (n = 4 – 8).

Calix[5]arene, being an odd numbered macrocycle is difficult to synthesize, and the first "high" yielding method was found quite recently.[44] The yield in this method, while only 15%, allowed *p-tert*-calix[5]arene and its functionalized analogues to become more than just curiosities. It has properties similar in some respects to its larger and smaller cousin. Like calix[4]arene, calix[5]arene is more rigid than the floppy calix[6]arene or calix[8]arene, leading to the favored conformation being the cone. However like calix[6]arene it has a larger cavity than the calix[4]arene so it can complex larger guests than just solvent, gas or other small molecules.[45]

3.3.1   Fullerene interactions with curved hosts.

There are now many types of structurally different authenticated arrays of C_{60} involving large calixarenes and related molecules, and molecules with curved surfaces (Figure 3.3). Large enough arms on the upper rims of *p*-benzylcalix[5]arene or *p*-benzylhexahomooxacalix[3]arene lead to a complete encapsulation of the fullerene C_{60} resulting in discrete aggregates.[46] Mixtures of C_{60} and C_{70} with *p-tert*-butyl-calix[8]arene have been identified and characterized, it suspected that three calixarenes encapsulate

three C_{60} molecules or a ratio of 2:1 $C_{60}:C_{70}$ reside within.[47] A one-dimensional array of linear C_{60} molecules results in the solid state structure of the fullerene with *p*-bromocalix[4]arene propyl ether.[26,48] Showing how control of alignment of the fullerenes can be instigated, the use of the calixarene like molecule cyclotriveratrylene results in a zigzag array rather than a strict linear column.[49,50] Then by changing the concentration of C_{60} to cyclotriveratrylene results in a more complicated hexagonal-close packed two-dimensional arrays. Linear double strands were formed using the curved molecule bis(ethylenedithio)tetrathiafulvalene.[51] An even large Z-array of five strands resulted with calix[5]arene and C_{60} where co-crystallized on their own.[2] As will be seen in Chapter 4 saddle shaped molecules of Ni(TMTAA) produced corrugated sheets of fullerenes.[52] Finally using calix[6]arene results in more complex three dimensional constructs.[53]
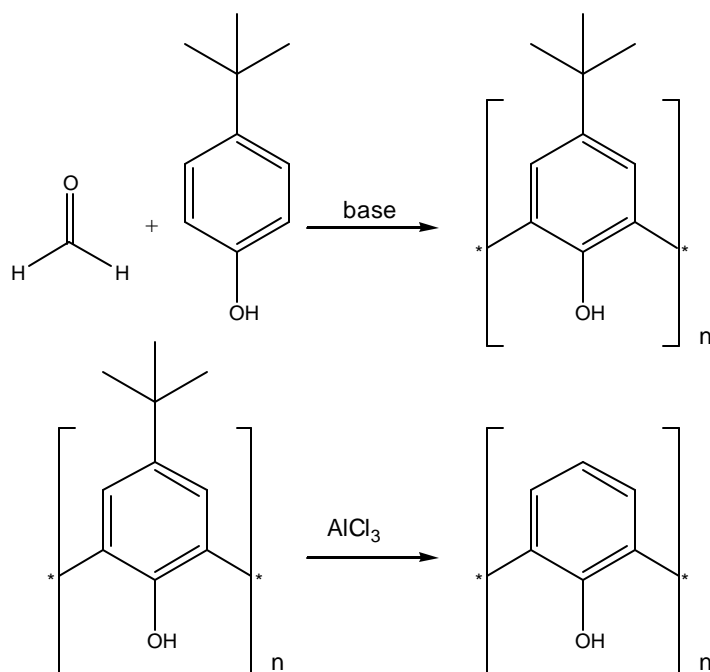
Scheme 3.1. General synthesis of calix[n]arenes (n = 4 – 8).

The discovery that calixarenes and fullerenes readily form host-guest complexes was initiated by our group in 1994.[11] It was found *tert*-butyl-calix[8]arene would selectively extract C_{60} and C_{70} from fullerite. The fullerene C_{60} could then be recovered from the complex with the addition of chloroform which binds stronger to the inner cavity of *tert*-butyl-calix[8]arene than C_{60}. This allowed for C_{60} to be separated from fullerite with >99.5% purity. It was this complex that was later determined computationally to be a micelle-like system formed between three *tert*-butyl-calix[8]arene and three fullerenes.[47] This was further supported by Langmuir-Blodgett film studies of *tert*-butyl-calix[8]arene and C_{60}.[54] The complexation between calixarene and fullerene in carbon tetrachloride was found to be strongest when the calixarene was preformed into a cone conformation.[55] Thus it was shown that it was difficult for *tert*-butyl-calix[6]arene and *tert*-butyl-calix[8]arene molecules to complex fullerenes when the lower rim hydroxyl groups were protected thus disrupting hydrogen bonding and stopping the hosts forming the cone conformation.

HPLC experiments using fullerenes covalently bonded to silica gel show that in solution *tert*-butyl-calix[8]arene has stronger binding in comparison to *tert*-butyl-calix[6]arene.[56] However the larger *tert*-butyl-calix[8]arenes, being so floppy, would bind in a different manner depending on functionality arranged on the ring. By changing the lower rim of *tert*-butyl-calix[8]arene from hydroxy- to methoxy-functional group and disrupting the hydrogen bonding that allows calixarenes to preferentially form cone conformations, it was found that both *tert*-butyl-calix[8]arene and *tert*-butyl-calix[6]arene would only encapsulate a single C_{60}, irrespective of the solvent.[57]

This inherent floppiness of calix[6]arenes leads to a preference to a double cone conformation not seen in the smaller calixarenes. While this somewhat attenuates its ability to maximize interactions with single large molecules it was found to be useful for binding multiple molecules of fullerene.[53] Two molecules of either C_{60} or C_{70} would reside within a single calix[6]arene. Surprisingly, despite C_{70} fullerene being larger, the solid state crystal analysis finds both fullerene-calix[6]arenes structures to be isostructural. This arrangement yields a 1:2 host–guest complex in which the fullerenes form an extended three-dimensional crisscrossed array of linear strands.[53]
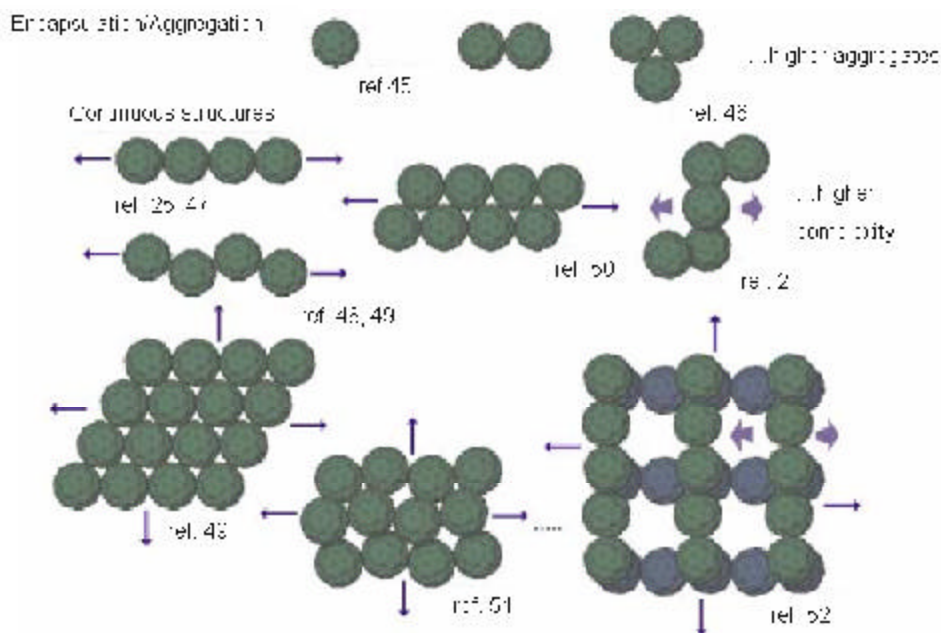
Figure 3.3. Structural arrays formed between curved molecular surfaces (guest molecules not shown to reveal fullerene positioning).

Calix[4]arenes have the shallowest cavity of the common calixarenes and are generally more difficult to complex with fullerenes. With the appropriate analogues it is however possible to co-crystallize. As mentioned previously our group managed to do so with *p*-bromocalix[4]arene propyl ether[48] and this structural motif was later used to form polymers of C_{60}.[26] Further structural engineering was possible and the importance of

substituents was shown when p-iodocalix[4]arene benzyl ether with fullerene C_{60} produced a bilayer structure in the solid state compared to the bromo- analogue.[58]

Like calix[4]arene, calix[3]arenes will not as the base compound complex with fullerenes. However as it is generally not possible to form the base calix[3]arene compound, the analogues that can be formed have a larger cavity than calix[4]arene. For instance, a hexahomotrioxacalix[3]naphthalene, a chiral calixarene, will form a 2:1 host-guest complex with C_{60}, as seen in solution and single crystal x-ray studies.[59] This was revealed by NMR to be solvent effected, the association constant being higher for the complex in toluene versus benzene (of which C_{60} is more soluble).

In 1998, Wang and Gutsche created a whole series of calixarenes that were singly or doubly bridged using covalent ether linkages between the calixarenes.[60] They showed that doubly bridged calix[n]arenes (n = 4 – 6) were too sterically restricted to allow into the resulting double cavity any fullerene. The more flexible mono-bridged bis-calixarenes were a different story, doubling or tripling the association constant for the respective complexation with C_{70} and C_{60} and highlighting the advantages of preorganization of supramolecular tectons. Bis-calix[4]arene still did not associate, the cavity still too small too hold a fullerene. However, the bis-calix[5]arene analogue was by far the best, a p-allyl-bis-calix[5]arene increasing complexation with C_{60} over normal calix[5]arene by over 40 fold. In an unusual synthesis the same authors produced a supermolecule of three or five calixarenes connected together by aryl ethynyl ketones.[61] The tri-calix[5]arene compound was found to form a 1:1 complex with C_{60}, supposedly with all cavities binding with the fullerene simultaneously.

3.3.2 Calix[5]arene-fullerene interactions.

One of the focus molecules of this project, calix[5]arene, has been found to be an excellent host for fullerenes due to it's unique properties compared to the other calixarenes. Besides the $\pi\cdots\pi$ bonding between the host and guest and common to all calixarenes, the C_{5v} cone conformation of calix[5]arene (Figure 3.4) are complementary to the pentagonal rings of C_{60} and this principle axis also matches the tapered end of C_{70}.[46] Accordingly it has been a popular choice for host-guest studies with fullerenes. Generally, 1:1 and 2:1 host-guest complexes result in which each fullerene is situated in the cavity of a calixarene. Various modified forms of calix[5]arene have also been used to probe the host-guest interaction, including substituted calix[5]arenes,[62,63] biscalix[5]arenes,[64-66] and calix[5]arenes self-assembled by means of non-covalent metal–ligand interactions.[67]
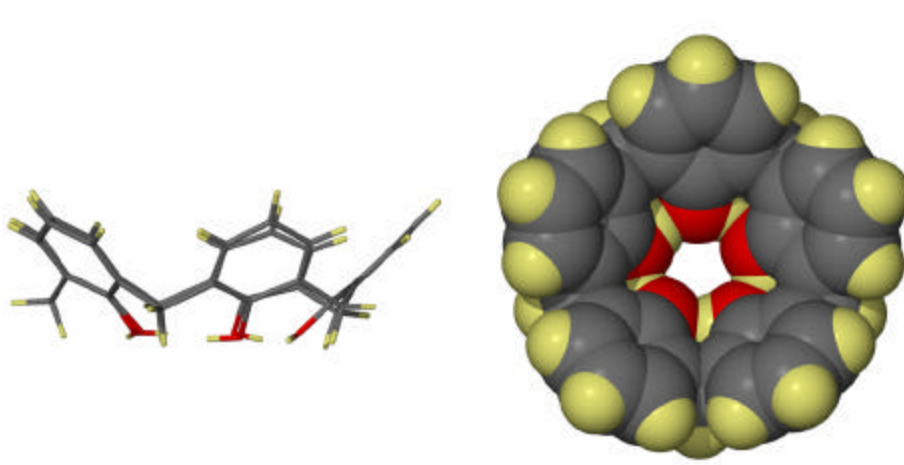
Figure 3.4. Side and top view of calix[5]arene showing shallow cavity, hydrogen bonding of the lower rim leading to a preferred cone conformation and five fold axis of symmetry (grey = carbon, red = oxygen, yellow = hydrogen).

Previous research in the Atwood and Raston groups has investigated the interplay between fullerene and calix[5]arene analogues extensively. *P*-benzylcalix[5]arene was

found to form an 2:1 host:guest complex with C_{60}.[46] The benzyl groups where mobile enough to make shallow an otherwise deep cavity and allow $\pi^{..}\pi$ between the two hosts. In solution however, it is thought that a 1:1 host:guest interaction occurs, the outer phenyl rings bonding with the fullerene in preference.[63] By making the outer rim substituents fixed using *p*-phenyl rather than *p*-benzyl functional groups, interdigitation occurred rather than overlap between the outer arms.

Calix[5]arene has been used with a variety of metals to improve the complexation characteristics of the guest. For instance Fukazawa's group has been very active in this regard. Initially they noted how calix[5]arenes with halogens or methyl groups decorating the upper rim at the *para*-position strongly bound C_{60}.[62,68] It was proposed that the halogens on the upper rim contributed to the 2:1 complexation due to inter-halogen attraction. Using calix[5]arene bound together at one point each, they have created a clam shell-like structure in which to ensnare fullerenes.[64] This supermolecule captured and kept the fullerene with an association constant of $76(\pm5) \times 10^3$ dm^3/mol, one of the largest constants to date. Next they developed a more complicated linker with pH dependent conformations.[69] It was proven that the two calix[5]arenes would open up when acid was added to the solution thus providing a switching mechanism for fullerene encapsulation. They have also found that rather than a pH dependent linker, a more complicated joining molecule that will preferentially complex silver and close the two calix[5]arenes can also allow the complexation of fullerenes.[70] Later they found that by adjusting the metal to copper and changing the linker between the calix[5]arenes it was possible to selectively bind C_{70} over C_{60}.[67] Meanwhile the group led by Gutsche managed to get a crystal structure of a bis-calix[5]arene with C_{60} fullerene.[66] The linker was a simple single

carbon-carbon bond across the para-position of the upper rim and produced a more open, larger cup that only encapsulated and covered just over half the fullerene C_{60}.

An extensive set of solution studies by Shinkai's group in 1997 revealed that calix[5]arene and homooxacali[3]arenes provided the strongest binding to fullerenes.[71] In solution and using *p-benzyl*-Calix[5]arene as the complexing agent, it has been shown that the typical four electron reduction of fullerene via voltammetry will split to eight indicating host-guest complexation.[21] All in all then, calix[5]arene has been a well studied and important encapsulating agent for fullerenes.

3.4 Controlling van der Waals *Contacts in Complexes of Fullerenes*

3.4.1   Calixarene:fullerene structure that instigated project.

There has been to date few studies on what occurs when C_{60} and C_{70} are present together. Besides the extraction procedure from fullerite[11] and some colloidal studies,[72] little research has probed into the interactions between differing fullerenes. Controlling the assembly of fullerenes into arrays, depending on the presence of a third component which itself does not form part of the assembly is an important development in the materials science of fullerenes and promises to expand the structural types possible for C_{60} as well as for C_{70} and higher fullerenes. To determine the generality of this process, this project has also looked at calix[6]arene:fullerene mixtures. By comparing and contrasting between differing calixarenes, it may be possible to elucidate what are the factors behind the phenomenon.

The most common method of generating fullerenes, using an electric arc between two graphite rods, yields C_{60} and C_{70} in a ratio of roughly 19:5.[12,73] Consequently, the

ubiquitous coexistence of C_{70} with C_{60} has been somewhat of a hindrance in the purification of the latter.

Recently the solid-state structure of a C_{60} complex of the unmodified, shallow-cavity calix[5]arene been elucidated.[2] Here the fullerenes assemble in a Z-array (**42**), comprising five close-packed columns enshrouded by a sheath of calix[5]arene molecules. (Figure 3.6). Some of the fullerenes are capped by two trans-calixarenes, while others are associated with the cavity of only one calixarene, or are not associated with any cavities at all.
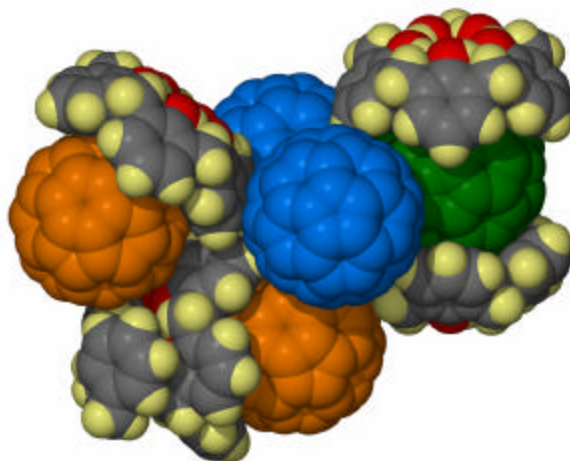
Figure 3.5. Unit cell of structure between calix[5]arene and C60 in toluene that reveals columns of fullerenes in a array in the shape of the letter Z (**42**). Fullerenes are encapsulated by zero (blue), one (orange) or two (green) calix[5]arenes. Two toluene molecules π…π stack with the external surface of a calix[5]arene (From Ref. 2, carbon = grey, hydrogen = yellow, oxygen = red).

3.4.2 A new structure from the "contamination" of C_{60}.

In further exploring the chemistry of fullerenes and calix[5]arene, we have now encountered yet another complex with the same structural tectons but with the calixarene and fullerene in a simple 1:1 ratio (**43**), compared with 4:5 for **42**.[1,2] Initially this new

complex formed in the presence of C_{70}, which is remarkable in that, far from being a hindrance, the larger fullerene actually facilitates the formation of a different complex of calix[5]arene and C_{60}. If the C_{60}:C_{70} molar ratio is varied while the total amount of calix[5]arene is kept constant (i.e. about 1.3:1 calixarene/fullerene) a progression of solid-state structures, from **42** to the new C_{60}/calix[5]arene structural motif, and then to a C_{70}/calix[5]arene complex, is obtained.

Using toluene as a solvent, calix[5]arene and C_{70} form a complex isolated as clusters of slender dark-red needles (Figure 3.6a), which have been unsuitable for single-crystal X-ray analysis. These clusters form in the presence of C_{60} up to a C_{60}:C_{70} molar ratio of approximately 2.3:1 (with 1.4 mole calix[5]arene) (Table 3.1). When the C_{60}:C_{70} molar ratio is close to approximately 4.5:1 (1.4 mole calix[5]arene), the new complex **43** forms along with the C_{70}/calixarene complex (Figure 3.6b and c). Complex **43** forms up to a 10:1 molar ratio of C_{60}:C_{70}, while at higher ratios **42** results (Figure 3.7d).[2] The ability of C_{70} to influence the composition of a system in a crystal by mediating the crystallization process is unprecedented and this not been noted in other fullerene/calixarene systems. In the absence of C_{70} and with excess calix[5]arene (1.3 mole) the C_{60}/calix[5]arene Z-array **42** also results (Figure 3.6d).
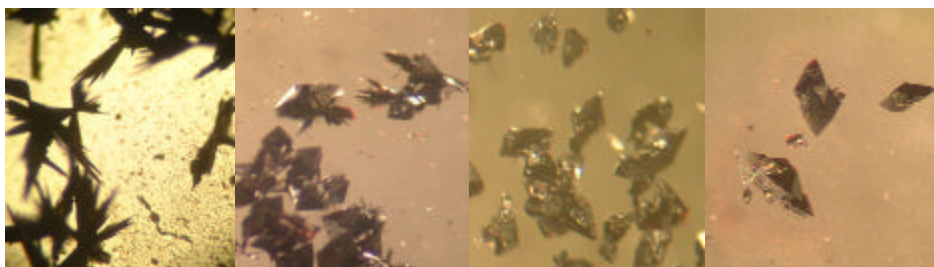
Figure 3.6. (Left to right) Photographs of crystals of: a) C_{70}/calix[5]arene, b) **43** and C_{70}/calix[5]arene (toluene solution: 2:1 C_{60}:C_{70} and calix[5]arene), c) **43** resulting from toluene solution: 4:1 C_{60}:C_{70} and calix[5]arene, and d) **42** (all at tenfold magnification).

X-ray diffraction analysis of **43** reveals a simple 1:1:1 complex of C_{60}, calix[5]arene, and toluene (Figure 3.7). The C_{60} molecules form a slightly helical, zigzag, one-dimensional oligomeric array. It is not surprising that the external surface of two adjacent calix[5]arenes abut close to each C_{60}, considering the electron-deficient nature of the fullerene and the electron-rich oxygen atoms and arene rings of the calix[5]arenes.[12]

Table 3.1. Crystallizations of calix[5]arene/C_{60}/C_{70} complexes from toluene (ca. 1 mg fullerene/mL toluene) and resulting complexes; yields approximately >75%.

C_{60}:C_{70}	C_{60}:Calix[5]arene	Crystal type
0–1.2:1	0–3.7:1	C_{70} complex(a)
2.3:1	0.49:1	helical(**43**) + C_{70} complex(b)
3.5–10.5:1	0.51–0.65:1	helical(**43**)
	0.07–0.7:1	helical(**43**)
	0.75–1.0:1	Z array(**42**)(c)

(a) C_{70}/calix[5]arene by comparison with X-ray powder diffraction data of C_{70}/calix[5]arene. (b) Ref. 1 (c) Ref. 2.

To further investigate the role of C_{70} in the formation of **43** we seeded toluene solutions of fullerite and calix[5]arene (close to the same molar ratios as above) with crystals of either **42** or **43**. In all cases the only complex formed was the new C_{60}/calix[5]arene complex **43**. Moreover, addition of crystals of **43** to a 1:1 solution of C_{60} and calix[5]arene in toluene also results in the formation of **43**. Thus here the crystal is seeding the crystallization of **43** at the expense of the Z-array, as opposed to the C_{70} mediation in the previous experiments. Complex **43** can therefore be regarded as the thermodynamically favored product, at least when the ratio of C_{60} to calix[5]arene is approximately 1:1. Seed crystals of **42** had no effect on the crystallization outcome for solutions of fullerite or C_{60} with calix[5]arene.
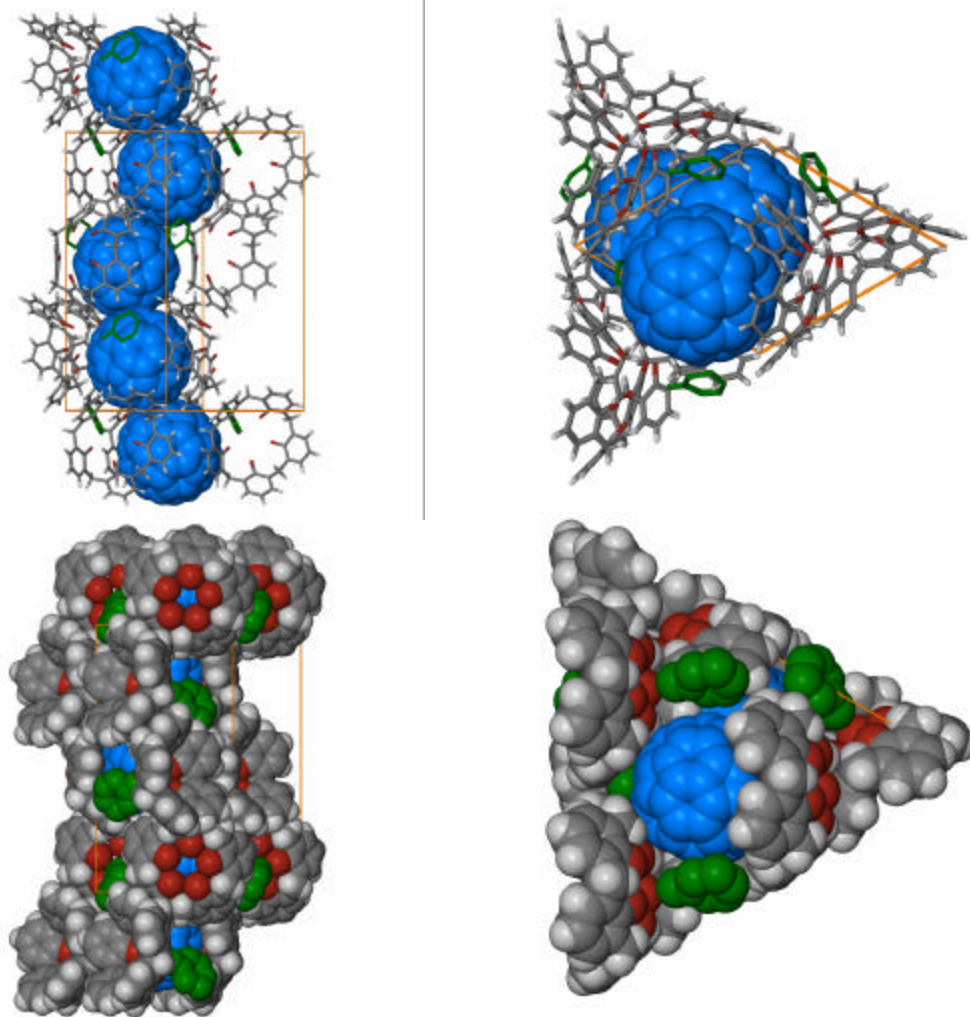
Figure 3.7. X-ray crystal structure of $[(C_{60})(calix[5]arene)] \cdot$ toluene, **43.** Left: projected at right angles to the zigzag array of fullerenes. Right: almost along the array.(Blue = C_{60}, dark and light gray = carbon and hydrogen atoms of the calixarene, red = oxygen atoms, dark green = toluene, orange box = unit cell).

Adding other globular molecules such as o-carborane $(1,2\text{-}C_2B_{10}H_{12})$ or C_{84} in place

of C_{70} to toluene solutions of C_{60} and calix[5]arene also results in the formation of **43,**

even though the carborane itself is known to form complexes with the calixarene.[74] Thus

these additives also mediate the crystallization of the new complex, although their role in

the crystallization process is as yet unclear. However, in solutions of C_{60} and bowl-

shaped molecules in a 1:1 ratio, aggregation of the fullerenes is proposed to occur by

101

polarization effects,[49,50,75] and aggregation could then lead to the fullerene-rich **42**. The other globular molecules could effectively disrupt the aggregation of C_{60} molecules *via* competitive encapsulation with calix[5]arene. This is further borne out by the fact that in the presence of an excess of calix[5]arene results in **43**, which can be rationalized by the dominance of the 1:1 supermolecule in solution, which possibly also minimizes aggregation of the fullerenes.

To confirm that either the Z-shaped or zigzag array **43** were representative of bulk samples, X-ray powder diffraction studies were undertaken (Figure 3.8). Distinct diffraction patterns were obtained, as was also the case for the C_{70}/calix[5]arene complex; we found no evidence for the presence of mixtures of two or three of the complexes and were found to conform to the diffraction pattern calculated from the single crystal.
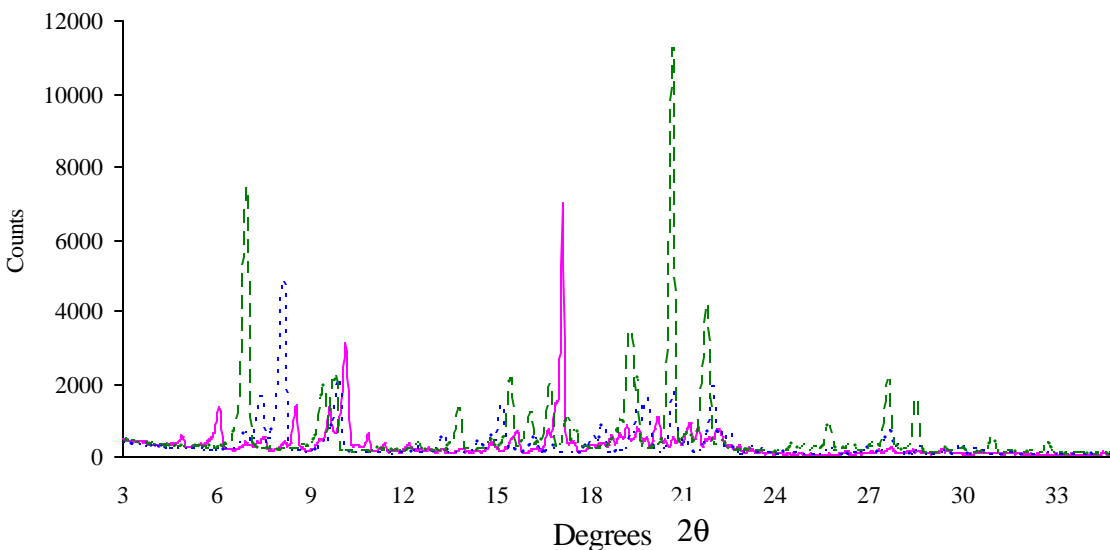
Figure 3.8. Powder diffraction patterns of bulk samples of C_{60}:Calix[5]arene Z-array complex (blue dotted line), C_{60}:Calix[5]arene zigzag complex (pink solid line) and C_{70}:Calix[5]arene complex (green dashed line).

UV/Vis studies in toluene or chloroform solutions prepared from single crystals of the **42** or **43**, and the ill-defined C_{70} complex were undertaken. Spectra were recorded after a single crystal had been dissolved slowly over a period of one week in either solvent and revealed no visible sign of C_{70}.

Crystals of complex **43** were also dissolved in toluene and using methanol:ether as the eluent, showed only traces of the higher fullerene according to HPLC analysis. Both the electronic spectrum and single crystal data show that the higher fullerene is not an integral part of the solid-state structure.[76,77]

3.4.3   Discussion on structural deviations.

The use of C_{70} as a mediator in crystallizing a new structural motif of C_{60} with calix[5]arene is interesting, since calix[5]arene is one of the few known hosts to complex C_{60} in solution.[8] We believe that the influence of globular additives on the resulting structure can be rationalized by considering how spherical molecules generally prefer to pack. In the fullerene-rich Z-array structure (**42**), the C_{60} molecules aggregate into several linear strands that make *van der* Waals contact with one another. Adjacent strands are staggered with respect to one another such that each C_{60} molecule is in close contact with four to six of its fullerene neighbors. Careful consideration of the individual C_{60} molecules shows that each is in a two-dimensional, pseudo-hexagonal-close-packed environment so as to maximize interfullerene contact.

Indeed, each of the molecules of the central strand is surrounded by six nearest neighbors, and this is the preferred arrangement for close-packed spheres. The C_{70}, *o*-carborane, or C_{84} molecules are similar in size and shape to C_{60}. However, we postulate that these molecules are sufficiently different that they disrupt the formation of the

pseudo-hexagonal-close-packed arrangement. Each of the additives is polar or has a dipole moment compared to the spherical C_{60}. Through interaction with the additives, it is possible that they disrupt the aggregation of C_{60} and therefore help produce the simpler **43**. From an entropic viewpoint, the disruption of a complicated organized structure like 42 would be favored over **43**.

Evidence for this disruption has been seen in colloidal studies of C_{60} and C_{70} mixed in solutions.[72] The authors found that whatever the solution used for aggregation, the mixture of C_{60} and C_{70} produced colloids of about half the diameter than when the individual fullerenes were alone. This and our research seem to show that the **42** is exquisitely arranged in solution before precipitating out as a crystalline complex.

It is likely that during crystal growth C_{60} molecules in the less constrained structure of **43** can be replaced by globular additives like C_{70} or carboranes. The association constants for C_{70} with calix[5]arene are consistently higher than for C_{60} in solution.[60,64,67] However, the growth of crystals from solution is a dynamic and reversible process in which the molecules can be deposited as well as removed from the growth boundary of the material. In most cases, this mechanism allows the crystal to "repair" itself by rejecting molecules that might fit but that do not conform to the minimum-energy packing mode. This allows the C_{60} molecules to adopt the alternative low-energy structure **43**, in which hexagonal packing does not play a role while C_{70} will more readily go back into solution and associate with other calix[5]arene.

A final study was conducted to determine if solvent effects were involved. The crystals were reconstituted in *p*-xylene at various ratios of fullerenes. When *p*-xylene was substituted for toluene, a similar trend in structural composition was inferred from the

determination of unit cell parameters with similar values obtained to those of the 5:4:2 and 1:1:1 C_{60}:calix[5]arene:solvent complexes (Table 3.2). As can be seen in, despite the addition of an extra methyl group on the solvent and though there are solvents of crystallization within the both Z-array and 1:1 structures, the structures with either toluene or *p*-xylene are essentially isomorphic. This shows that the solvent is having to all intents no effect on the crystal motif that is formed.

Table 3.2: Comparison of unit cells for structures formed when using toluene or *p*-xylene (*a*, *b*, *c* in Å; *a*, *b*, *g* in degrees; Volume in Å^3).

Crystal	Dimensions							Space
Solvent = toluene	*a*	*b*	*c*	*a*	*b*	*g*	Volume	Group
Z-array	20.71	31.44	37.78	90	90	90	24703	P2$_1$/c
1:1 C60:								
calix[5]arene	13.76	13.76	26.94	90	90	120	4420	P3$_2$
Solvent = p-xylene								
Z-array	20.60	31.50	37.81	90	90	90	20548	P2$_1$/c
1:1 C60:								
calix[5]arene	13.74	13.75	27.30	90	90	120	4472	P3$_2$

3.5   Structural elucidation of C_{70}:calix[5]arene

3.5.1   Structural knowledge of C_{70} complexes.

Until quite recently, only two solid state cavitand complexes with C_{70} have been described; other C_{70} solid state structures involving either flat macrocycles such as porphyrins[78-80] or saddle-shaped molecules such as Ni(OMTAA).[81] In the first instance, a third component (other than a solvent molecule) was involved: both C_{70} and *o*-carborane were cocrystallized with cyclotriveratrylene.[82] In the second case, two C_{70} molecules were cocrystallized with calix[6]arene to yield a structure which is isostructural to a similar complex with C_{60}.[53] The orientation of the fullerene in the cavitands is of interest in how the interplay of the two components is optimized. Only just in press, the Raston

group (now at the University of Western Australia) have published how having *tert*-butyl groups to calix[6]arene changes the conformation and interaction between calixarene and fullerene. In this final case, the C_{70} is endo- to the double cone cavity of *tert*-butyl-calix[6]arene.[83] The bulky *tert*- butyl groups block the already shrunken double cone and restrict entry by the fullerene.

3.5.2   Improved crystal morphologies with change in solvents.

With an understanding of the mechanics of how to build up different structural motifs of calix[5]arene with C_{60} fullerene, there was still a problem to elucidate.   Besides the formation of the crystals (Figure 3.9) there was still no evidence for what was happening to C_{70} fullerene with calix[5]arene. Something was occurring between host and guest. From solution studies it could be seen that C_{70} is actually a tighter fit with calix[5]arene compared with C_{60} (Association constants with calix[5]arene: $K_a = 30 \pm 2$ for C_{60} versus $K_a = 51 \pm 3$ for C_{70}).[60] Despite having the formation of separate red, needle-like crystals from toluene, the structure could not be elucidated owing to their small size. X-ray powder diffraction experiments indicated that the new phase is quite different in structure from either of the two known complexes of calix[5]arene and C_{60}.

It was with the previous study with fullerenes and calix[5]arene in *p*-xylene that a solid state structure was revealed. It was presumed that as with the C_{60}:Calix[5]arene complexes, the corresponding crystals with C_{70} may also be isostructural, and thus changing the solvent from toluene to *p*-xylene would afford the same structural types. In contrast, C_{70} gave a new complex at relatively high concentrations of the fullerene as small rectangular crystals which proved to be suitable for X-ray structural determination using synchrotron radiation.
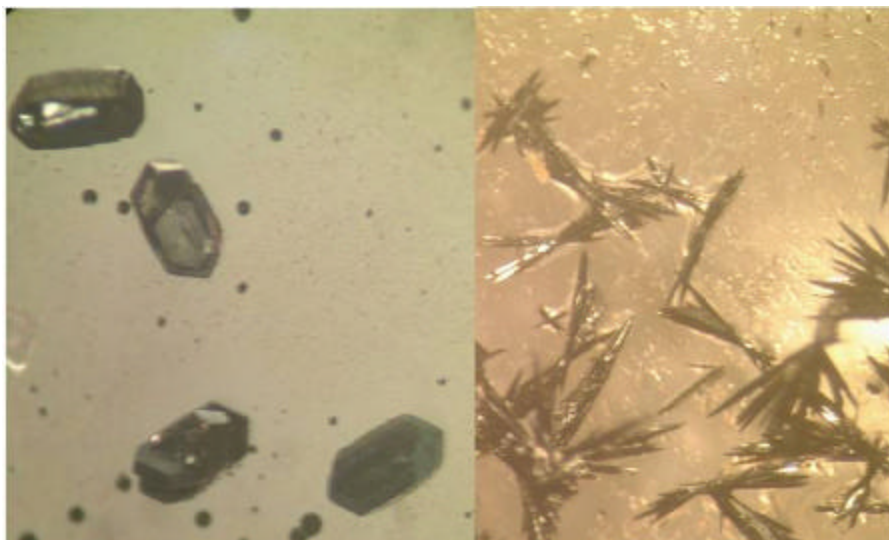
Figure 3.9. Crystals of C_{70} and calix[5]arene in *p*-xylene (left) and toluene (right).

Elucidation of the structure reveals a 1:1 complex of C_{70} and calix[5]arene, with no presence of *p*-xylene (**44**). Although both C_{70} and calix[5]arene possesses a five-fold rotation axis, symmetry matching of these axes does not occur in the complex. Instead, the five-fold axis of the C_{70} molecule is canted at an angle of approximately 40° relative to that of the calix[5]arene (Figure 3.10). A similar tilt of the C_{70} molecule occurs when complexed by the double cleft of calix[6]arene,[53] and possibly relates to optimizing complementarity of curvature of the two components or maximizing π··π stacking.

In the extended structure, columns of C_{70} molecules are aligned parallel to [001] (Fig. 3.11). Adjacent C_{70} molecules are at the van der Waals limit and are aligned with their major axes at 76° and 104° to the direction of the column. Each column is in close contact with two neighboring columns of C_{70} molecules, thus forming a two dimensional zigzag sheet parallel to (100) as shown. Adjacent undulating layers are well-separated by sheaths of calix[5]arene molecules.

3.5.3   Structure does not reflect toluene adduct

The calculated powder diffraction pattern for the structure does not comport with that measured for the crystals grown from a solution of calix[5]arene and C_{70} in toluene.[84] It is therefore reasonable to assume that the solid-state complexes of C_{70} obtained from *p*-xylene and toluene are not isostructural. This is an interesting observation since, as stated above, it is possible to obtain isostructural complexes for calix[5]arene and C_{60} from either solvent, even though one of the two known calix[5]arene:C_{60} structures incorporates solvent molecules into its lattice.
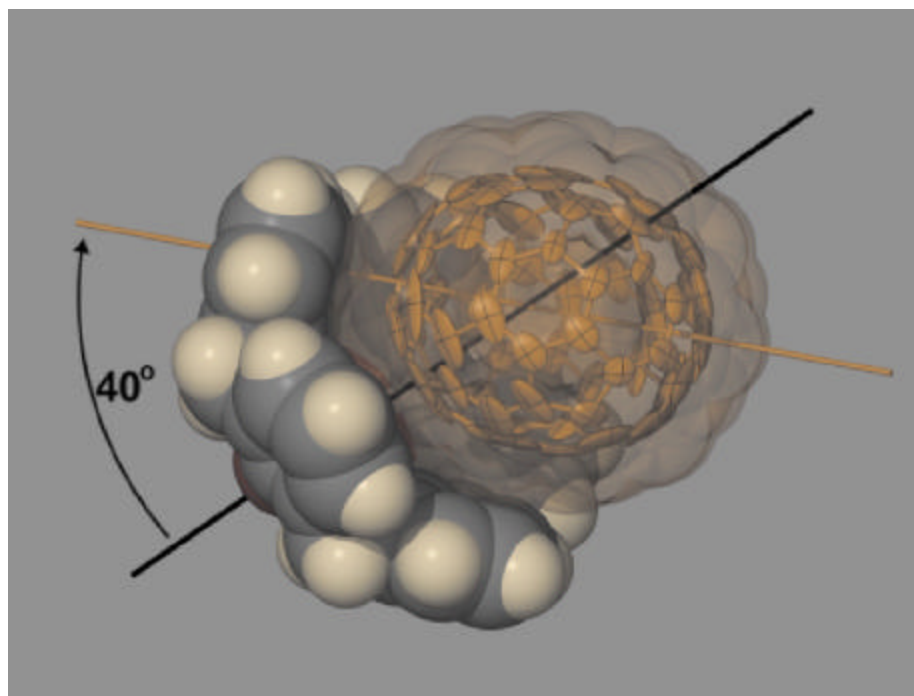
Figure 3.10. The asymmetric unit of calix[5]arene:C_{70} (**44**). The fullerene is shown in orange as a thermal ellipsoid (50% probability) plot within a semitransparent van der Waals surface. The five-fold axes of the calix[5]arene and C_{70} molecules are shown as black and orange lines, respectively.

Furthermore, thermogravimetric analysis of calix[5]arene:C_{70} crystals grown from toluene does not indicate the presence of solvent in that structure. We therefore conclude that while neither toluene nor *p*-xylene plays a structural role in the solid state complexes

of calix[5]arene with C_{70}, the choice of solvent certainly influences the form of the resultant structure, possibly in the way the fullerenes aggregate, compared with complexation of C_{60}.[1] Indeed, if the complex isolated from toluene proves also to consist of an exact 1:1 molar ratio of calix[5]arene and C_{70}, this would be the first known instance of true polymorphism in fullerene complexation.
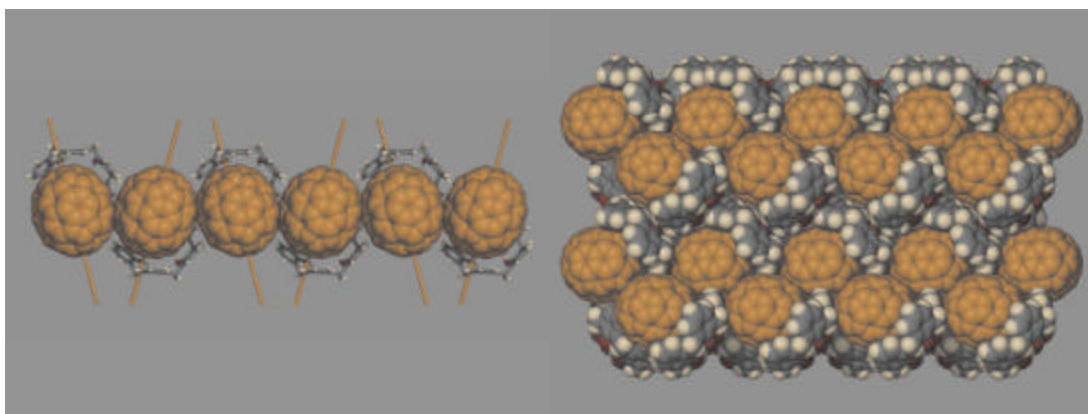
Figure 3.11. Left: A single column of calix[5]arene : C_{70} complexes aligned parallel to [001]. The 5-fold axes of the fullerenes are shown in orange. Right: Perspective view along [001] showing two zigzag layers of C_{70} molecules enshrouded by calix[5]arenes.

Although difficult to predict, the ability to control the close arrangement of fullerenes in the solid state is highly relevant to their subsequent covalent linking, *inter alia*. This second structural compound of C_{70} with a calix[n]arene (after calix[6]arene) seems to show a general preference for a non-spherical fullerene to form at an angle to their host. In this regard the maximizing of $\pi \cdots \pi$ interactions can be seen to be of more consequence than that of symmetry concerns. With the limited number of authenticated van der Waals complexes of C_{70} greatly enhanced by the above structure, the scene is now set for covalently linking these fullerenes in a controlled fashion.

3.6   *Varying ratios of fullerenes with Calix[6]arenes*

An examination similar to C_{60}:C_{70}:Calix[5]arene was also conducted to determine whether this induced crystallization of new solid state structures occurs with calix[6]arene. As with calix[5]arene and the fullerenes the amounts and ratios of C_{60} to C_{70} were varied with the same concentration of calix[6]arene. The experimental crystallization procedure followed closely to the previously known crystallization process from our research group.[53]

Calix[6]arene formed suitable crystals with the fullerenes for single crystal x-ray diffraction. The structure predominantly was that of the calix[6]arene with C_{60} discovered by our group in 1996.[53] Unit cells across the entire range of structures remained the same up to 9:1 mole ratio of C_{60}:C_{70}. Only pure C_{70} with calix[6]arene showed the unit cell for the previously discovered larger fullerene encapsulated within the macrocycle. These results show the special ability of calix[5]arene to bind to fullerenes. The floppiness of calix[6]arene no doubts allows for a more relaxed binding within the double cavity for the fullerene. This allows for more freedom to occur in binding during the crystallization process.

3.7   *Conclusion*

The research has shone light on how to build differing structural motifs from calix[5]arenes and fullerenes using a small almost catalytic amount of spheroidal material. Similar to the structures used by Sun and Reed[26] to form one dimensional fullerene polymers, the helical structures promoted by with the C_{60}:calix[5]arene allow for a complementary polymer to be envisioned. Such a helical structure could possibly be

used as shock absorbers for a future nanomachine.[85,86] The costs for such a construct could be reduced since there would be no need for any preprocessing to purify C_{60} from C_{70}, the larger fullerene an essential initiator to prevent a more aggregated and complicated sheet of fullerenes.

3.8 Experimental

Formation of crystals of C_{60}, C_{70} and calix[5]arene in toluene (**42 – 44**)

Calix[5]arene was synthesized in house using literature method.[44] Fullerenes were purchased from Bucky USA, Houston, TX and supplied as is. All solvents were HPLC grade.

Solutions of fullerenes at approximately 1 mg/ml of toluene or *p*-xylene were made up overnight. The solutions were filtered hot in case of any solid contaminant and added to calix[5]arene in a vial or beaker. The tops were covered but allowed some holes to allow for evaporation. After 1 – 3 weeks crystals would develop. Crystals were examined under the microscope for homogeneity.

Samples for X-ray powder diffraction were loaded onto silicon powder holders cut along the 510 hkl plane. XRD patterns recorded from 3 – 70° on a Phillips PW1050 diffractometer, using a CuKα tube, a diffracted beam monochromator, a 1° divergence slit, 1° receiving slit and a 0.2° antiscatter slit. Scan speed was 1°/min using 0.02° step size. The powders were damped with toluene to ensure that it stayed on the holder.

HPLC data was collected with samples of 20 μL injected into a Beckman 110B Solvent Delivery Module. The flow rate was at 0.3 ml/min through a Spherisorb S3ODS1 column using a 50:50 methanol:diethyl ether solvent phase. Absorption was measured at 366 nm using a Beckman 163 Variable Wavelength Detector and plotted on a Spectra-

111

Physics SP4290 Integrator. Absorption rates of C_{60} and C_{70} were calibrated using a 1:1 C_{60}:C_{70} solution in HPLC toluene as the control.

Crystal data for $[(C_{60})(calix[5]arene)]$·toluene (**43**): $C_{102}H_{38}O_5$, M = 1343.32, dark red prism, 0.20 x 0.20 x 0.15 mm^3, trigonal, space group $P3_2$ (No. 145), a = b = 13.7630(1), c = 26.9435(3) Å, V = 4419.88(7) Å^3, Z = 3, ρ_{calcd} = 1.514 g/cm^3, F_{000} = 2070, Nonius KappaCCD area-detector (ω scan mode, MoKα radiation, λ = 0.71073 Å), T = 173(2) K, $2\theta_{max}$ = 55.78°, 21952 reflections collected, 10980 unique (R_{int} = 0.0304). The structure was solved and refined using the SHELX-97 software package[87] and the XSeed[88] interface. Direct methods yielded all non-hydrogen atoms of the calixarene and toluene molecules of the asymmetric unit. While none of the C_{60} atoms could be located unequivocally, the position of the rotationally disordered fullerene was indicated by a spheroid of difference electron density. Two idealized C_{60} molecules were placed on this position in two different orientations, and each molecule was assigned a site occupancy factor of 50 %. This procedure allowed adequate refinement of a rotationally disordered model for C_{60} of known location. The calixarene atoms were refined anisotropically (full matrix least squares method on F^2). Hydrogen atoms were placed in calculated positions with their isotropic thermal parameters riding on those of their parent atoms. Final *GooF* = 3.393, R1 = 0.2557, wR2 = 0.6101, R indices based on 9974 reflections with $I > 2\sigma(I)$ (refinement on F^2), 375 parameters, 626 restraints. Lorentz, polarization, and absorption corrections applied, m = 0.092 mm^{-1}. All X-ray structure figures were prepared with X-Seed.[88] CCDC-202602 contains the supplementary crystallographic data for this paper. These data can be obtained free of charge via www.ccdc.cam.ac.uk/conts/retrieving.html

(or from the Cambridge Crystallographic Data Centre, 12, Union Road, Cambridge CB21EZ, UK; fax: (+44) 1223- 336-033; or deposit@ccdc.cam.ac.uk).

Crystal data for calix[5]arene:C_{70} (**44**): $C_{105}H_{30}O_5$, $M = 1371.29$, dark red prism, 0.08 x 0.05 x 0.05 mm^3, monoclinic, space group $P21/c$ (No. 14), $a = 19.710(3)$, $b = 14.582(2)$, $c = 20.427(3)$ Å, b $= 104.525(2)°$, $V = 5683.3(14)$ Å^3, $Z = 4$, Dc $= 1.603$ g/cm^3, $F_{000} = 2800$, synchrotron radiation, $\lambda = 0.68600$ Å, $T = 120(2)$ K, $2\theta_{max} = 58.8°$, 37334 reflections collected, 15903 unique (Rint = 0.0448). Final $GooF = 1.695$, $R1 = 0.1492$, $wR2 = 0.4027$, R indices based on 11230 reflections with $I > 2\sigma(I)$ (refinement on $F2$), 788 parameters, 10 restraints. Lp and absorption corrections applied, m $= 0.098$ mm^{-1}. O-Hydrogen atoms were included in a 50:50 disorder model for a cyclic array of hydrogen bonding. The structure was solved and refined using the SHELX-97 software package[87] and the XSeed[88] interface.

Formation of crystals of C_{60}, C_{70} and calix[6]arene

Solutions of C_{60} and C_{70} were made up in toluene as for **43**. Calix[6]arene solutions were made in chloroform and the two were layered together in vials in the appropriate ratios and allowed to evaporate until crystals formed. Crystals were examined on the Bruker SMART 1000 CCD diffractometer where unit cells were determined.

(1) Atwood, J. L.; Barbour, L. J.; Heaven, M. W.; Raston, C. L. *Angew. Chem. Int. Ed.* **2003**, *42*, 3254-3257.
(2) Atwood, J. L.; Barbour, L. J.; Raston, C. L. *Cryst. Growth Des.* **2002**, *2*, 3-6.
(3) Atwood, J. L.; Barbour, L. J.; Heaven, M. W.; Raston, C. L. *Chem. Commun.* **2003**, 2270-2271.
(4) Rohlfing, E. A.; Cox, D. M.; Kaldor, A. *J. Chem. Phys.* **1984**, *81*, 3322-3330.
(5) Kroto, H. W.; Heath, J. R.; O'Brien, S. C.; Curl, R. F.; Smalley, R. E. *Science* **1985**, *318*, 162-163.
(6) Fowler, P. W.; Manolopoulos, D. E. *An Atlas of Fullerenes*; Clarendon Press: Oxford, 1995.

(7) Kratschmer, W.; Lamb, L. D.; Fostiropoulos, K.; Huffman, D. R. *Nature* **1990**, *347*, 354-358.

(8) Taylor, R.; Hare, J. P.; Abdul-Sada, A. a. K.; Kroto, H. W. *J. Chem. Soc., Chem. Commun.* **1990**, *20*, 1423-1425.

(9) Liu, S.; Lu, Y.-j.; Kappes, M. M.; Ibers, J. A. *Science* **1991**, *254*, 408-410.

(10) Diederich, F.; Ettl, R.; Rubin, Y.; Whetten, R. L.; Beck, R.; Alavarez, M.; Anz, S.; Sensharma, D.; Wudl, F.; Khemani, K. C.; Koch, A. *Science* **1991**, *252*, 548-551.

(11) Atwood, J. L.; Koutsantonis, G. A.; Raston, C. L. *Nature* **1994**, *368*, 229-231.

(12) Hirsch, A.; Brettreich, M. *Fullerenes Chemistry and Reactions*; Wiley-VCH Verlag GmbH & Co.: Wehnheim, 2005.

(13) Taylor, R.; Langley, G. J.; Avent, A. G.; Dennis, T. J. S.; Kroto, H. W.; Walton, D. R. M. *J. Chem. Soc., Perkin Trans. 2* **1993**, 1029-1036.

(14) Taylor, R.; Langley, G. J.; Dennis, T. J. S.; Kroto, H. W.; Walton, D. R. M. *J. Chem. Soc., Chem. Commun.* **1992**, 1043-1046.

(15) Kikuchi, K.; Nakahara, N.; Wakabayashi, T.; Honda, M.; Matsumiya, H.; Moriwaki, T.; Suzuki, S.; Shiromaru, H.; Saito, K.; Yamauchi, K.; Ikemoto, I.; Achiba, Y. *Chem. Phys. Lett.* **1992**, *188*, 177-180.

(16) Marcus, Y. *J. Phys. Chem. B* **2001**, *105*, 2499-2506.

(17) Prassides, K. In *Proceedings of the Symposium on Recent Advances in the Chemistry and Physics of Fullerenes and Related Materials*; Kadish, K. M., Ruoff, R. S., Eds.; The Electrochemical Society, Inc.: San Francisco, 1994; Vol. 1, p 1736.

(18) Catalán, J.; Saiz, J. L.; Laynez, J. L.; Jagerovic, N.; Elguero, J. *Angew. Chem. Int. Ed.* **1995**, *34*, 105-107.

(19) Nath, S.; Pal, H.; Palit, D. K.; Sapre, A. V.; Mittal, J. P. *J. Phys. Chem. B* **1998**, *102*, 10158-10164.

(20) Beck, M. T.; Mandi, G.; Kiki, S. In *Proceeding of the Symposium on Recent Advances in the Chemistry and Physics of Fullerenes and Related Materials*; Electrochemical Society: Pennington, 1995; Vol. 95-10, pp 1510-1518.

(21) Olsen, S. A.; Bond, A. M.; Compton, R. G.; Lazarev, G.; Mahon, P. J.; Marken, F.; Raston, C. L.; Tedesco, V.; Webster, R. D. *J. Phys. Chem. A* **1998**, *102*, 2641-2649.

(22) Reed, C. A.; Kim, K.-C.; Bolskar, R. D.; Mueller, L. J. *Science* **2000**, *289*, 101-104.

(23) Matt, S.; Echt, O.; Scheier, P.; Märk, T. D. *Chem. Phys. Lett.* **2001**, *348*, 194-202.

(24) Roth, S.; Carroll, D. *One-Dimensional Metals: Conjugated Polymers, Organic Crystals, Carbon Nanotubes*; Wiley-VCH Verlag GmbH & Co. KGaA: Weinheim, 2004.

(25) Iwasa, Y.; Tanoue, K.; Mitani, T.; Izuoka, A.; Sugawara, T.; Yagi, T. *Chem. Commun.* **1999**, 1411-1412.

(26) Sun, D.; Reed, C. A. *Chem. Commun.* **2000**, 2391-2392.

(27) Margadonna, S.; Pontiroli, D.; Belli, M.; Shiroka, T.; Ricco, M.; Brunelli, M. *J. Am. Chem. Soc.* **2004**, *126*, 15032-15033.

(28)   Chauvet, O.; Oszlànyi, G.; Forro, L.; Stephens, P. W.; Tegze, M.; Faigel, G.; Jànossy, A. *Phys. Rev. Lett.* **1994**, *72*, 2721-2724.

(29)   Konarev, D. V.; Khasanov, S. S.; Otsuka, A.; Saito, G. *J. Am. Chem. Soc.* **2002**, *124*, 8520-8521.

(30)   Prassides, K.; Brown, C. M.; Margadonna, S.; Kordatos, K.; Tanigaki, K.; Suard, E.; Dianoux, A. J.; Knudsend, K. D. *J. Mater. Chem.* **2000**, *10*, 1443-1449.

(31)   Prassides, K.; Vavekis, K.; Kordatos, K.; Tanigaki, K.; Bendele, G. M.; Stephens, P. W. *J. Am. Chem. Soc.* **1997**, *119*, 834-835.

(32)   Soldatov, A. V.; Roth, G.; Dzyabchenko, A.; Johnels, D.; Lebedkin, S.; Meingast, C.; Sundqvist, B.; Haluska, M.; Kuzmany, H. *Science* **2001**, *293*, 680-683.

(33)   Cao, H.; Xu, Z.; Wei, X.; Mab, X.; Xue, Z. *Chem. Commun.* **2001**, 541-542.

(34)   Hardie, M. J.; Raston, C. L. *Chem. Commun.* **1999**, 1153-1163.

(35)   Hardie, M. J.; Torrens, R.; Raston, C. L. *Chem. Commun.* **2003**, 1854-1855.

(36)   Schön, J. H.; Kloc, C.; Batlogg, B. *Science* **2001**, *293*, 2432-2434.

(37)   Schön, J. H.; Kloc, C.; Siegrist, T.; Steigerwald, M.; Svensson, C.; Batlogg, B. *Nature* **2001**, *413*, 831-833.

(38)   Fleming, R. M.; Ramirez, A. P.; Rosseinsky, M. J.; Murphy, D. W.; Haddon, R. C.; Zahurak, S. M.; Makhija, A. V. **1991**, *352*, 787-788.

(39)   Service, R. F. *Science* **2001**, *293*, 1570.

(40)   Jansen, M.; Waidmann, G. *Z. anorg. u. allgem. Chem.* **1995**, *621*, 14-18.

(41)   Dinnebier, R. E.; Gunnarsson, O.; Brumm, H.; Koch, E.; Stephens, P. W.; Huq, A.; Jansen, M. *Science* **2002**, *296*, 109-113.

(42)   Akada, M.; Hirai, T.; Takeuchi, J.; Hiroshiba, N.; Kumashiro, R.; Yamamoto, T.; Tanigaki, K. *Phys. Rev. B* **2005**, *72*, 132505-132508.

(43)   Gutsche, C. D. In *Calixarenes: A Versatile Class of Macrocyclic Compounds*; Vicens, J., Böhmer, V., Eds.; Kluwer Academic Publishers: Dordrecht, 1991; Vol. 3, p 264.

(44)   Stewart, D. R.; Gutsche, C. D. *Oppi Briefs* **1993**, *25*, 137-139.

(45)   Thondorf, I.; Brenn, J. *J. Chem. Soc., Perkin Trans. 2* **1997**, 2293-2299.

(46)   Atwood, J. L.; Barbour, L. J.; Nichols, P. J.; Raston, C. L.; Sandoval, C. A. *Chem. Eur. J.* **1999**, *5*, 990-996.

(47)   Raston, C. L.; Atwood, J. L.; Nichols, P. J.; Sudria, I. B. N. *Chem. Commun.* **1996**, 2615-2616.

(48)   Barbour, L. J.; Orr, G. W.; Atwood, J. L. *Chem. Commun.* **1998**, 1901-1902.

(49)   Atwood, J. L.; Barnes, M. J.; Gardiner, M. G.; Raston, C. L. *Chem. Commun.* **1996**, *12*, 1449-1450.

(50)   Bond, A. M.; Miao, W.; Raston, C. L.; Ness, T. J.; Barnes, M. J.; Atwood, J. L. *J. Phys. Chem. B* **2001**, *105*, 1687-1695.

(51)   Izuoka, A.; Tachikawa, T.; Sugawara, T.; Suzuki, Y.; Konno, M.; Saito, Y.; Shinohara, H. *J. Chem. Soc., Chem. Commun.* **1992**, 1472-1473.

(52)   Andrews, P. C.; Atwood, J. L.; Barbour, L. J.; Nichols, P. J.; Raston, C. L. *Chem. Eur. J.* **1998**, *4*, 1384-1387.

(53)   Atwood, J. L.; Barbour, L. J.; Raston, C. L.; Sudria, I. B. N. *Angew. Chem. Int. Ed.* **1998**, *37*, 981-983.

(54)   Dei, L.; LoNostro, P.; Capuzzi, G.; Baglioni, P. *Langmuir* **1998**, *14*, 4143-4147.

(55)   Bhattacharya, S.; Nayak, S. K.; Chattopadhyay, S.; Banerjee, M.; Mukherjee, A. K. *J. Phys. Chem. B* **2003**, *107*, 11830-11834.

(56)   Gasparrini, F.; Misiti, D.; Negra, F. D.; Maggini, M.; Scorrano, G.; Villani, C. *Tetrahedron* **2001**, *57*, 6997-7002.

(57)   Bhattacharya, S.; Nayak, S. K.; Chattopadhyay, S.; Banerjee, M.; Mukherjee, A. K. *J. Chem. Soc., Perkin Trans. 2* **2001**, 2292-2297.

(58)   Barbour, L. J.; Orr, G. W.; Atwood, J. L. *Chem. Commun.* **1997**, 1439-1440.

(59)   Mizyed, S.; Ashram, M.; Miller, D. O.; Georghiou, P. E. *J. Chem. Soc., Perkin Trans. 2* **2001**, 1916-1919.

(60)   Wang, J.; Gutsche, C. D. *J. Am. Chem. Soc.* **1998**, *120*, 12226-12231.

(61)   Wang, J.; Gutsche, C. D. *J. Org. Chem.* **2002**, *67*, 4423-4429.

(62)   Haino, T.; Yanase, M.; Fukazawa, Y. *Angew. Chem. Int. Ed.* **1997**, *36*, 259-260.

(63)   Makha, M.; Hardie, M. J.; Raston, C. L. *Chem. Commun.* **2002**, 1446-1447.

(64)   Haino, T.; Yanase, M.; Fukazawa, Y. *Angew. Chem. Int. Ed.* **1998**, *37*, 997-998.

(65)   Biali, S. E.; Böhmer, V.; Columbus, I.; Ferguson, G.; Grüttner, C.; Grynszpan, F.; Paulus, E. F.; Thondorf, I. *J. Chem. Soc., Perkin Trans. 2* **1998**, 2261-2269.

(66)   Wang, J.; Bodige, S. G.; Watson, W. H.; Gutsche, C. D. *J. Org. Chem.* **2000**, *65*, 8260-8263.

(67)   Haino, T.; Yamanaka, Y.; Araki, H.; Fukazawa, Y. *Chem. Commun.* **2002**, 402-403.

(68)   Haino, T.; Yanase, M.; Fukazawa, Y. *Tetrahedron Lett.* **1997**, *38*, 3739-3742.

(69)   Yanase, M.; Haino, T.; Fukazawa, Y. *Tetrahedron Lett.* **1999**, *40*, 2781-2784.

(70)   Haino, T.; Araki, H.; Yamanaka, Y.; Fukazawa, Y. *Tetrahedron Lett.* **2001**, *42*, 3203-3206.

(71)   Ikeda, A.; Yoshimura, M.; Shinkai, S. *Tetrahedron Lett.* **1997**, *38*, 2107-2110.

(72)   Alargova, R. G.; Deguchi, S.; Tsujii, K. *J. Am. Chem. Soc.* **2001**, *123*, 10460-10467.

(73)   Kroto, H. W.; Fischer, J. E.; Cox, D. E. *The Fullerenes*; Pergamon Press: New York, 1993.

(74)   Hardie, M. J.; Raston, C. L. *Eur. J. Inorg. Chem.* **1999**, 195-200.

(75)   Drljaca, A.; Kepert, C.; Spiccia, L.; Raston, C. L.; Sandoval, C. A.; Smith, T. D. *Chem. Commun.* **1997**, *2*, 195-196.

(76)   Hare, J. P. K., H. W.; Taylor, R. *Chem. Phys. Lett.* **1991**, *177*, 394-398.

(77)   Diack, M. H., R. L.; Compton, R. N.; Guiochon, Georges. *Anal. Chem.* **1992**, *64*, 2143-2148.

(78)   Sun, D.; Tham, F. S.; Reed, C. A.; Boyd, P. D. W. *PNAS* **2002**, *99*, 5088-5092.

(79)   Konarev, D. V.; Neretin, I. S.; Slovokhotov, Y. L.; Yudanova, E. I.; Drichko, N. y. V.; Shul'ga, Y. M.; Tarasov, B. P.; Gumanov, L. L.; Batsanov, A. S.; Howard, J. A. K.; Lyubovskaya, R. N. *Chem. Eur. J.* **2001**, *7*, 2605-2616.

(80)   Konarev, D. V.; Kovalevsky, A. Y.; Li, X.; Neretin, I. S.; Litvinov, A. L.; Drichko, N. V.; Slovokhotov, Y. L.; Coppens, P.; Lyubovskaya, R. N. *Inorg. Chem.* **2002**, *41*, 3638-3646.

(81)   Croucher, P. D.; Marshall, J. M. E.; Nichols, P. J.; Raston, C. L. *Chem. Commun.* **1999**, 193-194.

(82)   Hardie, M. J.; Godfrey, P. D.; Raston, C. L. *Chem. Eur. J.* **1999**, *5*, 1828-1833.

(83)   Makha, M.; Raston, C. L.; Sobolev, A. N.; Turner, P. *Cryst. Growth Des.* **2005**, *in press*.

(84)   Yvon, K.; Jeitschko, W.; Parthé, E. *J. Appl. Cryst.* **1997**, *10*, 73-74.

(85)   Cao, A.; Dickrell, P. L.; Sawyer, W. G.; Ghasemi-Nejhad, M. N.; Ajayan, P. M. *Science* **2005**, *310*, 1307-1310.

(86)   Dahl, K. N.; Kahn, S. M.; Wilson, K. L.; Discher, D. E. *J Cell Sci* **2004**, *117*, 4779-4786.

(87)   Sheldrick, G. M.: Göttingen, 1997.

(88)   Barbour, L. J. *J. Supramol. Chem.* **2003**, *1*, 189-191.

Chapter 4: Nanotube-Nickel macrocycle composites

Abstract

This chapter presents the study of how nickel macrocycles interact with single wall carbon nanotubes and promote the formation of a sol-gel. Gelation is accelerated with the introduction of nickel macrocycles for certain solvents. However, experiments using solid state ^{13}C NMR were inconclusive and large scale TGA analysis seems to show that the macrocycles are not intrinsically interacting with the solvent or the nanotubes once the gel is formed. SEM/EDS however shows that the nanotubes are highly bundled and more than capable of gelling on their own and while the macrocycle is also present and not just in the solvent.

4.1 *Introduction to Carbon Nanotubes*

Since the discovery of Multi-Walled Carbon Nanotubes (MWNT) in 1991 by Ijima,[1] and the elucidation that Single-Walled Carbon Nanotubes (SWNT) could also be synthesized in 1993, also by Ijima,[2] carbon nanotubes have in many ways blazed ahead in interest and utility from their spherical progenitors the fullerenes.[3,4] Consisting of carbon rings with a range of diameters (1.0 – 1.5 nm for SWNT; 5.0 – 100.0 nm for MWNT) and lengths of up to many micrometers, carbon nanotubes come in a range of varieties. There are now many methods to produce, purify and characterize nanotubes.[5] There has been great interest also to functionalize nanotubes, both covalently[6] and non-covalently.[7] More importantly for this project, creation of composites has been another area of current academic and industrial interest.[8-11]

4.1.1 Types

There are two types of nanotube that consist of entirely of carbon (excluding "defects" and other functionalization). MWNT have to date seen more use in comparison to SWNT. This is due to the MWNT larger diameters and similarity to carbon fiber and so can be used for similar, successful applications. This is likely to change as manipulation at the nanometer level improves. Essentially MWNT are a series SWNT wrapped around each other. The smallest diameter nanotube was multiwalled, the central tube being only 0.5 nm in diameter and having half the fullerene C_{36} as a cap.[12]

However SWNT are of more academic interest because of the possibility and future opportunity for applications ranging from materials to electronics.[4] The SWNT is a large macromolecule of pure carbon that is essentially a graphite sheet wrapped around into a

tube. The way the carbon tube can be wrapped varies and this determines the electronic properties of the SWNT in question.[13] The SWNT are the strongest material known and with other materials may make extremely strong composites.[9,14-17] This project was an attempt to non-covalently bond SWNT and nickel-containing macrocycles.[15,18,19] *The hypothesis for this project is that saddle shaped molecules will allow the formation of a SWNT composite due to both the complementary curvature of the sub-units, the metal involved and the functionalities of the smaller sub-unit.*

4.1.2   Formation

The purity of the nanotubes is a problem for many reasons. First, the processes by which they are formed result in a mixture of products. Synthesis of carbon nanotubes is similar to the process of fullerene production and in fact fullerenes and associated buckyonions, buckycones and amorphous carbon soot is generally the unwanted material found with nanotubes.[20-22] Metal catalyst is also generally used: transition metals (e.g.: iron, nickel) and lanthanides (e.g.: yttrium) in various combinations.[23] While the catalyst's method of action is somewhat unclear, it does appear that the particles grow the tube around them and travel along one opening of the nanotube adding carbon atoms behind it.

There are three different methods of making carbon nanotubes.[24] SWNT in this project were produced from two different methods. The initial SWNT from Sigma-Aldrich are synthesized from the arc discharge method. The catalyst used is nickel and yttrium and produces SWNT of ~1.4 nm diameter with 50 – 70% yield. The other type of SWNT studied was created using the HiPCO method; high pressure laser ablation of

carbon monoxide that leads to a much higher yield of SWNT and is the method of choice to date.

Post processing generally involves the use of refluxing nitric acid followed by filtration. This however can shorten the nanotubes, open holes or form other defects in the sides of the tubes or either end and introduce carboxylic acid groups at these positions.[5] Sometimes this has been a deliberate process. For instance, nanotube pipes, carbon nanotubes only 100 – 300 nm long have been thought to be linkers between future nano computers based on SWNT.[3,25] A milder method developed uses refluxing hydrogen peroxide to remove the amorphous carbon and carbon disulfide to remove fullerenes impurities before filtration.

4.1.3   Properties

Due to their aspect ratio, a carbon nanotube has semi-one dimensional behaviors and can in some ways be thought of as a quasi-one-dimensional crystal.[23] One of the more researched electronic properties because of this one-dimensionality are Van Hove singularities; absorption peaks in the density of states (DOS).[26] This leads to peaks in absorption in the near infrared region. As the band gap is larger for metals compared with semiconductors, nanotubes of each type can be visualized at this area of the electromagnetic spectrum at different regions allowing for characterization of a sample of carbon nanotubes.

Spectroscopically, nanotubes have been well characterized by Raman spectroscopy and near infrared.[27-29] As seen with Raman spectroscopy, SWNT have a characteristic breathing mode at approximately 200 cm^{-1}, and a high energy mode with maxima at both 1593 and 1570 cm^{-1}. MWNT have a mode more typical of graphite at 1582 cm^{-1}, not

surprising perhaps when the spacing between the tubes making up a MWNT is the same distance as for adjacent layers of graphite, 0.34 nm.[23]

An unusual property of nanotubes was discovered after taking a photo of them.[30] The flash of the camera set them alight and decomposed the nanotubes into nanohorns and disordered graphene, depending on the atmosphere.

Solubility issues have been a constant problem with carbon nanotubes. This is in part because of their general intractability in any sort of solvent. This leads to difficulties of dealing with such unusual molecules in regards to characterization. A thorough attempt of a wide range of solvents that may allow nanotubes into solution for study was attempted.[31] While this found not unexpectedly that the nanotubes could not be solvated, suspensions of SWNT that did not precipitate out were found in five cases: NMP, DMF, hexamethylphosphoramide, cyclopentanone, tetramethylene sulfoxide, and *e*-caprolactone. This has been put to use in getting SWNT and MWNT more tractable to further processing.

Since carbon nanotubes consist of thousands of carbon atoms that that go to make a connected series of hexagonal rings, defects are a common if not inevitable situation. This leads to errors in formation process that leads to five- or seven-membered rings forming.[4] In both cases this defect creates a bending in the nanotubes leading to a twist of these otherwise ideally linear macromolecules.

Finally, the two ends of the nanotubes can be either open or closed, in that the ends of the SWNT is a rounded shape with a fullerene like motif or the carbon atoms are terminated with carboxylic acid groups.[32] Depending on the diameter of the nanotube in question, the curved surface is generally thought to be of fullerene type construction with

a single five-membered ring surrounded by six-membered rings. However modeling has shown that this smaller ring does not need to be symmetrically placed on the surface of the hemisphere making up the end. Open ended nanotubes are chemically more interesting with the end carbons decorated with carboxylic acid groups where it is believed the metal catalyst used to form the nanotube was or is still situated.

4.1.5   Uses

To date, carbon nanotubes have seen limited use in material strength enhancement. However, there is much promise in future technology based on these tubes.[4] They have been shown to be excellent backbones for molecular switches.[33] There is some controversy that they can take hydrogen up to 1.84 wt %, though this may also be due to impurities within the nanotube matrix.[34] Theoretically 10 wt % hydrogen could be stored within the typical carbon nanotubes when they are kept at low temperatures with liquid nitrogen.[35]

Composite materials are of immense interest in that it allows for the merging of the properties of both materials. This has been especially evident in traditionally brittle ceramics, with the introduction of nanotubes allowing for an enhancement of strength to the composite.[9-11,15,17,36-39] Since solubilizing SWNT is fraught with difficulties often a sol-gel matrix is used to form the composites.[14,17,36,40]

4.1.6   Covalent interactions

One of the main reasons for covalent functionalization is also solubility considerations. Functionalization is often conducted on nanotubes to tailor their properties for the task required.[6,41] Often the carboxylic acid groups from damaged areas

or open ends of the nanotubes are convenient functionalities. For instance by adding amines to the carboxylic acid groups it is possible to make the tubes soluble in water due to the zwitterionic nature of the resulting peptide(Figure 4.1).[42] By using the carboxylic acid moieties on the surface of the carbon nanotubes, it is possible to wrap them in a polymer that will react with the acid, making them soluble in water.[43] Thiolating the carboxylic acid moieties on the ends of carbon nanotubes allows them to be attached to
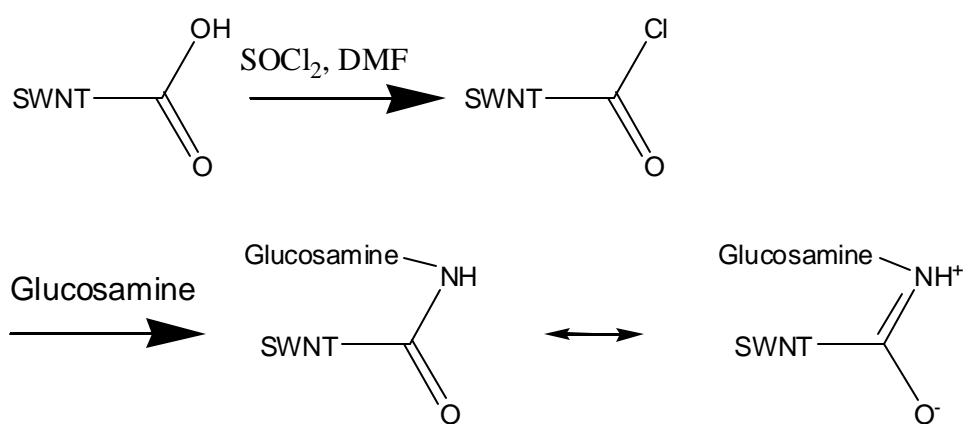
Figure 4.1. Carboxylic acid group defects on the end of tubes can be converted to amines functionalizing the nanotubes and making them water soluble.

gold and it has been shown that they stand orthogonal to the gold surface.[44] Attaching glycol molecules to nanotubes can solubilize them up to 50 mg/mL in chloroform.[45]

Due to the variety of nanotubes that come with every batch, measuring interactions with guests generally comes to studying the properties of the guest rather than the nanotube. For instance, after functionalization of nanotubes with pyrene, the interaction was monitored by studying the ^{1}H NMR peaks of the pyrene.[46]

Recently covalent interactions have been used to fine tune the separation process of nanotubes.[47,48] In a mixture of nanotubes and diazonium reagents, the metallic nanotubes

will give an electron to the diazonium ion while the semiconducting nanotubes will bond with the diazonium moiety. This leads to separation of the nanotubes *via* specific functionalization. Though this solubilization changes between metallic and semiconducting nanotubes and they can be extracted. A similar reaction is even possible

R = Cl, Br, t-butyl, CO_2CH_3, NO_2
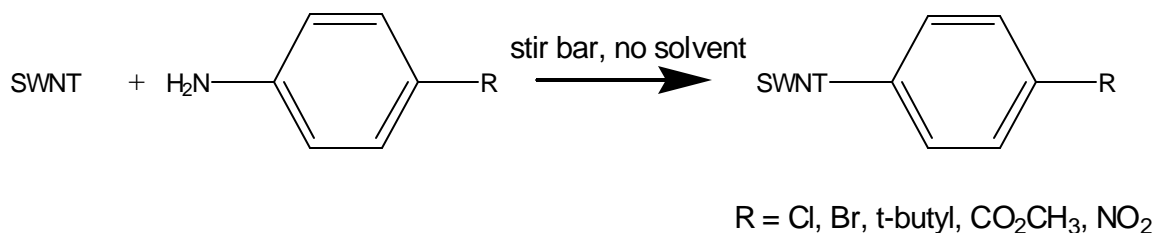
Figure 4.2. Functionalization of SWNT is possible using no solvent which allows for greater reaction rates due to no quenching by the solution.

without solvent(Figure 4.2).[49] By changing the properties of the subtype of nanotube it should be possible to separate metallic from semiconducting tubes.

The simplest covalent attachment has been to decorate carbon nanotubes with fluorine by acidifying the tubes in hydrogen fluoride.[50] This has allowed the tubes *via* sonication to be solubilized in alcohols which has allowed them to be reacted with reagents such as hydrazine or sodium methoxide. Other small molecule attachment such as dichlorocarbene has resulted in metallic nanotubes being converted to semiconducting tubes.[51]

By using a transmission electron microscope (TEM) it has been possible to covalently bond adjacent nanotubes with each other.[52] At low enough energy (~80 keV) under TEM irradiation it was possible to strengthen bundles of carbon nanotubes by up to 70% through covalent bonding and detect this by examining the conjoined tubes' bending modulus. At higher energies, the tubes were eventually found to coalesce, break down and convert to amorphous carbon. Covalent functionalization is problematic however

since the reason SWNT are of interest is attenuated when the other functionalities are attached.

4.1.7   Non-covalent interactions

Non-covalent functionalization gets around the problem of permanent change or destruction of nanotube properties at the expense of a more difficult process. The most common non-covalent compound used for nanotubes to date has been lipids; a particular favorite appears to be the anionic surfactant sodium dodecyl sulfate (SDS, Figure 4.3). At critical micellar concentration, the lipid has been seen *via* TEM to wrap itself around individual nanotubes or small nanotube bundles in a helical arrangement.[53] Under the right conditions SDS can be used to separate carbon nanotubes completely from the bundle.[54] Due to the carboxylic acid groups that are common at defects and at the end of open nanotubes, it has been possible to add zwitterionic lipids non-covalently to the tubes.[55] This then allows SWNT to solubilize in organic solvents.
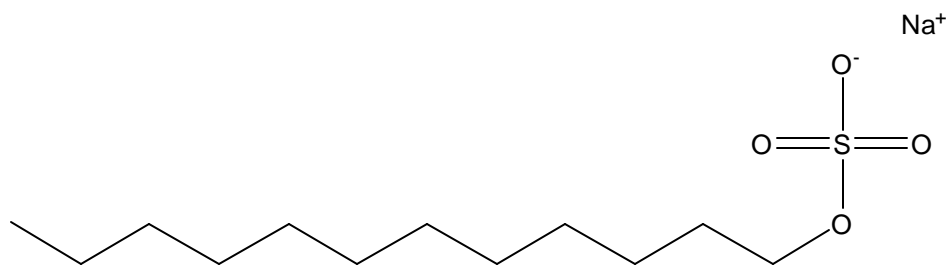
Figure 4.3. The common solubilizing agent for SWNT is the surfactant sodium dodecyl sulfate (SDS).

Common starch has also been found to solubilize SWNT in aqueous solutions.[56] In a wonderful experiment of supermolecular chemistry, the starch must be preformed into a

helical conformation with iodine for this process to work. Starch analogues that block this helical prearrangement leading to linear strands do not take up the nanotube.

Aromatic polymers have also been a favorite for solubilizing nanotubes. The aromatic aspect of the polymer is thought to π···π bonding and the alkyl chain allows for solvation in organic solvents.[57] On the other hand, crosslinking polymers can lead to a permanent sheath around the nanotubes which basically leads to a loss of all but the qualities of strength of the SWNT.[58,59] An improvement of this process is to use a polymer that consists of a linear rigid backbone and flexible arms (Figure 4.4).[60] Thus while the polymer can partially cover the nanotube and allow for solubilization, it also allows part of the tube open to the environment and so allows for other functionalization and access to other substrates to take place.
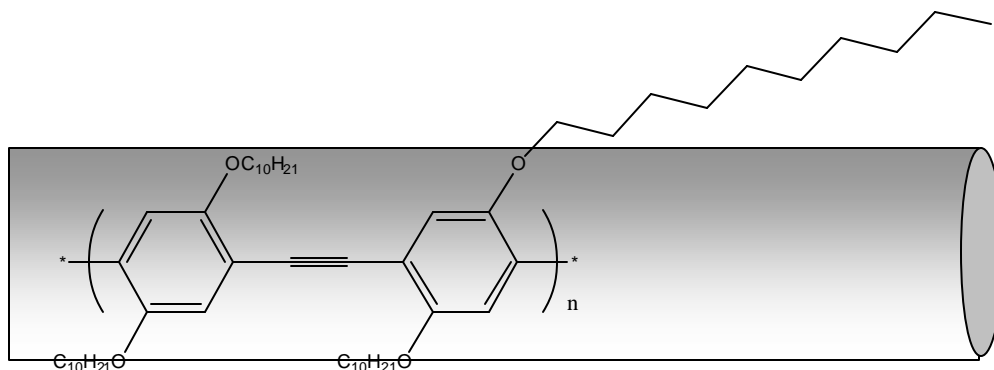
Figure 4.4. By using a rigid backbone with long alkyl chains SWNT can be solubilized and accessed for further modification simultaneously.

Smaller, non-polymeric molecules have been used to add some further functionality to nanotubes. Pyrene molecules attached to an ester were irreversibly adsorbed to the nanotube *via* π···π interactions.[61] The ester was shown to be favorable to reaction with many proteins due to amine functional groups on their surface. The proteins ferritin, streptavidin and biotin-PEO-amine were all shown to attach to the nanotube *via* the ester.

All these examples have SWNT in the role of an extremely long guest. The other sort of non-covalent interaction is in which carbon nanotubes are used as the host; generally with the inner cavity of the SWNT used as a container for gases and other molecules. Malcolm Green's group at Oxford has conducted a large amount of research in this area.[62] Where others have formed materials within the nanotubes during SWNT synthesis,[18] the Green group has managed to use the nanotube with open ends to act as a capillary. Using this they have managed to insert fullerenes, salts and carboranes.[63] The salts, such as potassium iodide, exhibit regular lattices within the nanotubes leading to "Feynman crystals," a once theoretical solid state construct constrained in one or two dimensions but infinite in the third.

Elsewhere, the metallofullerene $Sm@C_{82}$ has been inserted into nanotubes in a similar manner.[64] Through *in situ* heating *via* TEM they have coalesced the fullerenes together and using the energy electron loss spectroscopy (EELS) determine the samarium atom's electronic state. In another use of this technique, TEM allowed for visualization of nanotubes and EELS provided the evidence that nitrogen containing poly(propionylethylenimine) functionalization was successful.[42]

4.2   Nickel macrocycles

The macrocycle 5,7,12,14-tetramethyldibenzo[*b,i*][1,4,8,11]tetraaazacyclotetradecine = (TMTAA) has been around for many years. A integral part of the composites described within has been on the molecules based on Ni(TMTAA), **45**. Our group began using the framework and extending it with methyl groups to form Ni(OMTAA) **46**, first synthesized in 1975.[65] Ni(TMTAA) and it's analogues are themselves formed *via* a

supramolecular template reaction, a condensation between a central metal, two diones and two aromatic diamines (Figure 4.5).[66]

The extended looped chain followed a similar pattern to previously determined solid state structures of this class of molecules with the two macrocycles non-covalently dimerizing (Figure 4.2). The dimerization is common with Ni(OMTAA) in this case $\pi\cdots\pi$ stacking with a centroid$\cdots$centroid distance of 3.7 Å.[67]

From previous work, it was determined that the saddle shaped molecule, Ni(TMTAA)
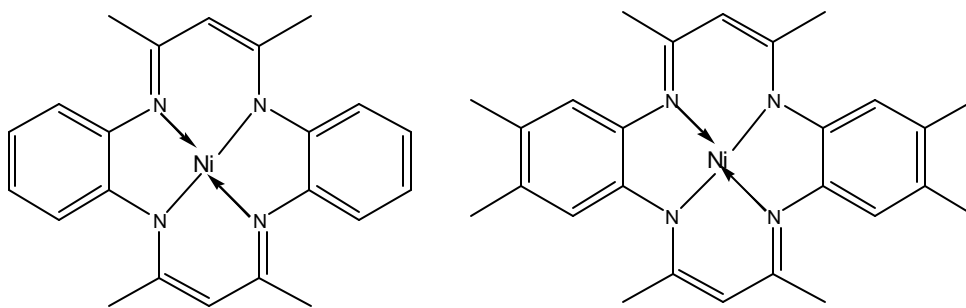
Figure 4.5. Left: Parent molecule nickel(II) 5,7,12,14-tetramethylidibenzo [*b,i*][1,4,8,11]tetraaazacyclotetradecine; more commonly known as Ni(TMTAA)(**45**). Right: With the addition of methyl groups at ortho positions the molecule is known as Ni(OMTAA)(**46**).

will crystallize out with fullerenes to form columns.[68-70] With the propensity for this macrocycle to $\pi\cdots\pi$ stack and the known affinity for nickel with nanotubes it was hypothesized then that a similar situation will occur with SWNT, in that Ni(TMTAA) and it's analogues will non-covalently bind around individual nanotubes.

There has been a little research done elsewhere that these molecules can wrap themselves around a carbon nanotube in much the way hypothesized. Basiuk *et al.* have conducted both theoretical and actual experiments with SWNT and Ni(TMTAA). Some evidence was presented that Ni(TMTAA) could be observed to aggregate upon carbon

nanotubes when examined by TEM.[71] The authors proposed that dark regular striations across the horizontal axis of visualized SWNT were the macrocycle. Computational
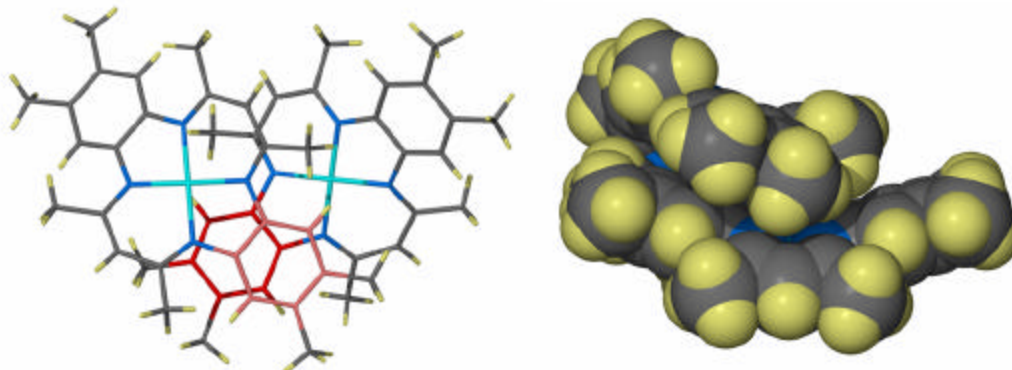
Figure 4.6. Solid state structure of **46**. Left: Structure found in solid state generally overlap as dimers due to π···π stacking (shown as red rings). Right: Space fill view shows how the dimers fit snugly into each others' larger cleft.

results of this research shows that due to the nature of the Ni(TMTAA) its exo-surface, the area with the largest cleft and aromatic groups is orthogonal to the surface and non-covalently attaches to the carbon nanotube.[72]

4.2.2   Synthesis of Nickel Macrocycles

Nickel is known to be a good template molecule for tetraza macrocycles.[73] The Ni^{2+} state is most common for this metal and the most stable energy levels for the 10 d electrons means that any surrounding ligands favor a square planar configuration over an octahedral one.[74] The square planar configuration matches up well with the four nitrogen atoms on the macrocycle in the same position. Even as late as 1986, the template effect was difficult to accomplish for such structures if the nickel was sterically hindered. Often only three of the four substituents will wrap around the metal, the fourth position taken up by a solvent molecule.

130

The M(TMTAA) (M = metal) molecule forms a backbone onto which further functionalization can be performed. A Ni(TMTAA) was turned into part of a crown ether by use of phosgene and various glycols.[75] An attempt to link two Ni(TMTAA) molecules with ethylene glycol was not so successful. The crown ether was shown to coordinate with cesium cobalticarborane in a solution of toluene-methylene chloride.[76]

4.2.3 Complexation

Research in our group regarding the macrocycle has been extensive. Nickel, zinc and copper TMTAA were investigated in the solid state with various molecules such as P_4Se_3 and S_8.[77] In such cases, the M(TMTAA) (M = Ni, Cu) structures would dimerize and then interact with the other molecule. All interactions between the guest molecule and M(TMTAA) molecules were occurring: both curvatures, edge on and aromatic face only for a total of four molecules per guest. Surprisingly both P_4Se_3 and S_8 fit snug in the same spatial position in both structures. There was essentially no change to the orientation of the surrounding M(TMTAA) molecules. The globular molecules fullerene C_{60}, P_4S_3 and o-$C_2B_{10}H_{12}$ where also surrounded by Ni(TMTAA).[68] The latter two produced solid state structures with Ni(TMTAA) almost isostructural as did P_4Se_3 and S_8. Using C_{60} fullerene as the guest produced a two dimensional zigzag sheet of fullerenes in close contact with dimerized Ni(TMTAA) insulating the layers. Our group has also examined multi component structures with sulfonated calix[4]arene, 18-crown-6 and H_4TMTAA^{2+} to form a "Russian Doll" complex.[78] Without the calixarene, Ni(TMTAA) will crystallize with 18-crown-6 as six sets of dimers surrounding the ether.[79]

More complicated structures could be formed with cryptand and carborane involvement.[80] The structure was compared to a perovskite, with the carboranes at the

vertices of a cube, a nickel or potassium 2.2.2 cryptate at the center of the cube and Ni(TMTAA) molecules surrounding it. Substitution of the larger cobalticarborane resulted in a simpler structure, a cryptate and a cobalticarborane taking up opposite sides of the faces of Ni(TMTAA).[81]

The initiation of this project resulted from the more interesting structures formed between fullerenes and the Ni(OMTAA) (Figure 4.7). The extension of the aromatic rings with two methyl groups led to a disengagement of adjacent columns of the C_{60} fullerenes.[70] The long one dimensional chain of fullerenes brought to mind a preformed nanotube. The fullerene C_{70} was isostructural with fullerene C_{60} with regard to Ni(OMTAA).[69] However due to the extended length of C_{70}, the molecule was found to be within van der Waals contact of adjacent C_{70} molecules. This results in a corrugated two dimensional sheet of the fullerene much as found with C_{60}:Ni(TMTAA).[68]
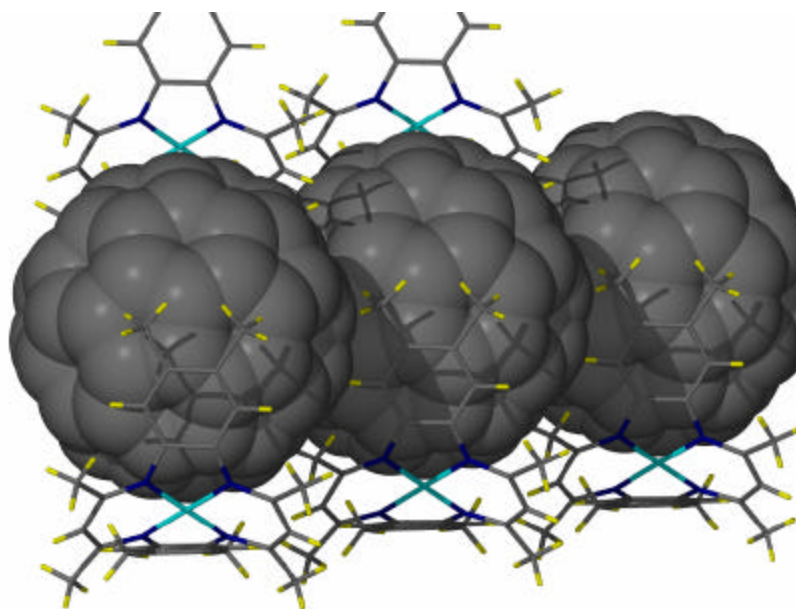
Figure 4.7. The crystal structure of C_{60} with Ni(OMTAA) producing a one-dimensional motif (Carbon = grey, hydrogen = yellow, nickel = aqua, nitrogen = dark blue).

Most importantly in regards to this research project has been work by Fukushima and coworkers.[16] They found that simply grinding in appropriate ionic liquids they could gel carbon nanotubes. Surprisingly they found that gelling did not occur upon sonication or with normal organic solvents.

4.3   *Carbon Nanotube-Ni(OMTAA)*

Other than that, Ni(TMTAA) has not been examined as a better host for SWNT. There is some evidence that methyl groups may enhance the interaction with carbon surfaces, albeit the evidence is in regards to a flat graphite surface.[82] A similar earlier study also concluded that the presence of nickel will help in regards to bonding (due to a greater free energy for bonding compared to the metal free macrocycle).[83] As such, it is a very ripe field for study. The known affinity of nickel as a catalyst for SWNT formation also makes this particular subset of azamacrocyles offer many possibilities. Nickel as a compound has also been implicated with the help of SWNT in the making of nanowires[18] and composite materials capable of removing heavy metal wastes.[19]

The purpose of this project and the hypothesis put forward tend to mitigate the need for most of the purity factors to be considered when dealing with SWNT. However both HiPco and arc-discharge SWNT were investigated. This work was primarily aimed at elucidating the conditions required to form a strong material composite, while purity factors are generally problems when it comes to issues of the electronic or chemical properties of nanotubes. However this proved an interesting challenge when it came to characterization of the composites formed. While there is a wide variety of methods on which to characterize carbon nanotube composites, the most telling for this type of research is the ability to determine the composites strength by simply pulling it apart or

133

deforming them.[16] However, one aspect of this composite is a known synthetic molecule with well studied characteristics. The Ni(TMTAA) or Ni(OMTAA) molecule can itself be used as a marker for interactions between itself and the nanotubes. It is liberally scattered with delocalized aromatic rings, four nitrogen atoms and a metal centre.

Finally in this project, as the aromatic aspects of the macrocycle would be one of the reasons for the interaction with the nanotubes, some modifications were attempted to the macrocycle by increasing the number and size of the methyl and aromatic groups it possesses. Availability of larger aromatic substrates and the simplicity of the template reaction to form the nickel macrocycle will allow for further elucidation on what the interaction between the host and guests and how to optimize it. This will affect both the chemical reactivity and the spatial characteristics of the macrocycle and may lead to a better fit with the nanotubes.

4.4   Synthesis of macrocycle
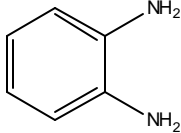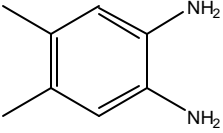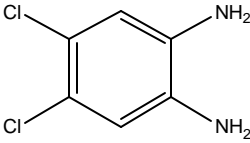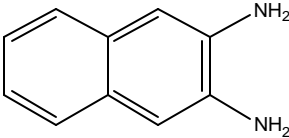
The macrocycles are produced from three precursors: the metal, the aromatic moiety and dione linker (Scheme 4.1). The metal and dione have been kept constant throughout the project, the precursors being nickel acetate and the dione, 2,4-pentanedione.
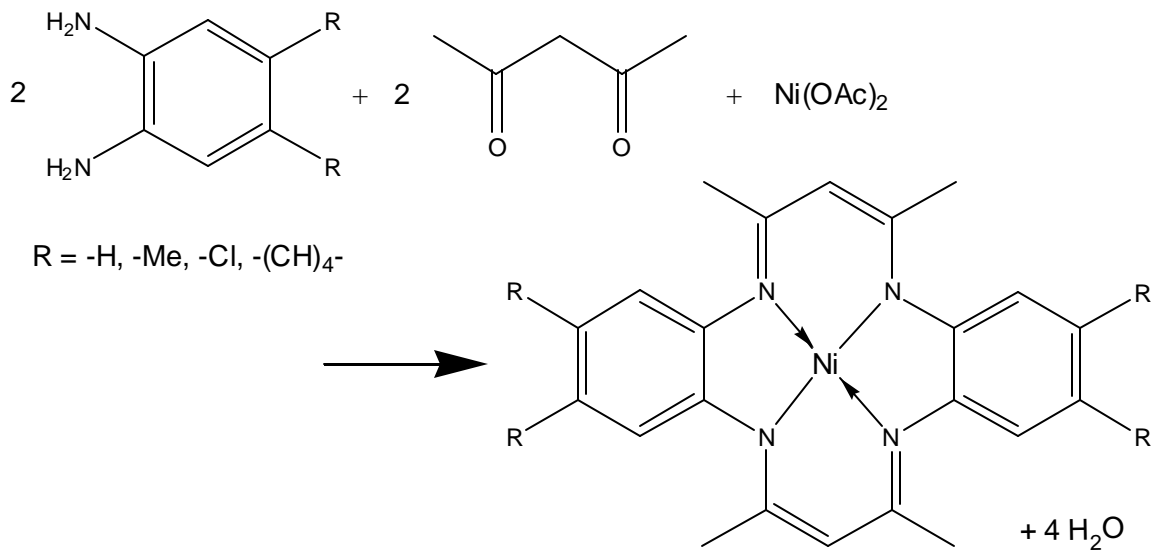
Scheme 4.1. Reaction profile to synthesize nickel

The aromatic group was also generally essentially the same, a 1, 2-diaminophenylene.

However at positions meta- to the amino groups, four different functionalities were added

(Table 4.1). Initially hydrogen atoms were the only "functionality" so that the actually

local functional group could be considered the delocalized phenyl rings. This is the

original compound designated Ni(TMTAA). By adding methyl groups on the phenyl ring

meta to the amine groups we now have Ni(OMTAA), used previously to form solid state

complexes with fullerenes and the impetus for this project.[69,70]

Table 4.1. Macrocycles synthesized for project

Precursor Name	Precursor Structure	Product Designation with Nickel
o-phenylenediamine		Ni(TMTAA) (**45**)
4,5-dimethyl-o-phenylenediamine		Ni(OMTAA) (**46**)
4,5-dichloro-o-phenylenediamine		Ni(TClTMTAA) (**47**)
2,3-diaminonaphthalene		Ni(TMNapTAA) (**48**)

Next was attempted the synthesis of two new macrocycles. Chlorine atoms replaced the methyl groups meta- to the amines on the two phenyl moieties. The reasoning behind this is that halogens have shown to be attracted to nanotubes and so it was thought that this may in fact help with the interaction between SWNT and macrocycle.[84-89] This macrocycle was designated Ni(TClTMTAA), **47**.

The single crystal X-ray structure of Ni(TClTMTAA) was determined (Figure 4.3). It revealed that the structural characteristic of adding the chlorine atoms had little effect on the overall structure. The interaction in the solid state with two molecules of **47** leading to mutual overlap is exactly that seen for molecules of Ni(OMTAA). Two molecules of **47** overlap with Ni··Ni distance of 3.47 Å. This pair then are offset with other sets of **47**

through $\pi\cdots\pi$ interactions. The chlorine atoms are of a similar volume to the methyl groups of Ni(OMTAA) and appear not to have had any effect on the solid state structure.
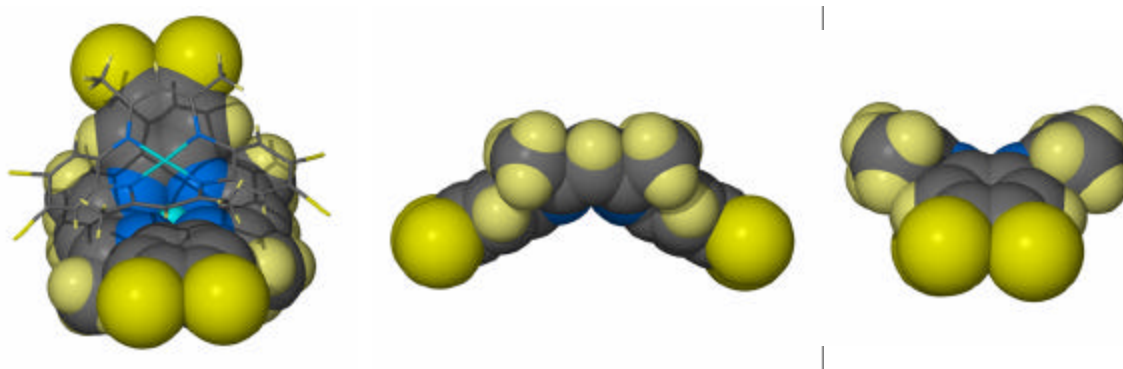
Figure 4.8. Left: Combined stick and space filling view of how **47** packs in the solid state. Center, right: Space filling view of orthogonal projections of **47** showing the two distinct clefts in the structure (Carbon = grey, hydrogen = yellow, chlorine = light yellow, nickel = aqua, nitrogen = blue).

The other macrocycle that was to be synthesized was planned in reference to the solid state fullerene structure with Ni(TMTAA) and Ni(OMTAA).[69,70,77] Since part of the reasoning for the solid state structure between the macrocycles and fullerenes is the aromatic $\pi\cdots\pi$ stacking between host and guest, it was thought that extending the aromatic backbone of the macrocycle using 1,2-diaminonaphthalene would allow for greater interaction. The single reference on the formation of this recently synthesized macrocycle has previously shown it to have luminescent properties.[90] This molecule was given the designation Ni(TMNapTAA), **48**.

The general synthesis is a template reaction whereby in a stepwise process two of the aromatic moieties are, through a process of condensation between the oxygen atom on the dione and the amino proton atoms, put together with the assistance of the nickel mediating this overall four molecule reaction. This has been elucidated with isolation of the intermediate for Ni(OMTAA).[70] The crystal structure of the intermediate has at the

fourth position where the second dione would be a molecule of acetate, the counterion for the nickel salt that was used for the reaction (Figure 4.4).
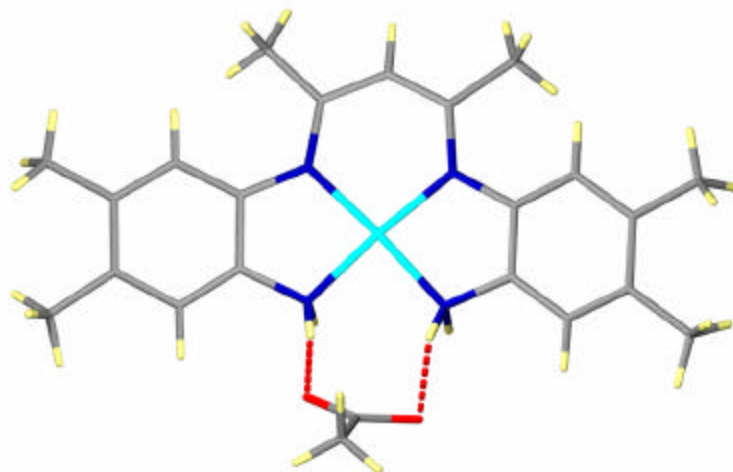
Figure 4.9. Crystal structure of Ni(OMTAA) intermediate with hydrogen bonded acetate (Carbon = grey, hydrogen = yellow, nickel = aqua, nitrogen = blue, oxygen = red).

Even refluxing the solution for a considerable time (upwards to a week) can still lead to both the desired product and the intermediate. As such, at the end of the reaction the solvent is removed before reducing heat, thus forcing the reaction to completion as the more stable product due to the loss of water (as synthesis of the intermediate is not water dependent). This process has led to a higher improvement in yield though by no means does it generally lead to complete conversion to the macrocycle.

However the intermediate with two amino groups is soluble in water whereas the metal ligand bonding of the completed macrocycle and aromatic moieties generally preclude them going into aqueous solutions to any great extent. Also, being a transition metal based macrocycle, it should not be surprising to note that there are intense colors involved in both intermediate and completed product. All macrocycles made are a dark green color (though the naphthalene analogue is a yellow-green) whereas the

138

intermediate is a dark red. As such, work up generally involves separating the intermediate into an aqueous phase while the macrocycle is soluble in organic chloroform or methylene chloride. The aqueous layer is used to wash the organic layer until the solution is clear. Overall this allows for an easy separation.

All compounds were able to be synthesized except for Ni(TMNapTAA), **48**. This compound, unlike **47**, was unable to be synthesized despite attempted reactions including refluxing for up to a week at a time. Mass spectral evidence pointed toward the trimer (with and without the metal center) forming as per Figure 4.4. NMR of the product, even after repeated washing to remove impurities produced a very broad spectrum which is typical for nickel when it is uncoordinated to the macrocycle, it most likely being in an octahedral configuration with the solvent which results in the Ni(II) have two unpaired electrons in the e_g orbitals.

4.5 Gels

A chemical system requires several aspects for it to become a gel. [91] There must be a loose collection of long chain molecules; in the case described here the long chains are SWNT. There must be a property of the system such that the long chain molecules can be linked together at random but fairly close spaced positions. This means the SWNT can't be aligned in bundles or form regular geometrical patterns else they would be more like a crystalline solid such as a zeolite. Finally they must be capable of being stiff enough to produce voids between the long chains so that small molecules, solvents or in the case of aerogels, gases can go in between. For sol-gels, the solution must be able to interact non-covalently with the backbone. If this were not the case the solution would easily leak out and the result would be separation of the solid nanotube matrix from the solvent.

By sonicating mixtures of nanotubes and Ni(TMTAA) or Ni(OMTAA) we have produced highly viscous gels. It was found that the gels formed quicker and were visually stronger when the macrocycle was part of the mix. Gels have previously been shown to form from with nanotubes mixed with polymers[92] or ionic liquids.[16]

If the carbon nanotube was to be part of the experiment it was put into a test-tube first. A solution saturated with the macrocycle was then added at approximately 10 mg/mL. The test tube was stoppered with a cork and parafilm wrapped around to stop any leakage. Sonication then occurred for one hour at a time. At the end of each hour examination of the matrix for signs of gelling occurred. The sonication was repeated until such time as complete gelling had occurred. For gels without the macrocycle this could take upwards of six hours, with the macrocycle generally less than two. If partial gelling had occurred then sonication for longer was performed to see if gelling could occur.

The solutions examined were put into four classes of product (Figure 4.10):

1.   Gelled: complete gelation, gel did not drop after turning test tube upside down.

2.   Partially gelled: Some gelation at the bottom of test tube but also liquid and loose nanotube seen.

3.   Hardly gelled: Mainly liquid and loose nanotube but some slight gelling as seen by some material stuck together.

4.   Ungelled: no visible sign of gelling, liquid loose.

Figure 4.10. Solutions of macrocycle and nanotubes after one hour sonication. Left: An ungelled solution (Solvent: carbon disulfide). Center: A partially gelled solution, not liquid at bottom of vial on cork (Solvent: NMP). Right: A completely gelled matrix (Solvent: Hexane).

A series of solvent were examined and basically came under three types (Table 4.2):

A.   The system gelled with the macrocycle at a much more appreciable rate than without;

B.   The system gelled with and without the macrocycle in the same amount of time;

C.   The system did not gel with or without the macrocycle.

Table 4.2. Solvents examined for gelling behavior (solvent/time (in hours))

A 1. gelled with macrocycle	time	B 2/3. partially gelled with and/or without macrocycle	time	C 3. didn't gel
hexane	1	toluene	1	water
1,2-dichloroethane	1	m-xylene	1	carbon disulfide
1,2-dichlorobenzene	1	mesitylene	1	dimethoxymethane
nitrobenzene	1	ethanol	1	
		2-propanol	1	
		acetonitrile	1	
		DMF	1	
		o-xylene	2	
		methanol	2	
		acetone	3	
		DMSO	3	
		ethyl acetate	4	
		NMP	4	
		chloroform	5	

The solvents chosen involved a wide range of types; polar, non-polar, aromatic, etc and were chosen on the basis of both accessibility and ease of use. For this reason no ionic liquids were studied on the grounds of the need to conduct pre-processing of the ionic liquid from its precursors and that they had been examined previously.

Many of the solvent conditions allowed for gelation even without the need for the nickel macrocycle. This is surprising because the key paper in gelation of solutions using nanotubes was quite specific in its claim that in ordinary organic solvents as mentioned gelation did not occur.[16] However our procedure was different to theirs since they used about 0.5 wt % nanotube while this research was conducted using a larger ratio of SWNT to both solvent and macrocycle. As there were solvents in category B indicates that the sonication is most likely causing defects to occur on the surface of the nanotubes.[93] This introduces defects into the sidewalls of the SWNT producing functional groups such as

carboxylic acid moieties that can then dimerize or further react with the same functional group on adjacent SWNT. It would seem then that the defects are also able to act as crosslinkers to the SWNT and produce gelation. It should also be noted that all four macrocycles performed identically.

For the solvents that gelled without the macrocycle most were the expected aromatic solvents that would expect to π-stack with the SWNT. Unusually NMP (1-Methyl-2-pyrrolidinone) a solvent known to provide stable suspensions of nanotubes was not very effective as a gelation agent, it taking four hours to adequately gel.[31] If the reason for the solvents in Group B gelling was that sidewall defects were occurring, it is possible that NMP may be protecting or somehow repairing the holes on the SWNT. Raman spectroscopy would be capable of detecting this by determining the deterioration of the nanotubes. That practically all solvents produced gelation eventually is probably due to the damage caused by sonication rather than the intrinsic properties of the solvent.

As this project was to do with the supramolecular composites between nanotubes and macrocycles, only systems of type A were further examined. This led to four solvents that seemed to be suitable for this purpose: hexane, 1,2-dichlorobenzene, 1,2-dichloroethane and nitrobenzene. Without the macrocycles extensive sonication was required (upwards of six hours) for gelling to occur compared to the single hour generally required when the macrocycle was present. Even then for all samples the entire solution had not gelled completely.

A series of experiments were devised to see how strong the matrices were at holding the solution and so to get an idea of the strength of the gel. Vials of the gelled solution with either Ni(OMTAA), Ni(TMTAA), no macrocycle and no solvent were placed in a

sand bath at a constant temperature set 10-50°C below that of the solvent boiling point. At regular intervals the vials were taken out, and the change in weight measured. From this the rate of loss of solvent could be measured and the strength of the gels could be compared. The results from three experiments were averaged and presented in Table 4.3.

Table 4.3. Average rate of solvent loss with and without nanotubes and/or macrocycle (mol/min (standard error in brackets), from three experiments, converted from mass/min.)

	1,2-dichloroethane	1,2-dichlorobenzene	nitrobenzene	hexane
SWNT	N/A	-1.99E-06 (1.86E-07)	-8.43E-07 (1.20E-08)	-5.63E-05 (2.71E-07)
SWNT + Ni(TMTAA	-2.40E-05 (2.52E-06)	-2.34E-06 (1.15E-07)	-2.12E-06 (2.19E-07)	-1.14E-06 (1.05E-07)
SWNT + Ni(OMTAA)	N/A**	-2.39E-06 (1.25E-07)	-1.18E-06 (1.50E-07)	-4.08E-06 (2.14E-07)
Solvent only	-3.14E-05 (9.28E-07)	-2.28E-06 (9.35E-07)	-1.19E-06 (2.20E-07)	-5.81E-05 (2.04E-06)

*Solution did not gel. **Contamination in vials negated results.

Within experimental error the solvent loss seemed to be the same with or without SWNT and/or macrocycle. So it would seem that the macrocycle while promoting the rate of gelation may not be actually being part of the backbone of the gel. Certainly the gels seem quite capable of keeping solvent without the macrocycle.

Solid state NMR was used to attempt to determine if any interaction between SWNT and the macrocycles could be detected. Ni(OMTAA) was used as the macrocycle with SWNT. Using at first 100 wt % macrocycle as a calibration, increasing amounts of nanotube were added (5, 10, 15, 17.5, 25 wt % SWNT). Macrocycle and SWNT were ground together in a ball mill with the idea that this would thoroughly mix them and allow for non-covalent attachment. The idea was that as the amount of SWNT was increased, there would be adsorption of the Ni(OMTAA) onto the nanotubes which would affect the magnetic environment of the carbon closest to the SWNT and depending

upon which face was non-covalently bonded too, the carbon peaks for the Ni(OMTAA) would shift.

In the final experiment using 25% SWNT (& 75 wt % Ni(OMTAA) there was no sign of any new peaks in the NMR spectra or loss of the original peaks indicating some change in the macrocycle's environment (Figure 4.11). The peaks did decrease in intensity and somewhat broaden with increasing nanotubes added. The compound was examined and found to be glassy in appearance though there was no sign of gelation. However the broadening can most likely be attributed to the nickel catalyst that is generally there as a contaminant and is difficult to remove even with standard purification processes.[94] Though peaks at approximately 192 and 75 ppm appear to be new, it was later determined that these were spinning side bands, artifacts of the spinning process and this was generally an inevitable process of solid state NMR.

X-ray powder diffraction of the sample at 25% wt SWNT revealed that the ball mill had not broken down the macrocycle enough, there being quite sharp peaks revealing that much of the macrocycle was micro-crystalline. As a crystalline solid, it would make it difficult for individual molecules of Ni(OMTAA) to free themselves from the crystal and non-covalently attach to the SWNT. Future work should entail using a solution or gel of the compounds allowing the macrocycle to intimately attach to the SWNT. It could then be dried to a powder and examined by solid state NMR.
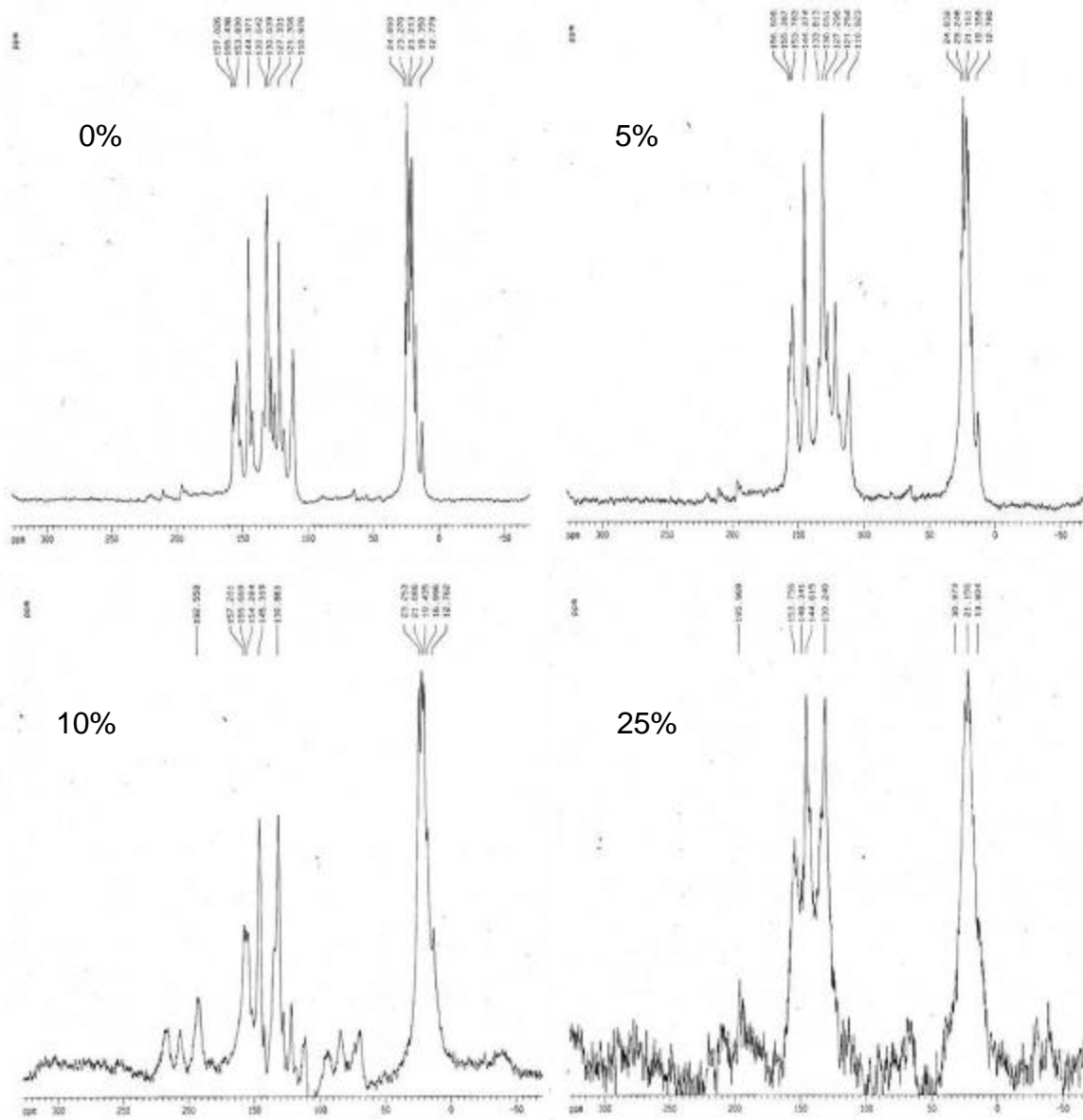
Figure 4.11. Solid state ^{13}C NMR of Ni(OMTAA) with 0, 5, 10 and 25 weight % SWNT.

SEM/EDS were used to examine if the nanotubes adsorb to the SWNT. Gels were deposited on a glass substrate coated in platinum. The gel was dried using a pipette to blow air over the compound and move the solvent away from the nanotube. Nickel was detected using the point detection mode of the EDS at randomly chosen points on the SWNT produced with the HiPco method (i.e.: the catalyst used was iron, not nickel). The iron present is no doubt the catalyst and while having the same counts does not necessarily mean the same concentration to that of nickel. At all points examined nickel could be detected in consistent numbers though the count was rather low compared to carbon (Figure 4.7). SEM with and without the macrocycles also revealed that visually the nanotubes looked to be in many chaotic bundles.
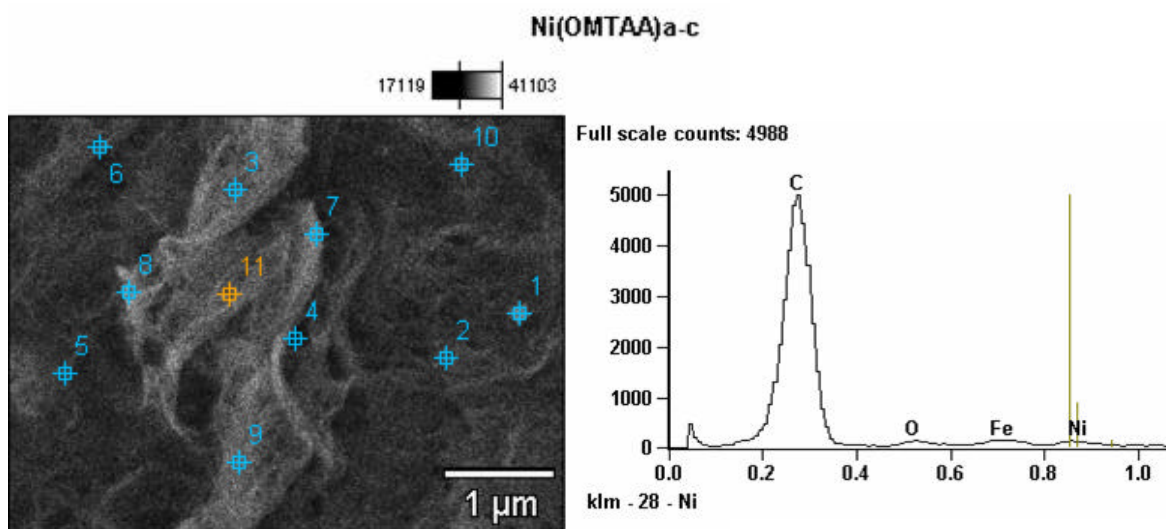
Figure 4.12. SEM/EDS of bundles of SWNT embedded with Ni(OMTAA). All points examined showed signs of nickel (Graph of point 11 shown). Iron is catalyst from SWNT process. (Accelerating Voltage: 5.0 kV Magnification: 25000)

Saturated solutions were used for the experiments to produce gels. Looking at the amount of macrocycle that was found in one milliliter of solution, the density at

147

saturation shows that the amount of macrocycle was enough to cover the SWNT by referring to the work by Basiuk (Table 4.4).[71,72] At a ratio of 10 mg/mL of SWNT to 600–700 mg/mL macrocycle for the least efficient solvent hexane it would appear that there is enough coverage of the solvent to encapsulate the nanotubes. Both theoretically and by experiment a mass ratio of 4:5 nanotube:macrocycle is all that is required to surround a typical nanotube of the diameter usually found synthesized *via* the arc-discharge process.[71,72]

Table 4.4. Solubility of nickel macrocycles in solvents that gel with SWNT

Density (g/ml)	**45**			**46**			**47**		
Hexane	0.62	±	0.05	0.66	±	0.02	0.68	±	0.04
1,2-dichloroethane	1.24	±	0.01	1.24	±	0.01	1.28	±	0.08
1,2-dichlorobenzene	1.30	±	0.004	1.30	±	0.01	1.30	±	0.01
Nitrobenzene	1.20	±	0.002	1.20	±	0.00	1.21	±	0.01

Ni(TMTAA) = **45**, Ni(OMTAA) = **46**, Ni(TClTMTAA) = **47**.

4.6 Conclusion

The results of this investigation into the SWNT-nickel macrocycle project are clear. Experiments such as SEM/EDS and solubility measurement show that the nickel macrocycle has the concentration in solution to be liberally spread and attracted to the SWNT. However, solid state NMR was inconclusive, as much because of the preparation as to whether there is a macrocycle-nanotube interaction. The method has not yet been found that makes Ni(TMTAA) and analogues have an interaction of the strength of that to the ionic liquids where recognizable results were available at 0.5 wt % SWNT.[16]

While the macrocycles are helping increase the speed of gelation there is no evidence that they actually are part of the linker molecules that hold the various tubes together to

create the gel. It is of course possible, especially with the aromatic solvents, there is π-stacking occurring between the macrocycle and the bulk. The rate of solvent loss seems to indicate that the interaction is between solvent and SWNT and not the macrocycles and SWNT. The best evidence to date of macrocycle-solvent interaction is that gelation is faster when the macrocycle is present in certain solvents, though gelation does occur with and without macrocycle present. It is possible that the macrocycles may be acting as catalysts to gel formation rather than as active substrates for it, as they have been implicated previously.[95]

4.7   *Experimental*

Single-walled carbon nanotube CarboLex AP-grade from Sigma-Aldrich (St. Louis, Missouri) were ball milled before use and in some cases purified using 6M nitric acid and washed with deionized water. Purified HiPco® single-wall carbon nanotubes were from Carbon Nanotechnologies Incorporated (Houston, Texas)and were ball milled before use. Nickel (II) acetate tetrahydrate, 98% was from Sigma-Aldrich (St. Louis, Missouri). O-phenylenediamine 98%, 4,5-Dimethylbenzene-1,2-diamine, 97%, 4,5-dichloro-o-phenylenediamine, 98%, 2,3-diaminonaphthalene and 2,4-pentanedione 99+% were from Acros Organics (Fair Lawn, New Jersey) and used as is. All solvents were ACS or HPLC grade. Test-tubes used were Fisherbrand borosilicate glass from Fisher Scientific. Sonicator was a Fisher ultrasonic cleaner, Model FS30, 1 gallon, 120V 50/60Hz, 1A, 130w, without heater.

Macrocycles **45** – **48** characterization

All macrocycles were synthesized as described in Section 4.4 of the text.

Ni(TMTAA) (**45**)

Yield: 85%. ^{1}H NMR (300 MHz; CDCl$_3$) δ 6.68 (dd, 4H), 6.56 (dd, 4H), 4.84 (s, 2H), 2.06 (s, 12H); ^{13}C NMR (75 MHz; CDCl$_3$) δ; *m/z* (ESI) 400.04 (M$^{+\cdot}$), 799.32 (2M$^+$). **47** was also crystallized and identified from its unit cell from comparison with the CCDC database.

Ni(OMTAA) (**46**)

Yield: 67%. ^{1}H NMR (300 MHz; CDCl$_3$) δ 6.45 (s, 4H), 4.75 (s, 2H), 2.02, 2.03 (s, 24H); ^{13}C NMR (75 MHz; CDCl$_3$) δ 154.9, 145.4, 129.6, 122.1, 110.5, 22.17, 19.73; *m/z* (APCI-MS) 457.31 (M+H$^+$), (ESI) 457 (M+H$^+$), 914 (2M + H$^+$). **46** was also crystallized and identified from its unit cell from comparison with the CCDC database. The intermediate structure was also identified from its unit cell from comparison with the CCDC database.

Ni(TClTMTAA) (**47**)

Yield: 45%. ^{1}H NMR (300 MHz; CDCl$_3$) 7.46 (s, 4H), 5.30 (s, 2H), 2.34 (s, 12H); ^{13}C NMR (75 MHz; CDCl$_3$) δ 159.2, 129.2, 128.7, 127.6, 121.4, 31.5.

Crystal data for Ni(TClTMTAA):

C$_{22}$H$_{18}$Cl$_4$N$_4$Ni, *M* = 538.91, colorless parallelepiped, 0.15 × 0.12 × 0.09 mm^3, monoclinic, space group *C*2/*c* (No. 15), *a* = 16.931(5), *b* = 19.917(5), *c* = 16.092(6) Å, ***b*** = 105.857(7)°, *V* = 5220(3) Å^3, *Z* = 8, *D*$_c$ = 1.371 g/cm^3, *F*$_{000}$ = 2192, Bruker SMART 1000 CCD diffractometer, MoKα radiation, λ = 0.71073 Å, *T* = 173(2)K, 2***q***$_{max}$ = 54.2°, 17278 reflections collected, 5687 unique (R$_{int}$ = 0.3007). Final *GooF* = 0.876, *R1* =

0.1299, $wR2 = 0.2855$, R indices based on 1504 reflections with I $>2\sigma$ (I) (refinement on F^2), 189 parameters, 8 restraints. Lp and absorption corrections applied, $\boldsymbol{m} = 1.169$ mm^{-1}. (Note: Squeeze on the Platon suite was used to refine structure due to weak data set; Spek, A. L. (1999). *PLATON*. Version of July 1999. Utrecht University, The Netherlands.)

Attempted synthesis of Ni(TMNapTAA) (**48**)

The reaction was attempted at various time lengths after the usual time length (~18 hours) did not seem to produce a completed template reaction, mass spectral evidence showing only a 2:1 diaminonaphthalene:dione with or without the nickel atom present. Longer times of up to a week did produce a small amount of dark green powder that however was yellow-green in solution, the majority product still the red incomplete template reaction.

Solid state NMR

Ni(OMTAA) (247mg) was ball milled for five minutes and then packed into a ceramic solid state NMR rotor with Teflon top. Once the NMR tube was placed in the 300 MHz NMR and calibrated the rotor was spun up to 5000 Hz and the NMR collected (from 1 hour for pure Ni(OMTAA) up to 12 hours for 25 wt % SWNT). At the end of each run, the Ni(OMTAA) was removed from the rotor. The appropriate amount of SWNT (Sigma-Aldrich) was mixed (between 13 and 15 mg added per run) in with the Ni(OMTAA) and ball milled for a further five minutes before placement in the rotor. The ball milling was later found not to disperse the macrocycle enough as was determined by powder X-ray diffraction.

Large scale "TGA" to determine solvent loss of gels: Gels were made up (or just solvent as control) in borosilicate vials and sonicated to form gel. The gels in the vials were weighed and placed in a constant temperature sand bath at just below boiling point (Hexane (b.p. = 69°C) at 51°C; 1,2-dichlorobenzene (b.p. = 160°C) at 179°C; Nitrobenzene (b.p. = 210°C) at 160°C); 1,2-dichloroethane (b.p. = 81°C) at 52°C). At regular intervals, the tubes were taken out and capped to stop solvent loss, reweighed and returned to the sandbath. The results were plotted mass versus time and the slope taken to determine the rate of loss per unit time (g/min). After averaging from three sets of data, the combined data was converted to mol/min.

SEM/EDS: A sample of gelled SWNT (HiPco) with Ni(OMTAA) in hexane or 1,2-dichlorobenzene was blow dried on a platinum coated (~5 nm) microscope slide and placed in the SEM/EDS. The hexane gel produced no results though SWNT could be visualized. The 1,2-dichlorobenzene dried gel was found on the grid and 11 random points picked scanned with the EDS. The graph depicted in this chapter is to all intents and purposes identical with the other 10 graphs in both quantitatively and qualitatively. Iron is from the catalyst and oxygen from the borosilicate glass.

(1) Iijima, S. *Nature* **1991**, *354*, 56-58.
(2) Iijima, S.; Ichihashi, T. *Nature* **1993**, *364*, 737.
(3) Edelmann, F. T. *Angew. Chem. Int. Ed.* **1999**, *38*, 1381-1387.
(4) Baughman, R. H.; Zakhidov, A. A.; de Heer, W. A. *Science* **2002**, *297*, 787-792.
(5) Zhou, O.; Shimoda, H.; Gao, B.; Oh, S.; Fleming, L.; Yue, G. *Acc. Chem. Res.* **2002**, *35*, 1045-1053.
(6) Banerjee, S.; Kahn, M. G. C.; Wong, S. S. *Chem. Eur. J.* **2003**, *9*, 1898-1908.
(7) Sun, J.; Gao, L.; Iwasa, M. *Chem. Commun.* **2004**, 832-833.
(8) Xiao, X.; Elam, J. W.; Trasobares, S.; Auciello, O.; Carlisle, J. A. *Adv. Mater.* **2005**, *17*, 1496-1500.

(9) An, L.; Xu, W.; Rajagopalan, S.; Wang, C.; Wang, H.; Fan, Y.; Zhang, L.; Jiang, D.; Kapat, J.; Chow, L.; Guo, B.; Liang, J.; Vaidyanathan, R. *Adv. Mater.* **2004**, *16*, 2036-2040.

(10)   Wang, X.; Padture, N. P.; Tanaka, H. *Nat. Mater.* **2004**, *3*, 539-544.

(11)   Lau, K.-T.; Shi, S.-Q.; Zhou, L.-M.; Cheng, H.-M. *J. Comp. Mat.* **2003**, *37*.

(12)   Sun, L. F.; Xie, S. S.; Liu, W.; Zhou, W. Y.; Liu, Z. Q.; Tang, D. S.; Wang, G.; Qian, L. X. *Nature* **2000**, *403*, 384.

(13)   Roth, S.; Carroll, D. *One-Dimensional Metals: Conjugated Polymers, Organic Crystals, Carbon Nanotubes*; Wiley-VCH Verlag GmbH & Co. KGaA: Weinheim, 2004.

(14)   Liu, C.; Zhang, J.; He, J.; Hu, G. *Polymer* **2003**, *44*, 7529-7532.

(15)   Chen, X.; Zhang, G.; Chen, C.; Zhou, L.; Li, S.; Li, X. *Advanced Engineering Materials* **2003**, *5*, 514-518.

(16)   Fukushima, T.; Kosaka, A.; Ishimura, Y.; Yamamoto, T.; Takigawa, T.; Ishii, N.; Aida, T. *Science* **2003**, *300*, 2072-2074.

(17)   Gavalas, V. G.; Andrews, R.; Bhattacharyya, D.; Bachas, L. G. *Nano Lett.* **2001**, *1*, 719-721.

(18)   Matsui, K.; Pradhan, B. K.; Kyotani, T.; Tomita, A. *J. Phys. Chem. B* **2001**, *105*, 5682-5688.

(19)   Lin, Y.; Cui, X. *Chem. Commun.* **2005**, 2226-2228.

(20)   Zhu, C.; Xie, Z.; Guo, K. *Diamond Relat. Mater.* **2004**, *13*, 180-183.

(21)   Arepalli, S.; Nikolaev, P.; Gorelik, O.; Hadjiev, V. G.; Holmes, W.; Files, B.; Yowell, L. *Carbon* **2004**, *42*, 1783-1791.

(22)   Loa, I. *J. Raman Spectrosc.* **2003**, *34*, 611-627.

(23)   Reich, S.; Thomsen, C.; Maultzsch, J. *Carbon Nanotubes Basic Concepts and Physical Properties*; Wiley-VCH Verlag GmbH & Co. KGaA: Weinheim, 2004.

(24)   Hirsch, A. *Angew. Chem. Int. Ed.* **2002**, *41*, 1853-1859.

(25)   Liu, J.; Rinzler, A. G.; Dai, H.; Hafner, J. H.; Bradley, R. K.; Boul, P. J.; Lu, A.; Iverson, T.; Shelimov, K.; Huffman, C. B.; Rodriguez-Macias, F.; Shon, Y.-S.; Lee, T. R.; Colbert, D. T.; Smalley, R. E. *Science* **1998**, *280*, 1253-1256.

(26)   Kim, P.; Odom, T. W.; Huang, J.-L.; Lieber, C. M. *Phys. Rev. Lett.* **1999**, *82*, 1225-1228.

(27)   Hartschuh, A.; Pedrosa, H. N.; Novotny, L.; Krauss, T. D. *Science* **2003**, *301*, 1354-1356.

(28)   Liu, Y.; Pan, c.; Wang, J. *J. Mater. Sci.* **2004**, 1091-1094.

(29)   Rao, A. M.; Richter, E.; Bandow, S.; Chase, B.; Eklund, P. C.; Williams, K. A.; Fang, S.; Subbaswamy, K. R.; Menon, M.; Thess, A.; Smalley, R. E.; Dresselhaus, G.; Dresselhaus, M. S. *Science* **1997**, *275*, 187-191.

(30)   Ajayan, P. M.; Terrones, M.; Guardia, A. d. l.; Huc, V.; Grobert, N.; Wei, B. Q.; Lezec, H.; Ramanath, G.; Ebbesen, T. W. *Science* **2002**, *296*, 705.

(31)   Ausman, K. D.; Piner, R.; Lourie, O.; Ruoff, R. S.; Korobov, M. *J. Phys. Chem. B* **2000**, *104*, 8911-8915.

(32)   Niyogi, S.; Hamon, M. A.; Hu, H.; Zhao, B.; Bhowmik, P.; Sen, R.; Itkis, M. E.; Haddon, R. C. *Acc. Chem. Res.* **2002**, *35*, 1105-1113.

(33)   Diehl, M. R.; Steuerman, D. W.; Tseng, H.-R.; Vignon, S. A.; Star, A.; Celestre, P. C.; Stoddart, J. F.; Heath, J. R. *ChemPhysChem* **2003**, *4*, 1335-1339.

(34)   Dai, G.-P.; Liu, C.; Liu, M.; Wang, M.-Z.; Cheng, H.-M. *Nano Lett.* **2002**, *2*, 503-506.

(35)   Lee, S. M.; An, K. H; Lee, Y. H.; Seifert, G.; Frauenheim, T. *J. Am. Chem. Soc.* **2001**, *123*, 5059-5063.

(36)   Vincent, P.; Brioude, A.; Journet, C.; Rabaste, S.; Purcell, S. T.; Brusq, J. L.; Plenet, J. C. *J. Non-Cryst. Solids* **2002**, *311*, 130-137.

(37)   Dalton, A. B.; Collins, S.; Razal, J.; Munoz, E.; Ebron, V. H.; Kim, B. G.; Coleman, J. N.; Ferraris, J. P.; Baughman, R. H. *J. Mater. Chem.* **2004**, *14*, 1-3.

(38)   Seeger, T.; Köhler, T.; Frauenheim, T.; Grobert, N.; Rühle, M.; Terrones, M.; Seifert, G. *Chem. Commun.* **2002**, 34-35.

(39)   Asai, M.; Fujita, N.; Sano, M.; Shinkai, S. *J. Mater. Chem.* **2003**, *13*, 2145-2149.

(40)   Gavalas, V. G.; Law, S. A.; Ball, J. C.; Andrews, R.; Bachas, L. G. *Anal. Biochem.* **2004**, *329*, 247-252.

(41)   Tasis, D.; Tagmatarchis, N.; Georgakilas, V.; Prato, M. *Chem. Eur. J.* **2003**, *9*, 4000-4008.

(42)   Pompeo, F.; Resasco, D. E. *Nano Lett.* **2002**, *2*, 369-373.

(43)   Huang, W.; Lin, Y.; Taylor, S.; Gaillard, J.; Rao, A. M.; Sun, Y.-P. *Nano Lett.* **2002**, *2*, 231-234.

(44)   Liu, Z.; Shen, Z.; Zhu, T.; Hou, S.; Ying, L. *Langmuir* **2000**, *16*, 3569-3573.

(45)   Georgakilas, V.; Kordatos, K.; Prato, M.; Guldi, D. M.; Holzinger, M.; Hirsch, A. *J. Am. Chem. Soc.* **2002**, *124*, 760-761.

(46)   Nakashima, N.; Tomonari, Y.; Murakami, H. *Chem. Lett.* **2002**, 638-659.

(47)   Strano, M. S.; Dyke, C. A.; Usrey, M. L.; Barone, P. W.; Allen, M. J.; Shan, H.; Kittrell, C.; Hauge, R. H.; Tour, J. M.; Smalley, R. E. *Science* **2003**, *301*, 1519-1522.

(48)   Dyke, C. A.; Stewart, M. P.; Maya, F.; Tour, J. M. *Synth. Lett.* **2004**, *1*, 155-160.

(49)   Dyke, C. A.; Tour, J. M. *J. Am. Chem. Soc.* **2003**, *125*, 1156-1157.

(50)   Mickelson, E. T.; Chiang, I. W.; Zimmerman, J. L.; Boul, P. J.; Lozano, J.; Liu, J.; Smalley, R. E.; Hauge, R. H.; Margrave, J. L. *J. Phys. Chem. B* **1999**, *103*, 4318-4322.

(51)   Kamaras, K.; Itkis, M. E.; Hu, H.; Zhao, B.; Haddon, R. C. *Science* **2003**, *301*, 1501.

(52)   Kis, A.; Csányi, G.; Salvetat, J.-P.; Lee, T.-N.; Couteau, E.; Kulik, A. J.; Benoit, W.; Brugger, J.; Forró, L. *Nat. Mater.* **2004**, *3*, 153-157.

(53)   Richard, C.; Balavoine, F.; Schultz, P.; Ebbesen, T. W.; Mioskowski, C. *Science* **2003**, *300*, 775-778.

(54)   O'Connell, M. J.; Bachilo, S. M.; Huffman, C. B.; Moore, V. C.; Strano, M. S.; Haroz, E. H.; Rialon, K. L.; Boul, P. J.; Noon, W. H.; Kittrell, C.; Ma, J.; Hauge, R. H.; Weisman, R. B.; Smalley, R. E. *Science* **2002**, *297*, 593-596.

(55)   Chen, J.; Rao, A. M.; Lyuksyutov, S.; Itkis, M. E.; Hamon, M. A.; Hu, H.; Cohn, R. W.; Eklund, P. C.; Colbert, D. T.; Smalley, R. E.; Haddon, R. C. *J. Phys. Chem. B* **2001**, *105*, 2525-2528.

(56)   Star, A.; Steuerman, D. W.; Heath, J. R.; Stoddart, J. F. *Angew. Chem. Int. Ed.* **2002**, *41*, 2508-2512.

(57)   Star, A.; Stoddart, J. F.; Steuerman, D.; Diehl, M.; Boukai, A.; Wong, E. W.; Yang, X.; Chung, S.-W.; Choi, H.; Heath, J. R. *Angew. Chem. Int. Ed.* **2001**, *40*, 1721-1725.

(58)   Kang, Y.; Taton, T. A. *J. Am. Chem. Soc.* **2004**, *125*, 5650-5651.

(59)   Fan, J.; Wan, M.; Zhu, D.; Chang, B.; Pan, Z.; Xie, S. *J. Appl. Polym. Sci.* **1999**, *74*, 2605-2610.

(60)   Chen, J.; Liu, H.; Weimer, W. A.; Halls, M. D.; Waldeck, D. H.; Walker, G. C. *J. Am. Chem. Soc.* **2002**, *124*, 9034-9035.

(61)   Chen, R. J.; Zhang, Y.; Wang, D.; Dai, H. *J. Am. Chem. Soc.* **2001**, *123*, 3838-3839.

(62)   Sloan, J.; Kirkland, A. I.; Hutchison, J. L.; Green, M. L. H. *Chem. Commun.* **2002**, 1319-1332.

(63)   Morgan, D. A.; Sloan, J.; Green, M. L. H. *Chem. Commun.* **2002**, 2442-2443.

(64)   Okazaki, T.; Suenaga, K.; Hirahara, K.; Bandow, S.; Iijima, S.; Shinohara, H. *J. Am. Chem. Soc.* **2001**, *123*, 9673-9674.

(65)   L'Eplattenier, F. A.; Pugin, A. *Helv. Chim. Acta* **1975**, *58*, 101-102.

(66)   Cotton, F. A.; Czuchajawska, J. *Polyhedron* **1990**, *9*, 2553-2566.

(67)   Steed, J. W.; Atwood, J. L. *Supramolecular Chemistry*; John Wiley & Sons: Chichester, 2000.

(68)   Andrews, P. C.; Atwood, J. L.; Barbour, L. J.; Nichols, P. J.; Raston, C. L. *Chem. Eur. J.* **1998**, *4*, 1384-1387.

(69)   Croucher, P. D.; Marshall, J. M. E.; Nichols, P. J.; Raston, C. L. *Chem. Commun.* **1999**, 193-194.

(70)   Croucher, P. D.; Nichols, P. J.; Raston, C. L. *J. Chem. Soc., Dalton Trans.* **1999**, 279-284.

(71)   Basiuk, E. V.; Rybak-Akimova, E. V.; Basiuk, V. A.; Acosta-Najarro, D.; Saniger, J. M. *Nano Lett.* **2002**, *2*, 1249-1252.

(72)   Basiuk, V. A. *J. Phys. Chem. B* **2004**, *108*, 19990-19994.

(73)   Hotz, R. P.; Purrington, S. T.; Singh, P.; Bereman, R. D.; Sinn, E. *Inorg. Chim. Acta* **1987**, *130*, 195-201.

(74)   Greenwood, N. N.; Earnshaw, A. *Chemistry of the Elements*; 2nd ed.; Butterworth-Heinemann: Oxford, 2002.

(75)   Hardie, M. J.; Malic, N.; Nichols, P. J.; Raston, C. L. *Tetrahedron Lett.* **2001**, *42*, 8075-8079.

(76)   Malic, N.; Nichols, P. J.; Raston, C. L. *Chem. Commun.* **2002**, 16-17.

(77)   Andrews, P. C.; Atwood, J. L.; Barbour, L. J.; Croucher, P. D.; Nichols, P. J.; Smith, N. O.; Skelton, B. W.; White, A. H.; Raston, C. L. *J. Chem. Soc., Dalton Trans.* **1999**, 2927-2932.

(78)   Ness, T.; Nichols, P. J.; Raston, C. L. *Eur. J. Inorg. Chem.* **2001**, 1993-1997.

(79)   Raston, C. L.; Nichols, P. J.; Baranyai, K. *Angew. Chem. Int. Ed.* **2000**, *39*, 1842-1845.

(80)   Hardie, M. J.; Malic, N.; Raston, C. L. *J. Chem. Soc., Dalton Trans.* **2002**, 295-296.

(81)   Hardie, M. J.; Malic, N.; Raston, C. L.; Roberts, B. A. *Chem. Commun.* **2001**, 865-866.

(82)   Drew, M. G. B.; Jutson, N. J.; Mitchell, P. C. H.; Potter, R. J.; Thompsett, D. *J. Chem. Soc., Faraday Trans.* **1993**, *89*, 3963-3973.

(83)   Drew, M. G. B.; Jutson, N. J.; Mitchell, P. C. H.; Potter, R. J.; Thompsett, D. *J. Mater. Chem.* **1992**, *2*, 817-822.

(84)   Wang, Y.-Q.; Sherwood, P. M. A. *Chem. Mater.* **2004**, *16*, 5427-5436.

(85)   Lee, J. Y.; An, K. H.; Heo, J. K.; Lee, Y. H. *J. Phys. Chem. B* **2003**, *107*, 8812-8815.

(86)   Gu, Z.; Peng, H.; Hauge, R. H.; Smalley, R. E.; Margrave, J. L *Nano Lett.* **2002**, *2*, 1009-1013.

(87)   Jin, Z.-X.; Xu, G. Q.; Goh, S. H. *Carbon* **2000**, *38*, 1135-1139.

(88)   Lu, C.; Chung, Y.-L.; Chang, K.-F. *Water Research* **2005**, *39*, 1183-1189.

(89)   Barthos, R.; Méhn, D.; Demortier, A.; Pierard, N.; Morciaux, Y.; Demortier, G.; Fonsec, A.; Nagy, J. B. *Carbon* **2005**, *43*, 321-325.

(90)   Costamagna, J.; Ferraudi, G.; Villagran, M.; Wolcan, E. *J. Chem. Soc., Dalton Trans.* **2000**, *15*, 2631-2637.

(91)   Horkay, F.; McKenna, G. B. In *Physical Properties of Polymers Handbook*; Mark, J. E., Ed.; AIP Press: Woodbury, New York, 1996, pp 379-400.

(92)   Fujita, N.; Asai, M.; Yamashita, T.; Shinkai, S. *J. Mater. Chem.* **2004**, *14*, 2106-2114.

(93)   Koshio, A.; Yudasaka, M.; Zhang, M.; Iijima, S. *Nano Lett.* **2001**, *1*, 361-363.

(94)   Kitaygorodskiy, A.; Wang, W.; Xie, S.-Y.; Lin, Y.; ShiralFernando, K. A.; Wang, X.; Qu, L.; Chen, B.; Sun, Y.-P. *J. Am. Chem. Soc.* **2005**, *127*, 7517-7520.

(95)   Caiut, J. M. A.; Nakagaki, S.; Friedermann, G. R.; Zarbin, S. M. D. A. J. G. *J. Mol. Cat. A: Chem.* **2004**, *222*, 213-222.

Chapter 5: Pyrogallol[4]arene large spheres

Abstract

This chapter elucidates the discovery of large scale structures of aggregates of pyrogallolarene supermolecules. Pyrogallolarenes have been shown to be excellent tectons for large supermolecules. The interest in them stems from the hexameric motif that self-assembles spontaneously in organic and sometimes polar solvents. The structures have been seen as encapsulating what was initially found to be disordered solvent molecules. Recently, efforts have to date have discovered methods whereby ordered solvent and more recently large aromatic fluorescent molecules can be locked in position within the cavity. The next stage of development from a structural viewpoint is to create larger edifices that could be a part of applications such as drug delivery. Pyrogallolarenes and associated calixarene-type molecules have been shown to form bi-layer or micellular constructs with modification to both upper and lower rims of the cup-shaped cavity. However we have discovered that the hexameric supermolecule will also aggregate into both spherical and tubular constructs. The design, characterization and hypothesis on how large scale structures can form from an unusual substrate will be discussed.

5.1 A question of scale: comparing chemistry and biology

Chemistry and biology, though of course interconnected, are often looked at on different scales. Biologists can look through light or electron microscopes as much of the cellular architecture is at the microscale (10^{-6} m). For chemists molecular building blocks are generally examined using Ångstroms (10^{-10} m) and even the large non-covalently bound capsules are a few nanometers in diameter (10^{-9} m). Science and chemistry in particular, is currently at the stage of building the molecules and architecture from the molecular level up to the realm that has been the preserve of biologists.[1] The need to explore the development of structures between the cellular and molecular level is pressing and full of opportunity for discovery. Manipulating matter at this level is a goal that will allow for applications in both the medical and engineering domains as well as gaining fundamental knowledge of cellular architecture.

A common avenue to expedite the understanding of molecular control is by building simpler repeating substructures capable of self-assembly.[2] This follows from the knowledge gleaned of evolutionary processes; nature's ability to form complex structures from smaller, identical units has many advantages in both the economies of energy and design. It is still difficult to elucidate larger scale formations by judiciously designing the smaller tectons. Nature has shown that it is possible from simple rules and systems to build up complex patterns found in inorganic shell structures that follow the Fibonacci number pattern or the regular organic architecture of viruses that exhibit icosohedral symmetry.[3,4]

This means that it is possible to get some headway into the workings of nature through mimicry. Rather than delve into biological complexity, the "bottom-up"

approach has inspired many and from this can be distilled the mechanics of supramolecular machinery. For example using liposomes as a template it has been possible to form complex interlocking capsules that can capture otherwise unstable substrates,[5] enhance reaction rates[6] and provide transportation through unfriendly environments.[7] Another example of particular interest for this project is of cellular organelle transportation through nanotube-like appendages[8] much in the way of the more synthetically formed carbon nanotubes[9] or non-covalent tube assemblies.[10] This example of 'sphere' and 'tubule' interaction include the observation of cell-to-cell communication *via* nano-tubular cytonemes (as probed with fluorescently labeled wheat germ agglutinin) and the synergic action between amphiphysin and dynamin in clathrin-mediated endocytosis (i.e.: the budding of vesicles from tubes).[11] Very few synthetic systems have been developed in this way though giant vesicles with connecting tubules have been formed from phospholipids *via* micromanipulation.[12]

5.2 *Pyrogallolarenes: the calix[n]arene analogues*

5.2.1 Synthesis of pyrogallolarene

Within the realms of supramolecular chemistry, these recently developed abilities to control self-assembly have been exploited in the design of interesting spherical or capsular architectures that are of high symmetry. This chapter describes a unique form of biological mimic formed from an analogue of a well known synthetic molecular system, the bowl-shaped calix[n]arenes of chapter 3 (Figure 5.1, left). Besides the possibility of p···p interactions of the aromatic rings, the upper and lower rim can be decorated with a multitude of functional groups allowing for a range of covalent and non-covalent interactions. Capsules formed from calix[n]arenes are capable of interactions both within

the self-assembled cavities and externally between each other[13,14] and with a variety of other substrates, including DNA.[15]

Phenyl alcohol pyrogallol (1, 2, 3 – trihydroxybenzene; Figure 5.1, left; W = –H and X, Y, Z = –OH) has been selected as a precursor due to the proximity and number of alcohol functionalities that allow for multiple hydrogen bonds.[16]   While the parent
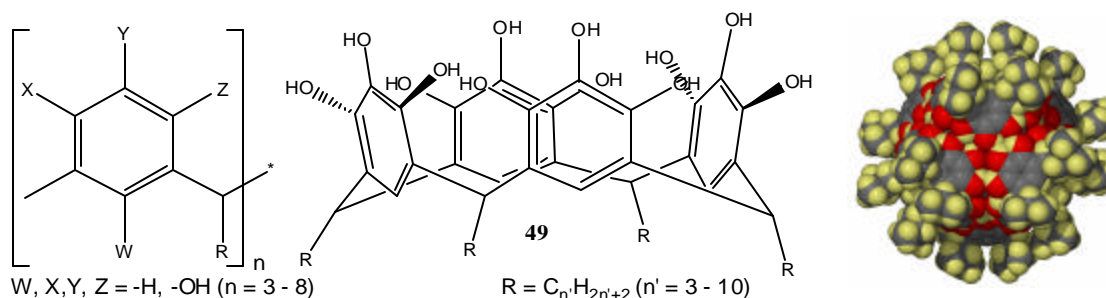
Figure 5.1. Calix[n]arene (left) and the pyrogallolarene analogue, **49**, (center) used to form the supermolecule. Right: Crystal structure of hexamer **49**$_6$.(EtOAc)$_6$(water) where R = -CH$_2$CH(CH$_3$)$_2$ (grey = carbon, yellow = hydrogen, red = oxygen, ethyl acetate molecules removed for clarity).

calix[n]arene macrocycle is a base induced condensation process, pyrogallolarene is easily synthesized from phenyl alcohols and aldehydes *via* an acidic condensation reaction (Scheme 5.1).[17]

The product pyrogallolarene (**49**) has been shown to be an excellent substrate for the formation of various supermolecules (Figure 5.2).[13] The bowl conformation is preferentially formed from four each of these substrates (n = 4). This resulting hydrogen bonding produces almost exclusively a cup-shaped tetramer, only in one recorded instance has a low yielding hexamer been found.[18] The other precursor for the pyrogallolarene is a set of alkyl aldehydes (Scheme 5.1). Using alkyl aldehydes provides access to the weaker van der Waals forces of fatty carbon chains to participate in self-assembly much as can be found with the cell wells within which lies a complex large mix

of lipid molecules.[19,20] Alkyl aldehydes used in this study produced pyrogallolarenes with alkyl tails in length from three to ten carbons long.

$$R = \text{-}C_3H_7$$
$$\text{-}C_4H_9$$
$$\text{-}C_5H_{11}$$
$$\text{-}C_6H_{13}$$
$$\text{-}C_7H_{15}$$
$$\text{-}C_8H_{17}$$
$$\text{-}C_8H_{16}Br$$
$$\text{-}C_9H_{19}$$
$$\text{-}C_{10}H_{21}$$
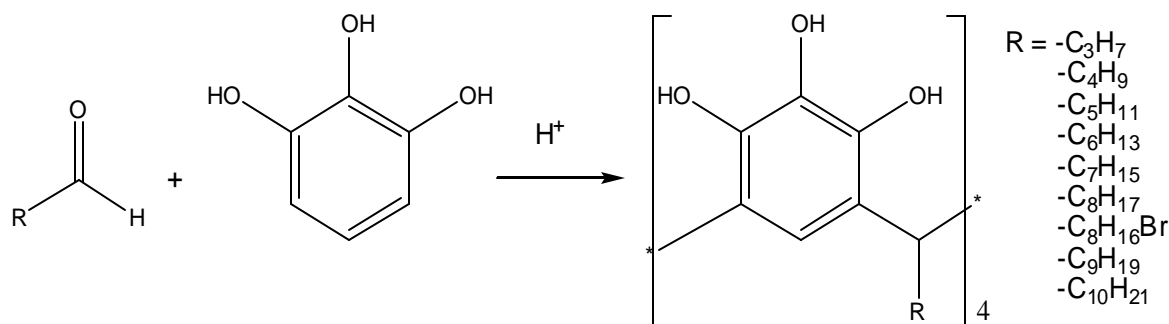
Scheme 5.1. Synthesis of pyrogallolarenes used for this project. A simple acid catalyzed reaction results in the tetramer being formed as the cup shaped molecule.

5.2.2   Formation of hexameric spheres

Pyrogallolarenes form differing motifs under solid-state conditions: bilayers, infinite regularly spaced channels[21] or discrete hexameric spheres.[22] These conformations are accessed by varying the solvent conditions during the recrystallization process. While each of the three conformations of the pyrogallolarenes produces differing properties in the bulk, the spherical motif provides a structural complexity not previously known.

The "sphere" consists of six pyrogallolarene molecules where each molecule of **49** is considered to be one face of a cube (Figure 5.2). However due to the cup shape of the calixarene base the overall shape appears spherical. The hexameric spheres are formed during approximately twelve hours of crystallization from a solution of ethyl acetate under ambient conditions, other solvents generally leading to the bilayer conformation (though it must be noted that anecdotally it is thought that recrystallization using acetone retained the conformation).
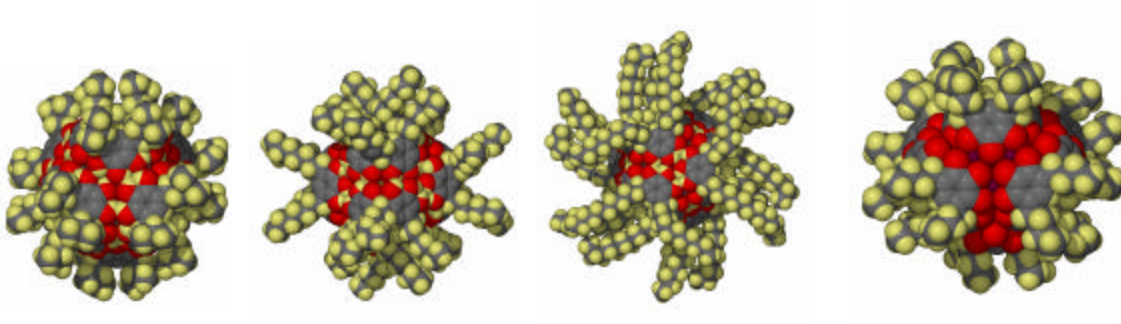
Figure 5.2. (left to right) Examples of solid state structures for **49**$_6$ showing areas of hydrophobicity (alkyl chains) and hydrophilicity (hydrogen/metal bonded oxygen atoms): R = –CH$_2$CH(CH$_3$)$_2$; R = –C$_6$H$_{13}$; –C$_{10}$H$_{21}$; R = –C$_3$H$_7$, X, Z = OGa^{3+}, Y = Ga$_2$. Atom color key: Grey = carbon; yellow = hydrogen; red = oxygen; purple = gallium. Solvent of crystallization removed for clarity. Not to scale.

The enclosed cavity consists of seven well ordered molecules (six of ethyl acetate, one of water), the strong hydrogen bonding between the encapsulated solvent and the individual parts of the hexamer producing a strongly bound capsule.[13] Solution-state studies reveal that the hexameric spheres, connected by a total of 72 hydrogen bonds, keep their supramolecular structure even in polar solutions.[23] Other studies revealed how the guest molecules have difficulty diffusing into solution.[24] With the substitution of metal atoms and water molecules for the protons on the deprotonated hydroxyl groups the hexameric spheres may even survive in mixed water/acetone solutions (Figure 5.2, right).[25,26]

Solid state studies show that an individual hexamer spans a maximum width of approximately four nanometers, actual width dependent on the length of the lower rim alkyl chain. The overall molecule can be considered to be oblate rather than perfectly spherical when taking the longer alkyl chains into account. The supermolecule takes on an asymmetric pose with the alkyl arms generally found together at opposite ends of the supermolecule leaving a hydrogen bonded equatorial space orthogonal to the alkyl chains open. Of course this position is not expected to be fixed this way in solution though this

does indicate an expected tendency for the hydrophobic and hydrophilic regions of the supermolecule to move so as to minimize repulsions.

5.3 Aggregation of the hexameric spheres

5.3.1 Initial discovery of aggregation

An investigation of the 4 nm hexameric supermolecules using dynamic light scattering (DLS) has shown they form larger molecular collectives in dilute solutions. At low concentrations (~1mg/mL) spurious signals were detected by DLS that were the same as that as found in pure solutions (~ 0 – 1 nm radius). At higher concentrations (~10 mg/mL) It was found that in acetone or chloroform, that besides detection of the individual hexamers (~4 nm diameter), it was also possible to detect aggregates on the size of 80 – 120 nanometers diameter with the smaller diameter structures being more prevalent (Figure 5.3). Sonication of the aggregates left only the smaller four nanometer hexamers but over time the larger species appeared to reform indicating a metastable aggregation and a tendency for further self-assembly overcoming entropic concerns. As the morphology of these aggregates could not be determined *via* DLS, electron microscopy techniques were used.
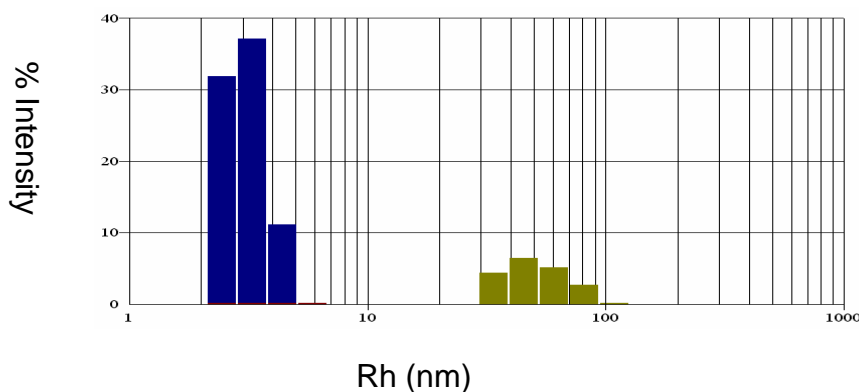
Figure 5.3. Typical DLS result of aggregation of 496 (R = -C$_{10}$H$_{21}$) in chloroform. Concentration: 10 mg/mL, bimodal distribution of 3.08 + 0.6 and 51.58 + 15.5 nm.

5.3.2   Electron Microscopy of Spherical aggregates

Formation of mostly spherical aggregates occurred in four solvents (acetone, acetonitrile, chloroform, methylene chloride) as determined by transmission electron microscopy (TEM) (Figure 5.4). Compared to DLS, a slightly more dilute solution was initially prepared for electron microscopy analysis (2.77 x 10^{-4} M *vs.* 1.39 x 10^{-3} M using DLS) and a 7 µl drop allowed to evaporate under ambient conditions onto a carbon coated copper grid. Upon drying in under a minute it was found that the aggregates detected *via* DLS were strong enough to not degrade upon loss of the liquid medium. Examination of the TEM grids reveals the deposition of groups of spherical aggregates. The spheres themselves seem to be of uniform shape and appear in a range of diameters (Table 5.1).

Solvent properties are important in the formation of these large structures. When the hexamers are examined in a solvent that they were non-soluble in such as water, DLS studies only detected aggregates the size of the individual supermolecule. TEM

examination revealed what appeared to be disorganized irregular compound. Water it seems completely blocks the ability of adjacent hexamers to communicate due to competitive hydrogen bonding.
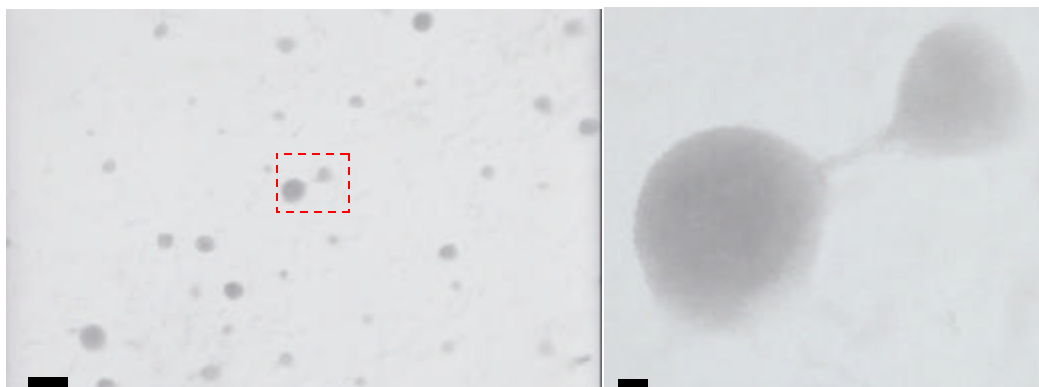
Figure 5.4. Left: TEM of spherical aggregates found from acetone solution of **49**$_6$ (R = –CH$_2$CH(CH$_3$)$_2$, Scale bar = 200 nm). Right: Close up of marked area showing tubular connection connecting two spheres (Scale bar = 20 nm).

It was also noticeable that for the purely organic hexamers (i.e.: those not containing metal linkers) that as the solvent used became increasingly hydrophilic, the spherical aggregates would form but would seem more deformed, with the structure of the sphere looking pushed in and rough. These small broken looking aggregates were seen in methanol or wet acetonitrile.

Neither was an aggregate found to form when using the crystallizing solution of ethyl acetate. A slower rate of evaporation seems to reduce the quantity of the spheres and concurrently led to crystal growth which was also visualized by TEM. Competition from crystallization was also a problem with high boiling point solvents and led almost exclusively to crystal formation in mixtures of water/acetone or methanol. It would appear that preferential crystallization is a competing process in aggregation.

Higher concentration of hexamers leads to larger aggregates of spherical structures rather than self-condensation into a larger motif (Figure 5.5). Using TEM with samples at

higher concentrations (1.39 x 10^{-2} M) revealed that the spheres piled atop one another rather than to coalesce. Due to the penetration of the electron beam, it is possible to see through a hollow sphere compared to a solid sphere which would result in an opaque entity. It is possible to see up to three to four layers thick of spheres piled atop one another. This was a somewhat haphazard technique as at this concentration the compound becomes so thick on the TEM grid that it was often impossible to obtain an image.

For a direct hexamer and bi-layer comparison using TEM, **49** was recrystallized in the bi-layer motif from acetone, a solvent known to retain the supramolecular assembly motif whether hexamer or bi-layer (n.b. ethyl acetate exclusively forms hexamers). Examination by TEM showed that the bilayer conformation resulted in only messy conglomerates (Figure 5.6) or at most a few spheres could be seen. Observing the spheres under these conditions seemed to imply some other process forms the spherical aggregates was taking place. However this anomaly was solved using X-ray powder diffraction.
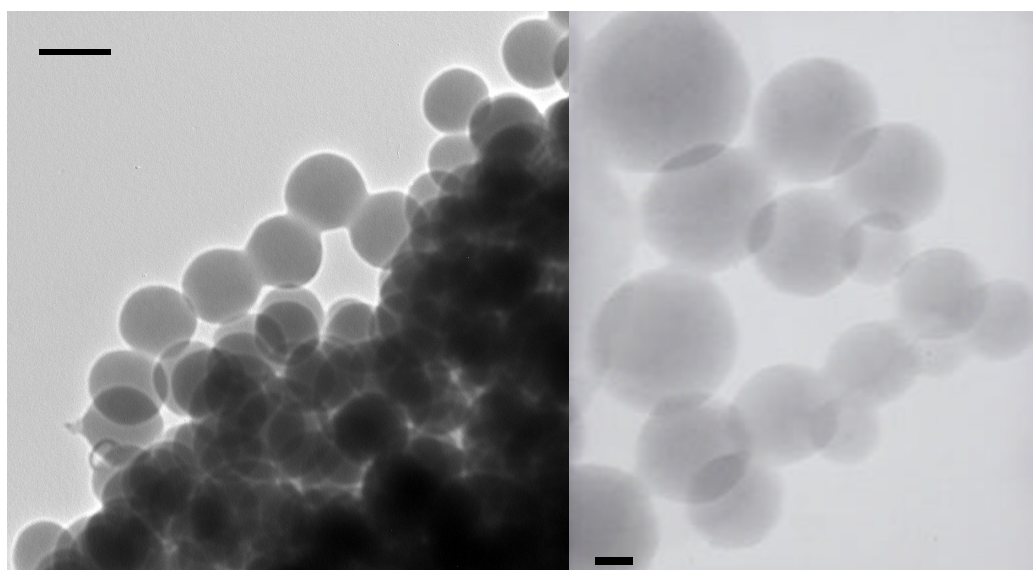
Figure 5.5. Left: TEM showing layering of spheres of **49**$_6$ from ε 1.39 x 10^{-2} M solution of chloroform (R = –CH$_2$CH(CH$_3$)$_2$, Scale bar = 100 nm). Right: Collection of aggregates from acetonitrile solution (R = –C$_3$H$_7$, Concentration of solution: 2.77 x 10^{-4} M, Scale bar = 20 nm).

It was revealed that a long standing bilayer sample in acetone solution (~24 hours) could be converted into the hexamer conformation. A sample of the bilayer conformation (pyrogallolarene, R = –CH$_2$CH(CH$_3$)$_2$ or –C$_8$H$_{17}$) was examined by powder diffraction, redissolved (1.39 x 10^{-3} M) and examined the following day by TEM which revealed the powder pattern for the spheres (Figure 5.7). The remaining sample was evaporated and another powder diffraction scan taken. Comparison with the known hexamer powder diffraction sample revealed the bilayer had converted to the hexamer conformation with concurrent spherical aggregates.
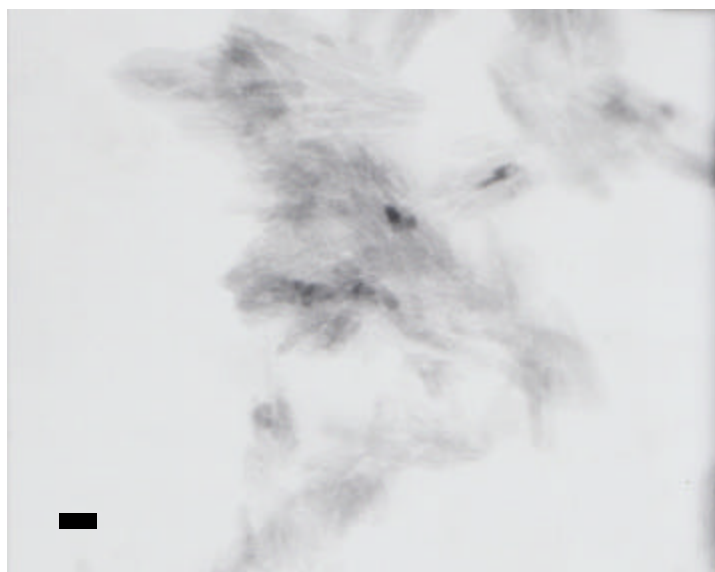
Figure 5.6. TEM of typical morphology of sample found in acetone solution of bilayer crystal for hexamer **49**$_6$ (R = –CH$_2$CH(CH$_3$)$_2$, Scale bar = 20 nm).

The crystals of pyrogallolarene were useful as supporting evidence for the hexamers conformation forming the spherical aggregates. Freshly crystalline material of hexamers **49**$_6$ (R = –C$_{10}$H$_{21}$) was slightly dissolved into chloroform by reducing the amount of solvent that was added to the crystal. After evaporation of the solvent the resulting mixture was examined under TEM. Some crystals had not completely dissolved but were

in a condition that allowed them to be decomposed under the electron beam (Figure 5.8). Conducting *in situ* experiments with the electron beam it was discovered that as the beam heated and decomposed the crystals; spherical aggregates could be seen to be forming.[27-29]

The approximate diameters of these *in situ* created spheres matched that of the structures examined *via* DLS and TEM previously. As the beam is producing the image and decomposing the crystal, a careful adjustment has to be made for this phenomenon to be filmed at a slow enough rate and a bright enough electron beam flux (~50 pA/cm^2) to visualize the formation (Movies 1–3, on CD-ROM).
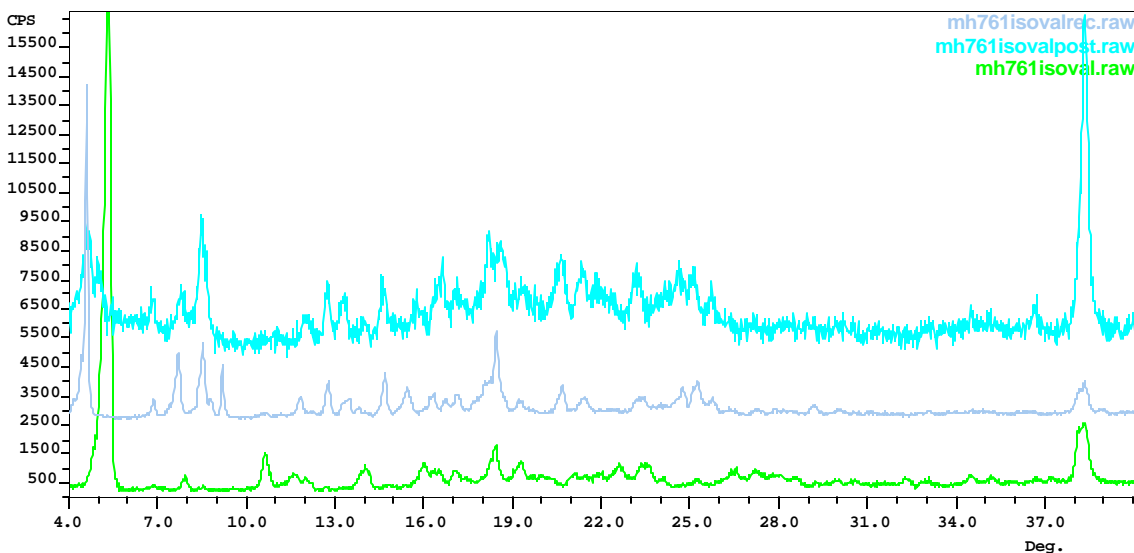
Figure 5.7. X-ray Powder diffraction scans showing change of conformation of pyrogallolarene **49** (R= –CH$_2$CH(CH$_3$)$_2$). Scan mh761isoval.raw showing bilayer conformation (bottom), Scan mh761isovalpost.raw showing sample after TEM (top) and comparison with sample crystallized from ethyl acetate, mh761isovalrec.raw

Due to the high energy of the beam the aggregates form, decompose and reform quickly compared to evaporation. It is clear that under non-crystallizing conditions the spherical aggregate is a preferred conformation. Crystals of the bilayer of **49** did not reproduce this event and neither did hydroxy alkyl functionalized pyrogallolarene examples in acetone/water solutions that crystallize in a columnar formation (R = –C_3H_6OH or –C_4H_8OH). Crystals from a sulfonated calixarene supramolecular product previously discovered in this lab and found to form tubular and spherical solid state structures also did not produce this phenomena.[30]
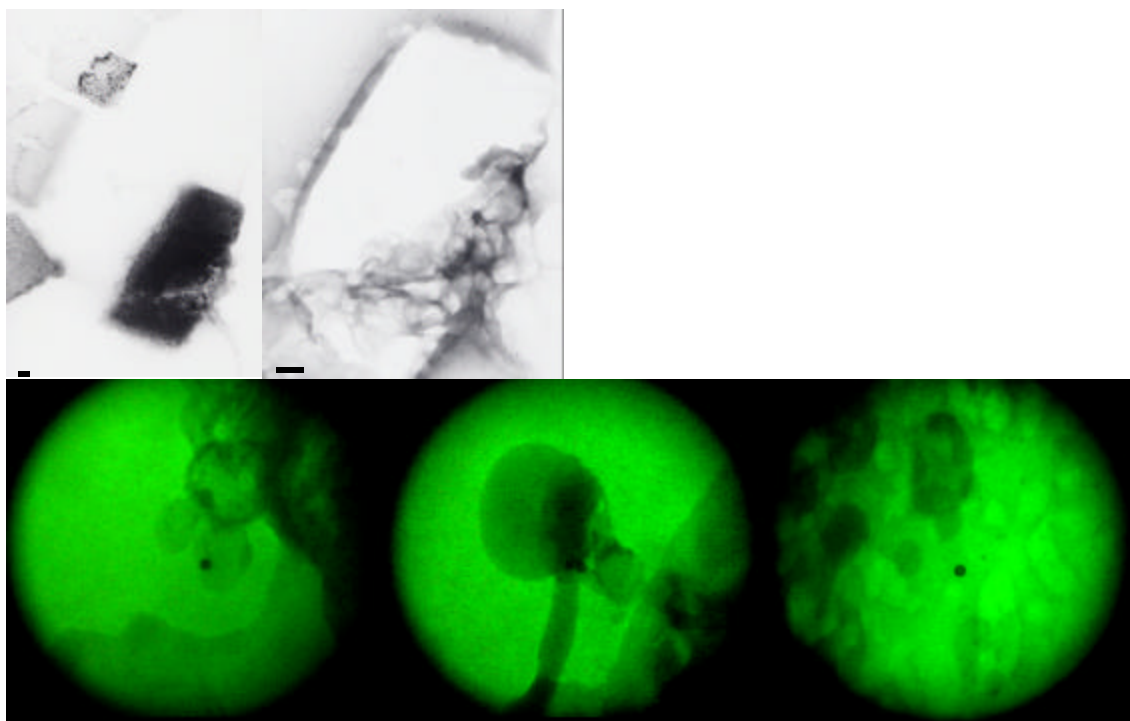
Figure 5.8. Top: TEM of crystal of hexamer **1**$_6$ (R = –$C_{10}H_{21}$) before (left) and after (right) showing decomposition *via* the electron beam. (Scale Bar = 100 nm). Bottom: Video grabs from movies 1 – 3 of spheres forming under TEM beam
(R = –$C_{10}H_{21}$, contrast varied for visibility, central spot diameter = 12 nm).

5.3.3   Tubular structure formation

A deeper examination of the pyrogallolarene hexamers revealed more remarkable entities in the shape of rods or tubes (Figure 5.9). The tubes could be found quite readily though not as common by using the same conditions as for the spheres above. Generally these longer assemblies were discovered when they were attached in some way to the spherical aggregates. The tubes dimensions were found to be smaller in diameter than the spheres but to extend in length a distance up to a maximum of 980 nanometers. Usually the tubes were found to have at each of the ends a sphere attached though there were examples of what appeared to be an exploded sphere and another example of three small spheres in a triangular cross-section (Fig. 5.10, center). The strength of these tubes could

be distinguished with one instance where the tube seemed to have broken in two, the two broken edges showing up quite sharply using SEM.

The tubes themselves could be distinguished by two types. The smooth tubes were most often seen; most commonly from solutions of chloroform but occasionally from other solvent systems like acetonitrile or acetone. These tubes showed no perturbations across their length, only ending in a sphere at either end. The tubes were quite long, some measuring close to a micrometer in length. Spheres could be seen attached at either end of the tube and other spheres seemed to have some contact with the tube along its length.

Spheres, when examined at high resolution, do appear to show a darker area around the edges (Figure 5.10). This possibly indicates some sort of visualization of the wall of the spheres, though of course this maybe open to other interpretation. It is for instance not seen for all spheres, some being completely dark or of uniform intensity.
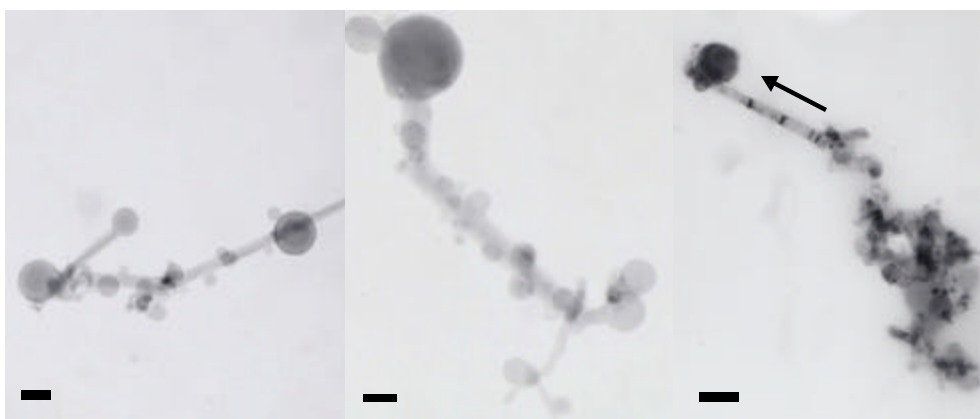
Figure 5.9. Left, center: TEM of spheres and tubes formed from $\mathbf{49}_6$ in a solution of chloroform (Scale bar left = 100 nm; center = 50 nm). Right: Pyrogallolarene sphere and tube network from a solution of methylene chloride showing what appears to be solvent moving along tube (Arrow indicates direction of movement; scale bar = 200 nm)(R = $-CH_2CH(CH_3)_2$).

Figure 5.10. Blowup of left image in Figure 5.9. Some of the spheres seem to have a darker area around their edges, perhaps indicating the wall of the sphere. Estimates from this structure put the wall at about 4 nm thick (Scale bar = 100 nm).

The other type of tube seemed deformed and thicker along its length (Figure 5.11, center). Examination of the deformation showed hemispheric, bulbous, swelling that appeared as though the spherical aggregates were budding. These external structures could be quite rare or liberally spread across the length of the tube. All appear to have the same approximate diameter per individual tube. These stubby tubes overall length were also comparatively shorter in comparison to the smooth tubes.
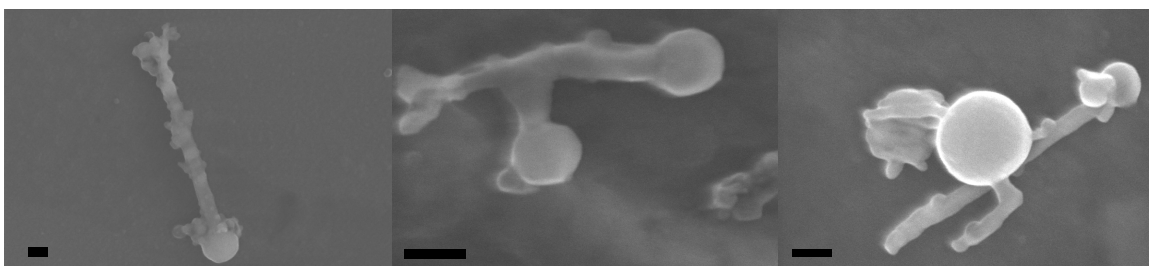
Figure 5.11. SEM of spheres and tubes of 49_6 made in chloroform. Both left and right micrographs show the initial smooth tubes with budding along the length. The center picture shows a rougher structure with a stubby tube coming off at right angles to the longer tube. At the end of both left and center micrographs the sphere appears to have burst or decomposed. (Scale bar = 100 nm, (R = $-CH_2CH(CH_3)_2$)).

Further evidence in regards to the spheres and tubes hollow construction was what appeared at first to be *via* moiré effects visible in TEM.[31] This diffraction of the electron beam is visible when there is a change in the material being observed, either by deformation or a change in the composition of the structure. When observing the spheres and tubes using TEM, it could be seen that bands of dark material would travel down the length of the tube from one side to another (Figure 5.9, right). In some cases it was also seen that a tube connected by spheres had an electron dark region that began from the sphere. The region then diffused from the sphere down through the tube as a band.

While the stresses by the electron beam on the structure of both sphere and tube could result in moiré fringes the structures themselves showed no sign of stress despite this movement of the dark bands. It is proposed that the dark bands are actually enclosed

solvent. These dark bands lends credence to the spheres and tubes being both interconnected and filled with solvent rather than the structures themselves collapsing which would show visible signs of deformation. More likely the energy of the electron beam causes regional heating that forces solvent within the cavity of the sphere and/or tube network to undergo movement due to a temperature gradient. This moves the solvent from a highly energetic regime into the cooler zone. Supporting this, the effect only occurred on samples that were recently put on TEM grids before examination and so were still somewhat wet. Grids examined again after a number of days showed no sign of this band movement; it seems unlikely to be caused by the moiré effect by deformation of either the aggregates or the underlying carbon surface. It must also be noted that if the electron flux of the beam was too high (as happens all too easily unfortunately) the flow of electron dark matter would flow to fast even to take a picture let alone a movie of the phenomenon.

Atomic Force Microscopy (AFM) allowed complementary information to the electron microscopy results in regards to both structure and spatial height of the spheres. Examination of the aggregates using the same process to visualize them as per TEM/SEM but using glass plates, it could be seen that the spherical compounds exhibited heights in the 80 nm range corresponding to the diameters of those seen in DLS and TEM (Figure 5.12, top). The structures were found in all solvent systems examined *via* the electron microscopy techniques.

In one case it was possible that the cantilever tip was forceful enough to puncture the tube and displace a supermolecule of 49_6 (Figure 5.12, bottom). A depression was produced with the cantilever tip with a depth of four nanometers, the same diameter as the hexamer, so providing tantalizing evidence for the hollow nature of the aggregates.
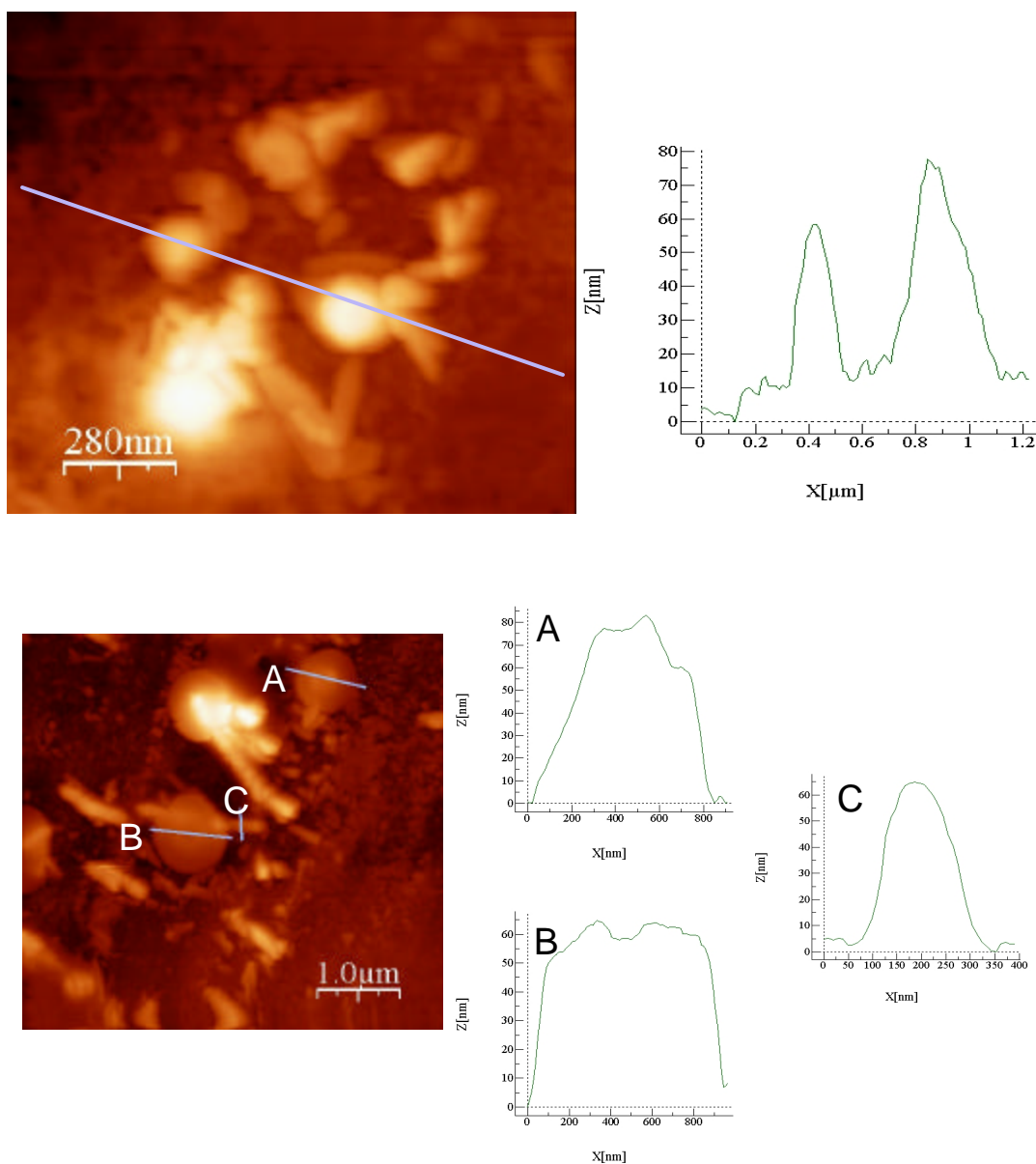
Figure 5.12. Top**:** Particles formed from 49_6 (R = –C$_5$H$_{11}$) on glass substrate from a solution of chloroform. Height measurements are shown across two spheres. Bottom: Spheres formed from hexamer 49_6 (R = –C$_5$H$_{11}$) from acetonitrile solution with height measurements for two spheres (A, B) and a tube-like structure (C). Both A & B appear to have been punctured by cantilever tip, with a 4 nm depression approximately equal in diameter to a single hexameric supramolecule.

5.3.4   Aggregation of gallium mediated hexamer spheres

To probe into the structure of what this larger aggregate consists of we moved away from a purely organic system and investigated the generality of the process using inorganic analogues. Gallium[25] and copper[26] have been found to complex with **49**, replacing some of the hydrogen atoms of the hydroxyl groups with metal atoms but otherwise retaining the spherical hexamer. A major difference in comparison to the organic analogue is that the structures formed by these metal-organic frameworks have exclusively been of the hexamer conformation; no bilayer or tube-like structure has been discovered. In part this seems due to the affinity for the metal to form an octahedral arrangement with only the hexamer conformation, other conformations leading to unfavorable metal-ligand interactions.

Examination of the aggregates formed *via* electron microscopy reveals the same spherical structures as with the purely organic moieties (Figure 5.13). The structures themselves seem quite varied in size and much darker, not surprising with the larger gallium metal within the framework that will absorb more of the electron flux. The evidence here seems to confirm that the tectons of the aggregates are indeed the hexamers.

It was during TEM examination of the aggregation of the gallium coordinated hexameric spheres that by serendipity a chance occurrence allowed for more visual confirmation of the three dimensional aspect of the aggregates (Figure 5.14). Occasionally, there are tears in the carbon sheet covering the copper grid used for TEM sample placement. In this case the heating of the electron beam caused the tear to roll around like a sheet of paper. The rate of roll up could be controlled by controlling the

intensity of the beam and it was seen that on the edge of this sheet some spheres had collected. Seeing them side on rather than from the usual position of face down was comforting to say the least. Of course due to perspective the scale bar gives only a minimum for the diameters as the sheet was rolling downwards.
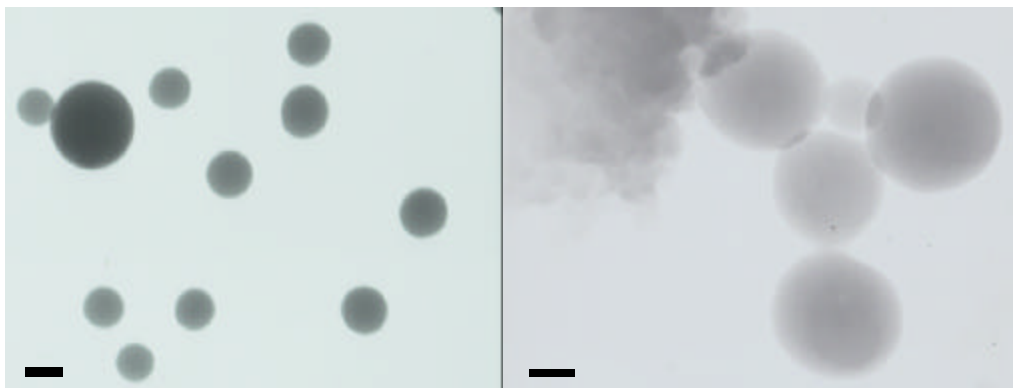
Figure 5.13. Gallium mediated hexamer spheres of 49_6 also form large spherical aggregates from the smaller supermolecule. At times they can be seen to overlay on top of each other (R= –C$_3$H$_7$, scale bar = 50 nm).

5.4   Proposed mechanism for aggregate formation

Aggregation such as elucidated in this project has been found in a couple of cases involving calixarenes or calixarene analogues called resorcinarenes (Figure 5.1, left, X, Z = –OH; Y, W = –H).[15,32] However, in both cases the monomeric unit is decorated along the upper rim opposite the alkyl chain derived lower rim and cannot form anything more complicated than a bi-layer with the upper rim acting as the polar head and the lower rim the hydrophobic tail.

Vesicles with tubes have also been formulated with phospholipids.[12] However this system requires micromanipulation to form both vesicle and nanotube structures. Unlike almost all examples of artificial molecular systems that make vesicles, the supramolecular system here is unique in that the self-assembly of the hexamer takes place

before the full assembly of the larger aggregates. A similar shaped entity are the functionalized fullerenes that were shown to exhibit a range of morphologies depending on the functionalities on the attached chain.[33] Even in this case the fullerenes only had the

Figure 5.14. A tear in the carbon sheet of the TEM grid reveals spheres hanging to the edge of the sheet as it rolls around from the energy of the electron beam (R = –C_3H_7, Scale bar = 50 nm).

organic long tail on one side.

Each individual unit of **49** is surfactant-like, a large charged head and a lipophilic tail consisting of the alkyl chains. Coming together in solution and solid state the supermolecule **49**$_6$ can be considered an inverse micelle, the hydrophilic centre with extensive hydrogen bonding and the lipophilic alkyl tails both into and out of the plane of the wall of the vesicle (Figure 5.15).

Compared to the precursor surfactants that make up micelles and generally have a single linear (i.e.: head and tail regimes) hydrophobic and hydrophilic region, our system seems to arrange itself into two separate but circular regions (Figure 5.15). At the center

of the supermolecule lies a hydrophilic core. This core is surrounded at the "equator" by a ring of hydrophobic alkyl chains. In the solid state, looking down the axis it can be seen
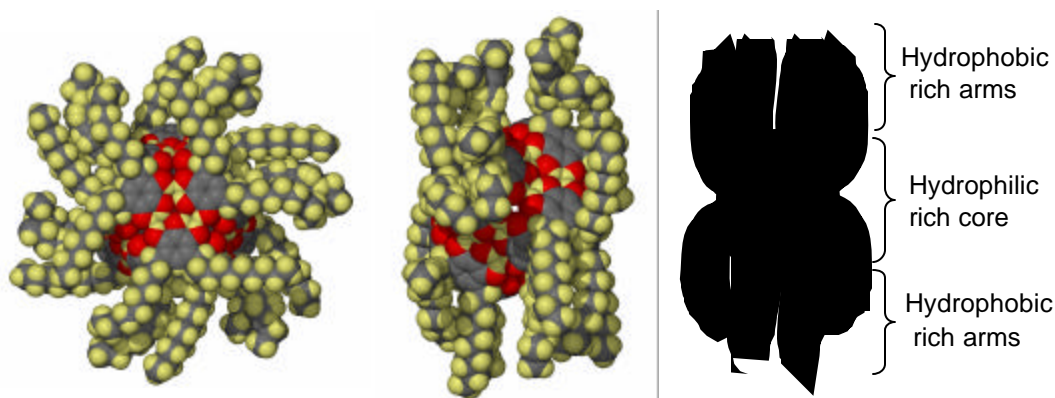
Figure 5.15. Crystal structure and cartoon showing how each hexamer of **49**$_6$ consists of a hydrophilic core surrounded by a hydrophobic outer surface (R = $-$C$_{10}$H$_{21}$). Left: Looking down the "axis" at the hydrophilic rich core. Center: Looking along the "equator" of the supermolecule.

that the alkyl chains conformation leaves open the hydrophilic center.

The unusual flexibility in this system occurs because of simple hydrophobic, hydrophilic considerations. Hydrogen bonding between adjacent hexamers of **49** has been observed in the solid state (Figure 5.16).[13] The hydrogen bonding occurs surrounded by alkyl chain arms from both the supermolecule and its neighbors. In solutions such as we have examined this would be advantageous to stop contact between the organic solvent and the polar oxygen rich core.
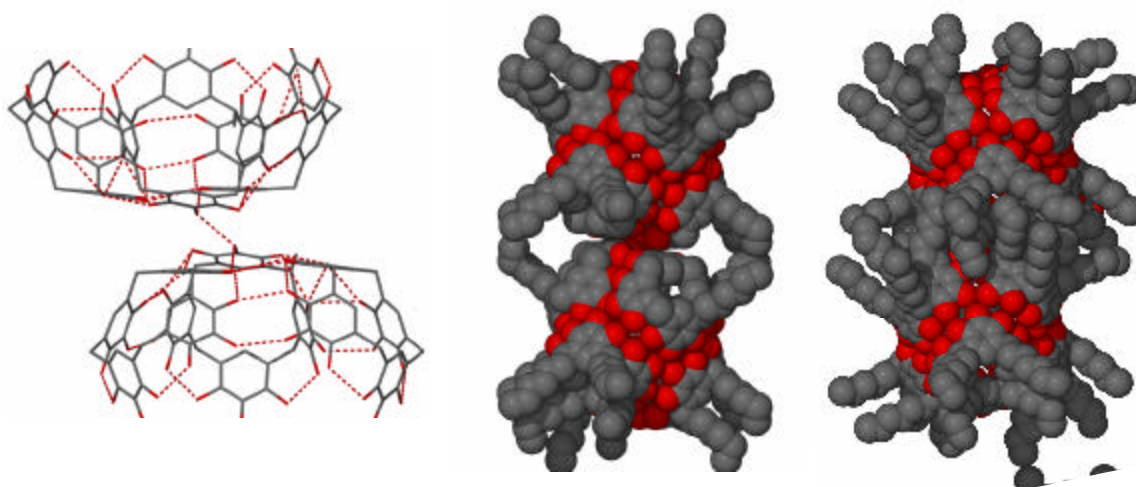
Figure 5.16. Pyrogallolarene **49**$_6$ (R = –C$_6$H$_{13}$) hydrogen bonding and van der Waals forces. Left: The hydrogen bonding between two hexameric supermolecules. Center: Space filling view of the two molecules (some alkyl chains removed for clarity). Right: Same picture but with all alkyl chains present (Hydrogen atoms in all pictures removed for clarity).

This arrangement may entail why a variety of morphologies are able to be produced rather than just a single morphology that is usually expected when aggregation into geometric moieties occurs.[34] A single morphology occurs for typical aggregates with a linear "head and tail" type domains since the tectons for spherical or tubular aggregation have a fixed length of surface as shown by:

$$\frac{v}{al} = 1 + Hl + \frac{Kl^2}{3}$$
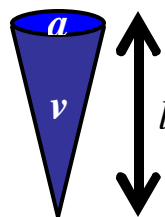
where *v*, *a* and *l* are the volume, cross-sectional area and length of the long alkyl chain and *K* and *L* are the radii of curvatures that occur when many of these tectons come together.

These values are fixed in most tectons and so the structure formed can generally be predicted in the first instance to be sphere, bi-layer or tube depending on the determined values (though further consideration must be made to the chemical aspects as well). In the case of pyrogallolarene hexamer system there are now six non-covalently bound tectons which form a large more complicated subunit. While the alkyl chains would nominally be orthogonal from each other, the solid state structures show there is a more flexible and dynamic morphologies available and so variable values in K and L possible. This leads to the possibility of two types of aggregate occurring simultaneously as we have observed.

Especially in hydrophobic solvents such as chloroform, the hexamers are known to form spontaneously.[35] In this situation there is further opportunity to further minimize the hydrophobic/hydrophilic interface within the hexamer itself. This naturally leads to a situation where the alkyl chains will move to the extremities leading to a similar structure as found in the solid state. With the hydrophilic core being open in this way though it would be only natural for the system to aggregate and remove the polar core from the organic solvent and end up in a situation as is found in the solid state. In this manner, it is reasonable to expect that eventually sheets of hexamers would aggregate *via* two dimensional hydrogen bonding. Since the edges of this sheet are still subject to the hydrophobic solvent, the simplest solution is for these larger morphologies to wrap around and thus enclose space as a sphere or a tube (Figure 5.17). Further evidence for this is that it is rare for the tubes to not have a sphere on the end, an open ended tube subjecting the hydrophilic region to the hydrophobic solvent. Hydrogen bonding rather

than lipophilic interactions would also explain the preference for these structures to break down as a more hydrophilic solvent is used, the hydrophilic solvent both more amenable to the inner core of the hexamer and capable of disrupting the inter-hexamer bonding.

The ability to self-assemble such a range a connections between spheres and tubes reflects a reason why there is a biological-like affinity for these constructs. Since the discovery of cytonemes[36] or tunneling nanotubes in multicellular eukaryotes, this phenomenon for creating tubes from spheres has been observed from cells exhibiting the ability for intracellular communication,[37] and organelle transportation.[8] The tubes are thought to be comprised of actin, a polarizable protein that can form long chain like networks and thus create the tubular structure, in essence very similar to the hexamers presented here. While many aspects of the cytonemes formation have been determined, the underlying chemical formation of them has yet to be fully elucidated. Our system shows that material from the cell wall can easily be transformed from a spherical bilayer system into a tube with out some complicated external process. Movement proteins, implicated in cytonemes research as instigators of the phenomena, could be merely directors of the process rather than active participants, once initiation of a tube from a sphere begins, self-assembly will complete the construct.
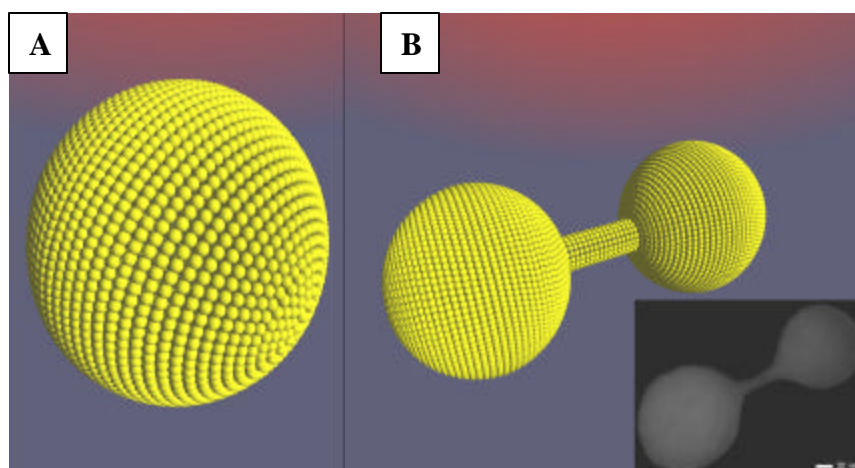
Figure 5.17. (**A**) Representation of hexamers (each small yellow sphere a supermolecule of **49**$_6$) making up the larger aggregate. (**B**) Representation of how spheres and tubes would form. Inset: Negative of Figure 5.4. (**B**) (Scale bar = 20 nm).

5.5   Conclusion

The evidence provided suggests that the pyrogallol[4]arenes are quite possibly hollow, though this has not been shown conclusively. The system we have developed can be easily tailored to form inner and or outer layers of both the cell-like spheres and the tubes to provide confirmatory evidence of the nature of the transport and means of formation through an otherwise impermeable cell wall. The system created from **49** is the simplest of models, stripped from it all the biological interfaces that create these complex morphologies and mimicking just the chemical aspects and response to supramolecular and solvent interactions. The individual hexamers can be tailored in a variety of ways. The structures have been shown to exist when using alkyl chains of different lengths and with certain functional groups including halogens.

In conclusion we have produced a simple, easily produced and tunable molecular system that can model fundamental mechanical aspects of the biological cell structure using a judicious use of substrate modification. Recent work on fluorescent guests within

hexamers of 49_6 allows for observation of structures under a variety of situations.[24] The ability to attach a range of functionalities to the alkyl chains and to modify the interior of the hexamers with a range of guests will allow for both an exploration of the mechanics of the larger biological mimic and as micromachines capable of transport properties as found with cytonemes and much larger vessels. As the system is tunable a wide variety of functionalities can easily be attached for whatever molecular engineering task may be desired. If the single pyrogallolarene can be considered the primary structure, the hexamer the secondary structure, it is now possible *via* supramolecular chemistry to create a tertiary structure, something nature has conducted with aplomb since the existence of the cell. Our research reveals that the general makeup of biological systems does not necessarily require an evolutionary blueprint to form intricate frameworks but is a general behavior that takes place at the molecular level and leads to increased complexity in form as the scale is increased beyond the nanoscale to the microscale.

5.6   Experimental

Methods to form the pyrogallolarenes can be found in Reference 13 and were supplied in house. Before commencing experiments samples were checked *via* unit cells using single crystal X-ray diffraction. All solvents and materials used were HPLC grade from Sigma Aldrich (St. Louis, MO). Hexamers of **49** were crystallized from ethyl acetate over 12 hours. The crystals of the hexamer were weighed and then the appropriate solvent was added. All samples were analyzed within 12 hours of the crystals being placed in solution except in the instance where they were checked for long term viability. All were placed in appropriate concentrations of solvent in a vial (5 ml or 20 ml) or flat top microcentrifuge tube (1.5 ml).

184

DLS was performed on a Protein Solutions DynaPro 99 molecular sizing instrument and with a solid-state laser operating at 655 nm with a temperature controlled Protein Systems MicroSampler at 20°C (Proterion Corporation, Piscataway, NJ). The autocorrelation function of the signal from the scattered intensity was measured by a multichannel digital correlator. The normalized intensity correlation function was analyzed by a regularization method included in the data analysis software package (Dynamics V5.19.06), to give the information on the distribution of the exponential decay function with decay rate Γ. The translational diffusion coefficient can be determined through $\Gamma = Dq^2$ where q is the scattering vector. The hydrodynamic radius R_H is calculated from D via the Stokes-Einstein equation, $R_H = kT/(6\pi\eta D)$, where k is the Boltzmann constant and η the solvent viscosity at temperature T(K). A data collecting strategy of multiple runs at short acquisition time was employed. The acquisition time for each run was set at 10 seconds. The experiment continued for 60 – 100 runs which corresponded to 10 – 15 minutes.

TEM was performed on a JEOL 210 TEM operating at 200kV, tungsten filament and a JEOL 1200 EX transmission electron microscope operating at 80 – 120kV. Carbon coated copper grids (300 mesh) were used for sample substrate. Samples were pipetted from the stock solution of appropriate hexamer and allowed to dry in air at the ambient temperature. Increasing evaporation rate using a pipette to blow air over the grid did not appear to cause any change to the resulting samples except that spheres more often appeared to be found on top of each other. Movies were taken with a Sony DSC-P73 Digital Camera through the microscope lens at +2EV.

SEM was performed on a Hitachi S4700 cold-cathode Field Emission Scanning Electron Microscope. Grids from the TEM experiment were used, or glass microscope slides coated with 5 nm platinum using a sputter coater. Samples prepared on these substrates were the same as per TEM.

AFM: All AFM measurements were performed in contact mode using a MultiMode Nanoscope SPM (Model MMAFM-2, Digital Instruments, Santa Barbara, CA). AFM experiments used the glass samples from SEM or naked glass plates with sample preparation the same as per TEM.

In Situ TEM experiment Movies (All movies had contrast adjusted for better visibility. Zoom is at x 60 000, central spot diameter = 12 nm).

Movie S1: From crystal of hexamer 49_6 (R = $-C_{10}H_{21}$). Approximately 20 seconds after zooming in on area. As crystal is being burned off, bubbles appear and disappear quite quickly. One in particular crosses an empty area as a thick tube before deflating.

Movie S2: From crystal of hexamer 49_6 (R = $-C_{10}H_{21}$). Large bubble formed on debris. After deflation another sphere forms and grows out of a squat tube like structure. A further rectangular bubble grows to the right of it.

Movie S3: From crystal of hexamer 49_6 (R = $-C_{10}H_{21}$). Many spheres forming, budding off one another and deflating.

(1) Service, R. F. *Science* **2005**, *309*, 95.
(2) Atwood, J. L.; Davies, J. E. D.; MacNicol, D. D.; Vögtle, F. *Comprehensive Supramolecular Chemistry*; Elsevier Science: Oxford, 1996; Vol. 1-11.
(3) Li, C.; Zhang, X.; Cao, Z. *Science* **2005**, *309*, 909-911.
(4) Zandi, R.; Reguera, D.; Bruinsma, R. F.; Gelbart, W. M.; Rudnick, J. *PNAS* **2004**, *101*, 15556-15560.
(5) Dye, J. L. *Science* **1990**, *247*, 663-668.
(6) Rebek Jr., J. *Angew. Chem. Int. Ed.* **2005**, *44*, 2068-2078.

(7) Kocer, A.; Walko, M.; Meijberg, W.; Feringa, B. L. *Science* **2005**, *309*, 755-758.

(8) Rustom, A.; Saffrich, R.; Markovic, I.; Walther, P.; Gerdes, H.-H. *Science* **2004**, *303*, 1007-1010.

(9) Baughman, R. H.; Zakhidov, A. A.; de Heer, W. A. *Science* **2002**, *297*, 787-792.

(10) Fernandez-Lopez, S.; Kim, H.-S.; Choi, E. C.; Delgado, M.; Granja, J. R.; Khasanov, A.; Kraehenbuehl, K.; Long, G.; Weinberger, D. A.; Wilcoxen, K. M.; Ghadiri, M. R. *Nature* **2001**, *412*, 452-455.

(11) Takei, K.; Slepnev, V. I.; Haucke, V.; Camilli, P. D. *Nat. Cell Biol.* **1999**, *1*, 33-39.

(12) Karlsson, A.; Karlsson, R.; Karlsson, M.; Cans, A.-S.; Stromberg, A.; Ryttsen, F.; Orwar, O. *Nature* **2001**, *409*, 150-152.

(13) Cave, G. W. V.; Antesberger, J.; Barbour, L. J.; McKinlay, R. M.; Atwood, J. L. *Angew. Chem. Int. Ed.* **2004**, *43*, 5263-5266.

(14) Palmer, L. C.; Julius Rebek, J. *Org. Lett.* **2005**, *7*, 787 -789.

(15) Nakai, T.; Kanamori, T.; Sando, S.; Aoyama, Y. *J. Am. Chem. Soc.* **2003**, *125*, 8465-8475.

(16) Cometti, G.; Dalcanale, E.; vose, A. D.; Levelut, A.-M. *J. Chem. Soc., Chem. Commun.* **1990**, *2*, 163-165.

(17) Atwood, J. L.; Barbour, L. J.; Jerga, A.; Schottel, B. L. *Science* **2002**, 1000-1002.

(18) Luostarinen, M.; Ahman, A.; Nissinen, M.; Rissanen, K. *Supramol. Chem.* **2004**, *16*, 505-512.

(19) Plant, A. L. *Langmuir* **1999**, *15*, 5128-5135.

(20) Perez-Salas, U. A.; Faucher, K. M.; Majkrzak, C. F.; Berk, N. F.; Krueger, S.; Chaikof, E. L. *Langmuir* **2003**, *19*, 7688-7694.

(21) Dalgarno, S. J.; Cave, G. W. V.; Atwood, J. L. *Angew. Chem. Int. Ed.* **2006**, in press.

(22) Atwood, J. L.; Barbour, L. J.; Jerga, A. *Chem. Commun.* **2001**, 2376-2377.

(23) Gerkensmeier, T.; Iwanek, W.; Agena, C.; Fröhlich, R.; Kotila, S.; Näther, C.; Mattay, J. *Eur. J. Org. Chem.* **1999**, 2257-2262.

(24) Dalgarno, S. J.; Tucker, S. A.; Bassil, D. B.; Atwood, J. L. *Science* **2005**, *309*, 2037-2039.

(25) McKinlay, R. M.; Thallapally, P. K.; Cave, G. W. V.; Atwood, J. L. *Angew. Chem. Int. Ed.* **2005**, *44*.

(26) McKinlay, R. M.; Cave, G. W. V.; Atwood, J. L. *PNAS* **2005**, *102*, 5944-5948.

(27) Hashimoto, A.; Yorimitsu, H.; Ajima, K.; Suenaga, K.; Isobe, H.; Miyawaki, J.; Yudasaka, M.; Iijima, S.; Nakamura, E. *PNAS* **2004**, *101*, 8527-8530.

(28) Bonar, J. M.; Hull, R.; Walker, J. F.; Malik, R. *Appl. Phys. Lett.* **1992**, *60*, 1327-1329.

(29) Benyoucef, M.; Clément, N.; Coujou, A. *Mater. Sci. Eng.* **1993**, *A164*, 401-406.

(30)   Orr, G. W.; Barbour, L. J.; Atwood, J. L. *Science* **1999**, *285*, 1049-1052.

(31)   Walker, C. A. *Handbook of moiré measurement*; Institute of Physics: Bristol, Philidelphia, 2004.

(32)   Lee, M.; Lee, S.-J.; Jiang, L.-H. *J. Am. Chem. Soc.* **2004**, *126*, 12724-12725.

(33)   Zhou, S.; Burger, C.; Chu, B.; Sawamura, M.; Nagahama, N.; Toganoh, M.; Hackler, U. E.; Isobe, H.; Nakamura, E. *Science* **2001**, *291*, 1944-1947.

(34)   Antonietti, M.; Förster, S. *Adv. Mater.* **2003**, *15*, 1323-1333.

(35)   Cohen, Y.; Avram, L.; Frish, L. *Angew. Chem. Int. Ed.* **2005**, *44*, 520-554.

(36)   Ramirez-Weber, F.-A.; Kornberg, T. B. *Cell* **1999**, *97*, 599-607.

(37)   Watkins, S. C.; Salter, R. D. *Immunity* **2005**, *23*, 309-318.

Chapter 6: Conclusion: contrasts between projects.

At first glance, the four projects of this PhD seem somewhat isolated from each other. The systems involve disparate elements in both the molecule investigated and the techniques to characterize them. The cucurbituril project was mainly about synthesis and functionalization of the macrocycle. The fullerene project dealt with fairly pre-made molecules and focused on their crystallographic aspects. The carbon nanotube project was involved in how a whole tangle of differing class of molecules (chirality, metallicity, length, diameter of SWNT) could come together and make a more organized gel. The pyrogallolarene project was synthetically similar to the curcurbituril project in that it involved some traditional organic chemistry but required techniques in the areas of biology and engineering.

All the structures studied in this project are common in their use of modern chemical systems. The fullerenes and cucurbiturils where only characterized properly in the 1980's. The first carbon nanotube was discovered by Iijima in 1991 and the pyrogallol[4]arenas are the youngest child in the family of calixarenes, the first reference to their existence coming about in 1990 and the discovery that they form hexamers only determined in 1999.

However, the projects were all useful in educating how to discover aspects of supramolecular chemistry and revealed the difficulty in fully characterizing molecular systems that by their nature can be of a tenuous existence. Standard chemical techniques must be supplemented with less used ones such as dynamic light scattering, electron and force microscopy.

The systems can obviously be compared in their form, the shapes of which are really of only two types; spheres and tubes. The purely carbon molecules are the easiest to distinguish, fullerenes obviously spheres and the nanotubes tubes. Cucurbituril could be considered a very squat tube, though it looks more donut shaped especially functionalized with cyclohexane rings as synthesized here. The pyrogallol[4]arenas are the least like the topology described in the title of this PhD, but with hydrogen bonding in the right solvent the hexamer motifs appear fairly spherical in gross appearance and go on to make both spherical and tubular aggregates.

Of the two spherical molecular systems, the fullerenes, were fundamental building blocks for a variety of crystal structures. The fullerene C_{60} was essentially the strut for which was assembled around it layers of calixarenes. The other fullerene C_{70} was also an important cog in both instigating the change in structure of C_{60} with the calixarene and as an integral part of the crystal structure when with calix[5]arene in p-xylene.

The other spherical amalgamation, pyrogallol[4]arene hexamers, was quite a contrast to the fullerenes. Compared to the complete covalent nature of the fullerenes, the hexamers are individually cup-shaped and need an extensive non-covalent hydrogen bonded network to form the spherical structure.

Both fullerenes and pyrogallolarenes are liberally decorated with aromatic rings. However, while carbon is the only element of fullerenes, the pyrogallol[4]arene have multiple elements arranged in differing zones of hydrophobicity (the alkyl chains) and hyrdophilicity (the hydroxyl groups). Fullerenes are certainly more difficult to functionalize and characterize, the simple synthesis of pyrogallol and aldehyde condensation certainly more controllable than the arc induced synthesis of fullerite.

The systems here show how exquisitely tuned molecular systems can be created and also need to be carefully controlled and understood else an undesirable result occurs. For instance, with the C_{60}:calix[5]arene Z array structure, the ratios of both substrates is crucial, a slight increase in calix[5]arene or the introduction of an impurity or a less homogeneous mix results in the different helical construct. Likewise, the pyrogallol[4]arene hexamers seem to have a preference for the spherical aggregates over the tubular ones, the latter structures seem to require finer tuning for them to form.

Of course the tube and sphere like structures of pyrogallol[4]arene have a commonality in shape with the pure carbon equivalents of the previous chapters. Fullerenes and SWNT are fine examples of how with essentially the same chemistry and same reaction procedures it is possible to create both spherical and tubular configurations. It is also not surprising that the pure covalent structures of fullerenes and nanotubes are easily examined and visualized due to the carbon-carbon bond network. Conversely the pyrogallol[4]arene equivalent structures are a more difficult study, even with an extensive network of hydrogen bonding, hydrophobic repulsions from solvent and a sheath of interlinking alkyl chains. Their non-covalent nature, the mainstay of supramolecular chemistry is an unfortunate but necessary difficulty to be overcome. The difficulty in characterizing such large aggregations is the price to pay for such a versatile and adaptable system.

The cucurbituril project can also be contrasted with the other projects. Like the others, the gist of the project was to manipulate the macrocycle so as to improve its ability to interact in a supramolecular way with other guests. That the covalent modifications where fraught with difficulties (though in the case of hydantoins not

191

completely unwanted) was probably the most unfortunate aspect of this PhD. This project compared with the others showed in some ways that non-covalent chemistry can in fact be an easier task to accomplish.

All these projects were involved in making structures, some being more successful than others and as always there are further avenues of exploration in all four areas researched. In particular regard though, these projects delved into how to make larger structures from smaller substrates, not a better drug or an improved absorbent. Cucurbiturils and nanotubes were both initially strong, rigid, molecules, more than capable of becoming sturdy backbones to larger molecular systems. The fullerenes and nanotubes, while being round globular molecules or collection of macrocycles, revealed that as building blocks they to, with perhaps some further modification, could produce interesting structures such as helical chains or possible hollow spherical aggregates. In comparison the tube-like substrates are essentially ready to go with easier supramolecular assembly from pre-organized ready made substrates.

The spherical compounds researched here would require more processing to become useful systems, possible requiring some covalent interactions so that they do not fall apart. However, the utility of the spherical pyrogallolarenes and fullerenes compared to the tubular nanotubes and cucurbiturils is that they are easier to manipulate and functionalize and so design. The tubular constructs strength and rigidity has come at the price of a more difficult road to functionalization.

In summary, it can be concluded that the various molecular systems examined for this PhD all have the potential to be valuable constructs for the burgeoning nanotechnology industry. We are at the stage of this new era that is set to take off over the next decade

and what should revolutionize the world. Here and now we are in the process of building the structural components, the cogs and wheels of future nanodevices. For supramolecular chemists, the knowledge that the parts and pieces of the various molecular systems we dabble in may go to make a future material that will change the world is gratifying indeed.

VITA

Michael William Heaven was born 6th July, 1972, in Adelaide, Australia. After attending public schools in Adelaide, he received the following degree from the University of Adelaide (1999): BSc (Honours) in Chemistry. Starting his Ph.D. in Chemistry at Monash University in Melbourne, Australia under Prof. Colin L. Raston, he transferred with his supervisor to the University of Leeds, England in 2001. Following the return of Prof. Raston to Australia in 2002, Michael transferred to the University of Missouri-Columbia to be supervised by Prof. Jerry L. Atwood where he earned his Ph.D. in Chemistry(2006). He is currently in a postdoctoral position at the University of North Carolina-Chapel Hill.